AMERICAN MUSEUM
Novitates

PUBLISHED BY THE AMERICAN MUSEUM OF NATURAL HISTORY
CENTRAL PARK WEST AT 79TH STREET, NEW YORK, NY 10024
Number 3501, 60 pp., 111 + 21 figures, 3 tables January 12, 2006

Nesting Biologies and Immature Stages of the Tapinotaspidine Bee Genera *Monoeca* and *Lanthanomelissa* and of Their Osirine Cleptoparasites *Protosiris* and *Parepeolus* (Hymenoptera: Apidae: Apinae)

JEROME G. ROZEN, JR.,[1] GABRIEL A. R. MELO,[2]
ANTÔNIO JOSÉ CAMILLO AGUIAR[3] AND ISABEL ALVES-DOS-SANTOS[4]

Appendix: Taxonomic Notes on *Monoeca* and Description of a New Species of *Protosiris*, by Gabriel A. R. Melo

CONTENTS

[1] Division of Invertebrate Zoology, American Museum of Natural History (rozen@amnh.org).
[2] Departamento de Zoologia, Universidade Federal do Paraná, Curitiba, Brazil (garmelo@ufpr.br).
[3] Departamento de Zoologia, Universidade Federal do Paraná, Curitiba, Brazil (ajaguiar@ufpr.br).
[4] Universidade do Extremo Sul Catarinense, Criciúma, Brazil (isa@unesc.rct-sc.br).

 ISSN 0003-0082

ABSTRACT

The nesting biologies of *Monoeca haemorrhoidalis* (Smith) and *Lanthanomelissa betinae* Urban (Tapinotaspidini) are described from southeastern Brazil. Both are ground nesting; the nests of the former are attacked by the cleptoparasite *Protosiris gigas* Melo (Osirini), and those of the latter are attacked by *Parepeolus minutus* Roig-Alsina (Osirini). Egg eclosion, larval feeding behavior, and cocoon spinning of *M. haemorrhoidalis* are detailed. A female of *P. gigas* opens the closed cell of *M. haemorrhoidalis* by making a large opening in the cell cap (which is plugged after ovipositioning) through which she apparently extends her metasoma. Indirect evidence suggests that she uses her metasomal apex, and perhaps even the sting, to kill the host egg or early instar. *Protosiris* eggs are either attached to the cell-wall surface of the nearly vertical host cells or dropped onto the surface of the provisions. First instars of *P. gigas*, with strongly curved, sharply pointed mandibles, are also capable of killing host immatures or competing cleptoparasites.

Cocoons of all four species are compared and contrasted. The egg, all larval instars, and pupa of *Monoeca haemorrhoidalis* are described, as are the egg and postdefecating larva of *Lanthanomelissa betinae*. The egg, all larval instars, and pupa of *Protosiris gigas* are described, as is the postdefecating larva of *Parepeolus minutus*.

Both *Monoeca haemorrhoidalis* and *Protosiris gigas* have four ovarioles per ovary. The egg indices and other ovarian features of both species are identified and discussed.

The possible phylogenetic relationship of the Tapinotaspidini with the Osirini is briefly explored on the basis of data from this study. Possible phylogenetic relationships of the Osirini with other cleptoparasitic apids are analyzed.

In the appendix, the identity of the species of *Monoeca*, whose nesting biology is presented in the main paper, is discussed. The species is *M. haemorrhoidalis* (Smith, 1854), a species closely related to *M. schrottkyi* (Friese, 1902) and *M. xanthopyga* Harter-Marques, Cunha, and Moure, 2001. An identification key for distinguishing these three species is presented. *Tetra-*

pedia piliventris Friese is placed as a junior synonym of *M. haemorrhoidalis* (new synonymy). A lectotype is designated for *Pachycentris schrottkyi* Friese. The species of *Protosiris* found attacking *M. haemorrhoidalis* is here described as new, *P. gigas* Melo sp. nov. It is structurally most similar to *P. caligneus* (Shanks), from which it differs by its abundant yellow marks, plumose pubescence on the lower paraocular area, protruding anterior mesoscutum, and sparser punctation on the metasomal terga.

RESUMO

A biologia da nidificação de *Monoeca haemorrhoidalis* (Smith) e *Lanthanomelissa betinae* Urban (Tapinotaspidini) é descrita a partir de estudos conduzidos no sul do Brasil. Ambas as espécies de abelhas nidificam no solo, sendo atacadas por duas espécies de abelhas cleptoparasitas da tribo Osirini; os ninhos da primeira são atacados pelo cleptoparasita *Protosiris gigas* Melo (Osirini) e os da segunda, por *Parepeolus minutus* Roig-Alsina (Osirini). Eclosão dos ovos, comportamento de alimentação das larvas e de construção dos casulos de *M. haemorrhoidalis* são descritos em detalhe. As fêmeas de *P. gigas* têm acesso às células recém-aprovisionadas e fechadas de *M. haemorrhoidalis* abrindo um buraco no tampão de fechamento (o buraco é fechado após a oviposição), pelo qual elas aparentemente inserem o metassoma. Evidências indiretas sugerem que as fêmeas do cleptoparasita usam o ápice do metassoma, e talvez o próprio ferrão, para matar o ovo ou a larva jovem do hospedeiro. Os ovos de *Protosiris* são colocados presos à parede vertical das células ou jogados sobre a massa de alimento. Larvas dos dois primeiros ínstares de *P. gigas* apresentam mandíbulas fortemente curvas e pontiagudas e são também capazes de matar os imaturos do hospedeiro ou de potenciais competidores cleptoparasitas.

Os casulos das quatro espécies são comparados. O ovo, todos os ínstares larvais e a pupa de *Monoeca haemorrhoidalis* e de *Protosiris gigas* são descritos, bem como o ovo e a larva pós-defecante de *Lanthanomelissa betinae* e a larva pós-defecante de *Parepeolus minutus*.

Tanto *Monoeca haemorrhoidalis* quanto *Protosiris gigas* apresentam quatro ovaríolos por ovário. Índices para os ovos e outras características dos ovários de ambas as espécies são apresentados e discutidos.

A possível proximidade filogenética entre Tapinotaspidini e Osirini é brevemente explorada com base nos dados do presente estudo. Possíveis relações filogenéticas de Osirini com outros grupos cleptoparasitas de Apidae são também analisadas.

No Apêndice, é discutida a identidade da espécie de *Monoeca*, cuja biologia é apresentada no artigo principal. A espécie corresponde a *M. haemorrhoidalis* (Smith, 1854), uma espécie próxima a *M. schrottkyi* (Friese, 1902) e *M. xanthopyga* Harter-Marques, Cunha & Moure, 2001. Uma chave de identificação para estas três espécies é apresentada. *Tetrapedia piliventris* Friese é colocada como sinônimo júnior de *M. haemorrhoidalis* (sinônimo novo). É designado um lectótipo para *Pachycentris schrottkyi* Friese. A espécie de *Protosiris* encontrada atacando *M. haemorrhoidalis* é aqui descrita como *P. gigas* Melo, n.sp. Estruturalmente, esta espécie assemelha-se mais a *P. caligneus* (Shanks), da qual difere pelas manchas amarelas abundantes, pela pilosidade plumosa na área parocular inferior, pelo mesoscuto projetado anteriormente e pela pontuação mais esparsa nos tergos metassomais.

INTRODUCTION

We present here information on the nesting biology of two species belonging to separate genera of the Tapinotaspidini, *Monoeca* and *Lanthanomelissa*.[5] Both genera and, indeed, all members of the tribe are thought to use floral and other plant oils in nest construction, nest provisioning, or both (Michener, 2000). The two species, *Monoeca haemorrhoidalis* (Smith) and *Lanthanomelissa betinae* Urban, nest in the ground. We found the nests of *M. haemorrhoidalis* attacked by an unnamed species of *Protosiris*, described and named *P. gigas* in the appendix. This is the first association of any species of *Protosiris* with a host. Nests of *L. betinae* were parasitized by *Parepeolus minutus* Roig-Alsina, mature larvae of which were recovered from

[5] Michener (2000) regarded *Lanthanomelissa* as a subgenus of *Chalepogenus*. For simplicity of presentation, we follow the usage adopted by Urban (1995).

the nests. This is the first confirmed host/parasite association of a member of *Parepeolus*, although Rozen (1984b) found an adult of *Parepeolus niger* Roig-Alsina in a nest of *Tapinotaspoides serraticornis* (Friese) (cited as *Tapinotaspis tucumana* (Vachal)), and Roig-Alsina (1989) tentatively associated *Ecclitodes stuardi* (Ruiz) with *Chalepogenus caeruleus* (Friese).

In addition to describing various aspects of the nesting biology of the two host species, we present biological information on their two cleptoparasites. The mode of cleptoparasitism of *Protosiris gigas* provides the first understanding of this matter for any member of the cleptoparasitic tribe Osirini. Because the immature stages of the Tapinotaspidini and Osirini are poorly known, we include an extensive treatment of eggs, larvae, and pupae of species whose nesting we investigated.

Data resulting in this report were accumulated over period of more than 3 years. The nesting biologies of *Monoeca haemorrhoidalis* and *Protosiris gigas* were studied at Mananciais da Serra, Piraquara, Paraná, Brazil. Melo (G.A.R.M.), Rozen (J.G.R.), and Aguiar (A.A.) gathered information for several days starting November 20, 2002, and G.A.R.M. and A.A. subsequently visited the nesting site on January 24, 2003. Starting on December 3, 2003, all authors, including Alves-dos-Santos (I.A.S.), returned to the same nesting site, which was again active, and examined it on and off over a 9-day study period. G.A.R.M. and A.A. carried out further observation on the site January 17, 2004, December 5, 2004, and January 30, 2005.

I.A.S. discovered one of the nesting sites of *Lanthanomelissa betinae* on the campus of Universidade do Extremo Sul Catarinense (UNESC), Criciúma, Santa Catarina, Brazil, in October 2002. All authors carried out excavations on it on November 15 and 16 of that year. Further studies were made there by I.A.S. in November 23–26, 2003. The other *Lanthanomelissa* site was on the campus of Universidade Federal do Paraná, Curitiba, Brazil. It was initially discovered by G.A.R.M. in late October 2001; J.G.R. excavated nests there in November 25, 2002.

Thus, all authors contributed to the biological information presented herein and to collecting and preserving immature stages. J.G.R. described the immature stages herein, and G.A.R.M. identified the adults and prepared the taxonomic description of the new species presented in the appendix.

Overview of Nesting Sites

Three nesting aggregations of tapinotaspidine bees were involved in this study at the following localities, all in Brazil. ***Monoeca* site**: The study site of *Monoeca haemorrhoidalis* is located in an area known as "Mananciais da Serra", in Piraquara, Paraná, which is administered by the state water company SANEPAR. This area has a high annual rainfall and is covered with dense, well-preserved Atlantic forest. The approximate coordinates and altitude of the study site are 25°28′40″S, 48°58′04″W and 1140 m. The nesting area itself is relatively flat, but its surroundings are very steep. Although the area is located on the western slopes of the Serra do Mar, the study site is within a long valley that opens to the east side of this mountain range. The soils there are derived from granitic rocks, which in some parts of the nesting area were still too consolidated to allow bees to burrow. ***Lanthanomelissa* (Curitiba) site:** This nesting site of *Lanthanomelissa betinae* is located on the campus of the Universidade Federal do Paraná (Centro Politécnico). The approximate coordinates and altitude of the site are 25°26′55″S, 49°13′54″W and 940 m. The region is mostly urbanized, with only a small patch of forest and wetlands about 500 m away. Most of the area around the bank containing the nests is maintained as a grass lawn. The soil and vegetation of the area suggests that it was originally a patch of native grass. These grass fields were relatively common in the region in areas with shallow soils in which *Araucaria* forest would not develop. ***Lanthanomelissa* (Criciúma) site:** This nesting site of *Lanthanomelissa betinae* is located at the edge of the campus of the Universidade do Extremo Sul Catarinense (UNESC), Criciúma, Santa Catarina. The coordinates and altitude of the town of Criciúma are 28°40′S, 49°22′W and 50 m. The site is bordered on one side by a small fragment

of secondary forest and by open areas covered by weeds and cultivated crops. The region is within the southern limit of the lowland Atlantic forest.

METHODS AND TERMINOLOGY

Preserved larvae were first illustrated while in ethanol, resulting in pencil illustrations of the entire specimen and enlarged frontal and lateral views of the head. Heads were then separated from the bodies, and both were cleared in a heated aqueous solution of sodium hydroxide until all tissue was removed. If large, specimens were examined in ethanol, or if small (usually), they were placed in glycerin. Details of anatomy such as setae and sensilla were added to the illustrations, and mandibles and spiracles were dissected and illustrated.

In estimating the approximate length of a strongly curved larva, four or five relatively straight sections of it were measured in lateral view at the level of the spiracles; these measurements were then summed, as illustrated in figure 52.

The term *mature larva* refers to the fifth instar after it has finished feeding. We use the term *postdefecating larva* (often called the prepupa by others) for the mature larva after it voids its feces. The term *predefecating larva* refers to the mature larva before it defecates. These two stages, although of the same instar and therefore usually identical in such structures as mandibles and spiracles, are quite different in overall shape, integumental texture, and behavior. The predefecating form is more robust, its integument is thinner and far less wrinkled, often of a different hue, and it is active (i.e., its head and body can move and its mandibles open and close). The postdefecating larva is more slender, often with body tubercles more pronounced, its integument is thicker and more wrinkled, and, when in full diapause, the larva is completely inactive. For most univoltine species, the postdefecating larva is the stage in which the bee diapauses until the next nesting season.

Because postdefecating larvae are the forms most frequently collected, descriptions of bee larvae are usually based on that stage. Descriptions of the mature larvae presented here are based on postdefecating forms. However, in cases where we also have been able to study mature predefecating larvae, we described significant differences with respect to body tubercles and the shape of the terminal abdominal segments, following the description of the postdefecating form. Other differences, such as body color of predefecating forms, are not mentioned, and similarly the more extensive expression of internal head ridges of predefecating larvae are not described, except in the case of *Lanthanomelissa betinae*, which will serve as an example. It seems likely that the less prominent internal ridges in the head of postdefecating forms result from the thickening of the cuticle elsewhere as the larva enters diapause, so that there is less contrast between ridges and nonridged areas.

In the frontal-view diagrams of larval heads, sensilla and internal ridges are indicated on only their left side.

Larvae and eggs were examined with a Hitachi S-5700 scanning electron microscope (SEM) in the Microscopy and Imaging Facility of the American Museum of Natural History after they were critical-point dried and coated with gold/palladium. Mature larvae so examined unexpectedly revealed elongate, setiform papillae associated with the salivary openings (figs. 60, 68, 96, 99). These structures are termed salivary papillae rather than spicules because they appear to be nonsclerotized. Their patterning differed from one species to another but suggests that they may have some function associated with the application of the silk in cocoon construction, such as serving like the end of a paint brush in distributing liquid over a broad surface. The papillae were scarcely visible when viewed with a light microscope and thus may have been overlooked in previous studies of other taxa. The extent to which other cocoon-spinning mature larvae have them should be investigated.

The egg index, referred to in the descriptions of eggs and in the section on Ovarian Statistics, is a method of defining the size of a bee's egg relative to the size of the female's body, as developed by Iwata and Sakagami (1966). It is calculated by dividing the length of the egg or mature oocyte by the distance between the outer rims of the tegulae. We

gathered these data two ways. For the section on Ovarian Statistics, we measured the length of the longest mature oocyte in a female and divided that figure by her intertegular distance. For the descriptions of eggs of the taxa, we averaged the lengths of eggs recovered from nests and then divided the resulting figure by the average intertegular distance of a sampling of females. Iwata and Sakagami (1966) proposed a five-category classification of bee eggs (mature oocytes) based on their indices; that is, length of the egg (oocyte) (E) divided by the distance between the outer rims of the tegulae, or metasomal width (M):

dwarf ($E/M \leq 0.50$);

small ($0.50 < E/M \leq 0.75$);

medium ($0.75 < E/M \leq 1.00$);

large ($1.00 < E/M \leq 1.10$);

giant ($0.10 < E/M$).

The abbreviations used for adult structures are: T for metasomal tergum and S for metasomal sternum, followed by an Arabic number denoting the segment (e.g., T6 refers to sixth metasomal tergum).

BIOLOGY OF *MONOECA HAEMORRHOIDALIS* (SMITH)

Several nesting sites of *Monoeca haemorrhoidalis* were discovered in 2002, 2003 and 2004 along a seldom-traversed, unpaved road extending more than 3 km through the heavily forested mountainous area. The largest site (fig. 1) was excavated during these 3 years to provide the information presented here. It occupied about a 12-m-long, horizontal section of the roadway. Being about 3 m wide at either end, its midsection widened to about 6 m and contained the most nests. The site was shielded marginally by the forest canopy so that much of it received considerable sunlight on clear days. Ground cover, mostly grasses, obscured much of the surface, so that many nest entrances were partly or completely hidden (fig. 2). In 2002, several smaller nesting sites along the forested roadway were discovered, but none of these showed activity of *Protosiris gigas*. However, in 2003 we discovered this cleptoparasite at a less populous site about 1 km from the study site.

In early December 2003 the main site was extremely active midmorning to late afternoon, with flying *Monoeca haemorrhoidalis* and *Protosiris gigas* producing a constant hum. Both species tended to fly no more than 0.5 m above the ground, although occasionally individuals briefly landed a meter or more above the surface on surrounding vegetation. Because of the dense, low groundcover, nest density could not be measured. Rough estimates of the number of individuals of both species combined ranged from approximately 50 per m^2 on December 4, 2003, during a very active period, to 25 per m^2 the following day, a reduction presumably resulting from different weather conditions. At these times, most of the *Protosiris* were males, whereas the *Monoeca* population was of both sexes, though males seemed more abundant. Although hosts and cleptoparasites were generally scattered over the entire nesting area, we frequently saw small flying aggregations of mostly male *Protosiris*, suggesting that they may have been pursuing a receptive female.

In December 2003, females of *Monoeca haemorrhoidalis* were seen near the nest aggregation, visiting flowers and flower buds of *Tetrapterys guilleminiana* A. Juss. (Malpighiaceae), a tree-climbing woody vine that presents yellow flowers arranged in large inflorescences. Most plants were in the tops of trees, but some branches had fallen onto the forest edge. One female collected on these *Tetrapterys* flowers carried only oil in the scopae of the hindlegs. On one plant of *T. guilleminiana* with nonglandular flowers, we saw one *Monoeca* female collecting pollen and another female with barren scopae approaching three flowers but leaving without landing. The scopal loads of five females carrying pollen consisted of *Tetrapterys* pollen. Also, all samples of pollen from seven broad cells contained *Tetrapterys* pollen, with most of them composed solely of *Tetrapterys* pollen. Only two of the cells analyzed revealed a half-and-half mixture of *Tetrapterys* pollen and unidentified pollen grains (triangular pollen grains with three furrows, each one crossed by a transverse furrow).

Adult activity at the site was greatest on

December 4, 2003, and declined gradually afterward although both parasites and hosts were still moderately abundant when we last visited the site on December 11, 2003, at the end of the joint study period. When G.A.R.M. and A.A. revisited the site on January 17, 2004, they discovered many flying males and nesting females of *Monoeca haemorrhoidalis*, which seemed about as abundant as in early December, but adults of *Protosiris gigas* were completely absent.

The start of the nesting activities of the next generation in 2004 seemed to have been delayed at the site. The adult activity on December 5, 2004, was only about one-fifth to one-sixth of that observed in December 2003, despite the favorable weather conditions. Also, no fresh cocoons or full-grown larvae were found.

Copulating *Monoeca haemorrhoidalis* were occasionally observed on the low vegetation covering the nesting site, with one or more other males often attempting to intercede with the copulating pairs. Females of *Monoeca haemorrhoidalis* presumably spent the night in nest burrows. Sleeping places of males were not found.

Only a single female occupied each nest. Nest entrances of *Monoeca haemorrhoidalis* were surrounded by abundant moist tumuli of excavated soil, and they lacked distinct turrets, although the worked wall of the main burrow extend through the tumulus at least on some occasions. Entrances were randomly scattered, with some being 5 cm apart and others more distant. Many could be seen at one time over a broad area, but most were partly to nearly completely hidden by ground cover (fig. 2). Main burrows descended vertically with limited turning through the moist, nearly rock-free substrate and were open their entire length. Because of on-going rainy spells, the substrate was always moist, but heavy downpours did not flood our large study excavations, attesting to the drainage capabilities of the nesting substrate. Burrow diameters ranged from 7.0 to 9.0 mm, and burrow walls were smooth and moderately shiny (fig. 3). At least in one area, the burrow walls were lined with extremely fine, reflective, claylike material about 1 mm thick that was red and contrasted with the browner surrounding substrate. Their color matched that of the lower substrate and no doubt resulted from the lower substrate material being brought to the surface during nest building. However, whether the tunnel linings were an accidental byproduct of nest excavation or a special construction by the female *M. haemorrhoidalis* is unknown. The surface of the burrow lining showed distinct, obviously repetitive, tamping impressions only in some areas (fig. 3). These impressions are thought to have been from the female using her pygidial plate, an activity known in other bees. A water droplet applied to the wall remained beaded on the surface for at least a minute. The surface was not coated with the same waterproof material used on the cell walls, so that its shiny, hydrophobic surface may have resulted from the mechanical compression of soil particles through the tamping process. Water-retardant burrow walls are an uncommon feature among solitary, ground-nesting bees. Perhaps water leaking through the walls of deep burrows with large diameters is hazardous in wet environments.

Overall nest configuration of this species could not be determined, although nests were obviously deep and almost certainly consisted of numerous cells. Too many main tunnels from the current and previous generations penetrated the soil to permit any one to be followed to reveal the branching pattern, and too many cells, both current and old, were encountered to assign them to a single main burrow. In one area fresh cells were first encountered at a depth of about 70 cm, and others may have extended below the 1 m level. In other areas a few cells were found as shallowly as 30 cm. All cells tended to be vertical but were tipped slightly, although we noticed one inclined as much as 45°.

Cells were bilaterally symmetrical around their long axes. One side was more outcurved, and the opposite side was more or less incurved above and straighter below, so that the long axis of the cell tended to be curved (figs. 7, 9). This feature is uncommon in bees, but interestingly it is characteristic of the distantly related Diphaglossinae (Rozen, 1984a), where it is often more accentuated. (Andrenidae and Halictidae commonly have one side more outcurved and the opposite side nearly flat, but the opposite side

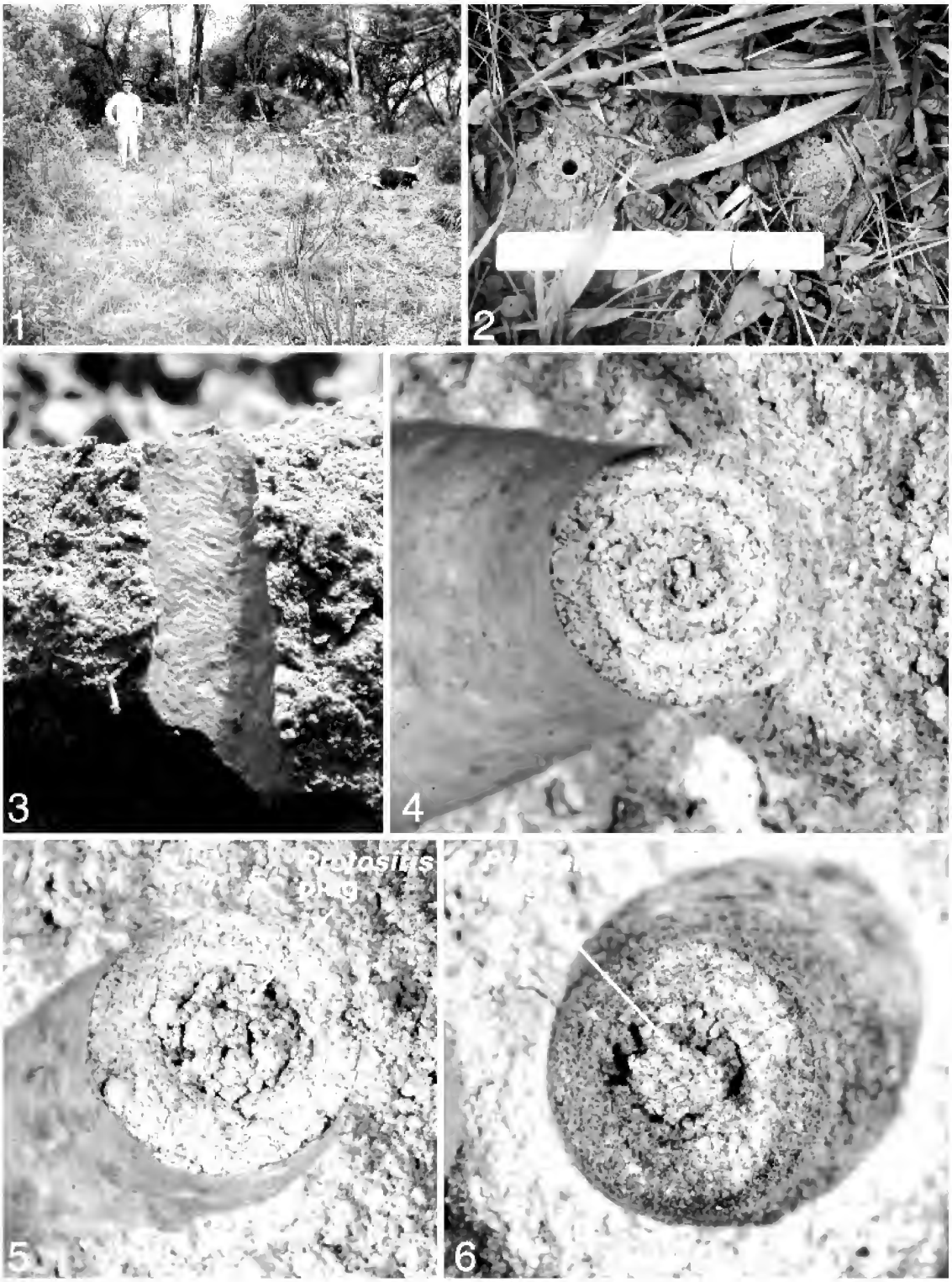

Fig. 1. Nesting site of *Monoeca haemorrhoidalis*, showing dense ground cover in foreground. **Fig. 2.** Close-up of two nest entrances of same. **Fig. 3.** Main burrow of *Monoeca haemorrhoidalis* show-

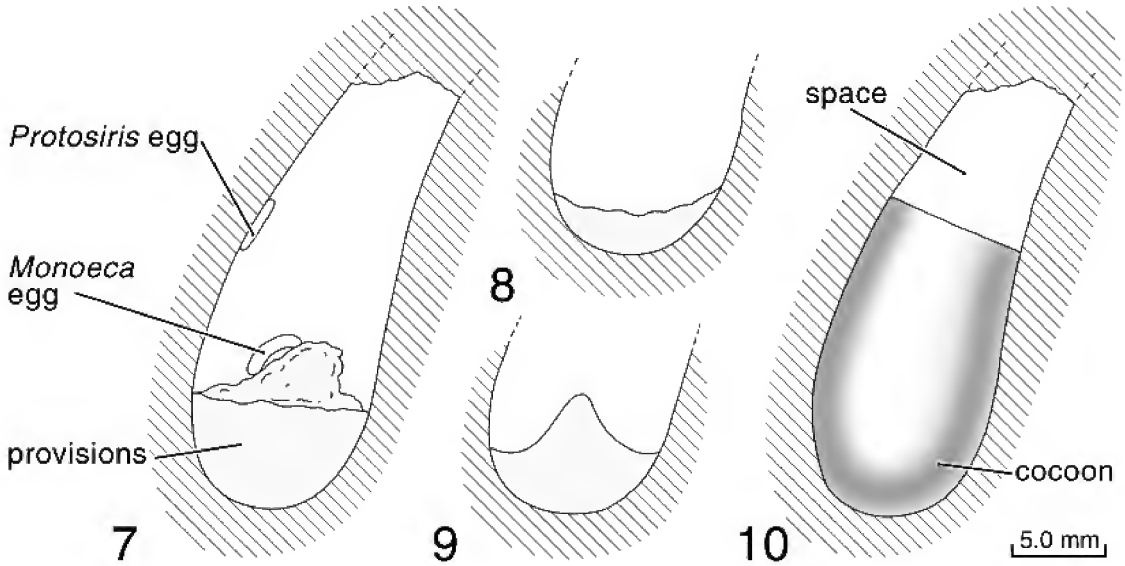

Figs. 7–10. Cells of *Monoeca haemorrhoidalis*, diagrammatically represented. **7.** Fully provisioned with *Monoeca* egg on provisions, and egg of *Protosiris gigas* attached to cell wall. **8.** In early stages of being provisioned. **9.** Depicting partially eaten provisions. **10.** Containing cocoon of *Monoeca haemorrhoidalis*, with empty space between top of provisions and cell closure. Scale line = 5.0 mm.

is not incurved as in the Diphaglossinae and *Monoeca haemorrhoidalis*.)

The cell lining was reflective, waterproof, and faintly milky. It not only coated the cell wall but also extended partly into the connecting lateral. When examined with a stereomicroscope, the material appeared brittle, fracturing rather than bending under stress. Its surface was patterned with faint curved parallel lines, one patch adjoining another, as if swept by a series of brushstrokes. A sweeping by the female's much enlarged pygidial plate (see fig. A7) will likely be found to account for these marks as she applies the coating to the cell surface. When cells were allowed to dry over time, their lining tended to fracture and pull away from the soil, so that pieces could be removed from the cell wall with forceps. When we placed a flake on a microscope slide that was then heated on a hotplate, the flake melted into a nearly clear liquid, which solidified when cooled to room temperature. The cooled material became less transparent, and, when scraped with forceps, the scrape mark was shiny. Thus, the material had the physical characteristics of wax. We would be surprised if this substance did not come from the large, pale dorsal wax gland on the anterior part of the female's sixth metasomal tergum (T6) that is normally hidden under the previous tergum (see also appendix, figs. A7–A8).

Santos et al. (2004) studied the histology of integumental glands in the metasoma of *Monoeca xanthopyga* Harter-Marques, Cunha, and Moure. The large gland present in the female's T6 was found to be a class I gland that histochemically produced lipids. We assume that the gland in *M. haemorrhoidalis* is homologous to that present in *M. xanthopyga*. We examined additional species of Tapinotaspidini and found that the external evidence of the gland (a transverse depression at the base of the female's T6) was

←

ing repetitive tamping impressions on shiny burrow wall. **Fig. 4.** *Monoeca haemorrhoidalis*, spiral inner surface of cell closure. **Figs. 5, 6.** Closure ends of cells of *Monoeca haemorrhoidalis*, showing plugged entrance holes made by females of *Protosiris gigas*; holes are filled by them as they depart.

present in *M. schrottkyi* (Friese) and *M. pluricincta* (Vachal) but absent from *Monoeca lanei* (Moure), *Monoeca* sp., *Trigonopedia glaberrima* (Friese), *T. ferruginea* (Friese), *Arhysoceble dichroopoda* Moure, *A. huberi* (Ducke), *Tapinotaspoides serraticornis* (Friese), *Paratetrapedia amplipennis* (Smith), *P. punctifrons* (Smith), *P. larocai* (Moure), and *Chalepogenus* sp.

The inner surface of the cell closure was a deeply concave spiral of 4–6 coils (fig. 4), which lacked a waterproof lining. It absorbed a water droplet immediately when tested.

Cell lengths measured from the apex of the concave spiral closure to the cell bottom were 18.0–26.0 mm ($\bar{x}$ = 23.2 mm, N = 15). The great range in lengths may have resulted from variation as to where the female placed the cell closure; for example, the shortest cell (18.0 mm) had the largest diameter at the closure (8.0 mm). Maximum cell diameters were 8.5–10.0 mm ($\bar{x}$ = 9.3 mm, N = 10). Cell diameters at the closure ranged from 5.5 to 8.0 mm ($\bar{x}$ = 6.3 mm, N = 9), with all closure diameters (except for the two extremes) between 6.0 and 6.5 mm. In general, cells were elongate relative to their maximum diameters, with their lengths being approximately 2.5 times their maximum diameters. We wonder if the unusual elongation of the cells of this species might have been driven by natural selection: host eggs farther away from the cell closure are distanced from the stings of the cleptoparasite (see Biology of *Protosiris gigas*, below).

Laterals appeared to approach cells from variable directions, sometimes rising shortly before bending downward to connect to a cell, and other times descending straight downward to connect to the cell. All were soil filled after cell closure, so that we were unable to trace them.

Pale cream-colored provisions when first brought into a cell were placed in the bottom and had a somewhat concave top surface (fig. 8), much as in *Lanthanomelissa betinae*. The full complement of provisions in a cell required a number of foraging trips, so that the basal portion with its concave upper surface appeared at more than one level among cells being provisioned. Completed provisions consisted of a homogeneous mass of moist pollen 4.5–7.0 mm deep (N = 4) from which arose a central mound, skewed away from the outcurved side of the cell (fig. 7). The height of the mound measured from the bottom of the cell was 8.5–9.0 mm (N = 5). The surface of the provisions was irregular. The female deposited her strongly curved egg on the less vertical side of the mass just below the summit, so that the posterior end of the egg pointed radially outward (fig. 7). Generally the anterior and posterior ends of the egg contacted the surface of the provisions, while its midsection was elevated above the surface.

The nature of our investigation did not permit us to measure developmental rates of eggs, larval instars, and pupae. However, casual observations suggested that the lengths of these stadia were not unusual for bees. Embryos of *Monoeca haemorrhoidalis* at first developed with the ventral surface dorsal within the chorion, and then they rotated 180° before hatching, so that the first instar's ventral surface rested next to the provisions, as mentioned, for example, by Torchio et al. (1988) for many other bees.

During eclosion, the embryonic fluid was ingested, so that the chorion adhered to the now defined, first-instar head capsule, and the trachea filled with air. The chorion split along the spiracular line on each side of the body (as was determined by examining preserved first instars for which the chorion had been partly removed by the wash of the preservative), while the ventral surface of the head was buried in the provisions. The rest of the body did not adhere closely to the food. By placing a droplet of a 1% aqueous solution of Fast Green on the provisions immediately in front of the head, we saw the green being ingested into the alimentary tract, an indication that the first instar was ingesting external fluid, not just embryonic fluid. During this time, the larva remained motionless except for faint contractions of the body surface presumably associated with fluid ingestion and tracheal ventilation. The body remained rigid and did not adhere closely to the provisions. Only when the second instar shed the chorion simultaneously with the first-instar integument did the ventral surface of the body come into complete contact with the provisions. At this time the mandibles started opening and closing, com-

mencing pollen ingestion, and the second instar crawled away from the previous exuviae.

To investigate how the first instar is able to ingest liquid from the provisions, we examined a preserved first instar, still surrounded by chorion. It revealed a large, circular, bowel-shaped invagination of the chorion in the vicinity of the larva's mouth (i.e., below the labrum and between the mandibles), possible external evidence of the passageway of the fluid into the foregut. From another preserved first instar, we were able to remove the chorion covering the head and examine it with a compound microscope. Although we expected to see an opening in the chorion on the innermost surface of the invagination, there was no visible rent. However, the micropylar array was there or near there, and this discovery raised the question of whether the micropyle pores might be the passageway for the liquid to be sucked into the foregut. We were able to examine yet another pharate first instar, this time with an SEM. Although the front of the chorion partly came away from the larva as it was being mounted on the SEM stub, the resulting images (figs. 11, 12) showed the inner surface of the chorion with the micropyle fully displayed, just below the larval head. This appears to be strong evidence that the micropyle is indeed the passageway that allows the first instar to ingest fluid from outside the chorion.

On this same specimen, we examined with the SEM the line of minute granules that extends longitudinally just above the spiracles (see description of first instar *Monoeca haemorrhoidalis*). Under very high magnification (figs. 14, 15), these granules are definitely spicules in that they do not articulate with the cuticle. They are stout at the base and most, if not all, are sharply pointed. We suggest that their position and shape may serve as the tearing mechanism that causes the chorion to split along the spiracular line as the body of the embryo/first instar swells from ingesting first embryonic fluid and then perhaps external fluid during eclosion. This hypothesis and the hypothesized ingestion of external fluid through the micropyle need further investigation, but they may well shed light not only about eclosion in *Monoeca haemorrhoidalis* but more broadly about eclosion in many other groups of bees, since the lateral splitting of the chorion has been observed in other bees (Alves-dos-Santos et al., 2002; Rozen, 1964, 1969; Rozen and Buchmann, 1990; Torchio, 1989a, 1989b; Torchio and Trostle, 1986).

While feeding, the second instar roamed actively over the surface of the provisions. It was remarkably agile, being able to raise the anterior part of its body into the air while only the terminal 2–4 body segments remained in contact with the provisions. Thus, it was capable of leaving the provisions to climb the cell wall and, when being reared in an artificial container, to leave the cell altogether. Later-stage larvae lay sideways on the provisions, with their dorsal surface against the cell wall as they fed and moved forward. As a consequence, the provisions developed a more pointed conical central peak surrounded by a trough containing the larva (fig. 9). As larvae became more enlarged, they looped the midsection of their body upward, so that the head could feed on the provisions on one side of the cell and the apex of the abdomen touched the provisions on the opposite side. While in this position, the larva's feeding caused the central peak of the provisions to become facetted, that is, flattened on one side rather than evenly cone-shaped.

It seems likely that the changes in body spiculation from one instar to the next (treated in the descriptions of the larval stages) relate to their mode of activity. Unfortunately, we were unaware of these changes when we were in the field where we could have studied them in greater detail. Nonetheless, changes in spiculation of the early instars seem clearly related to larval activity. The first instar does not crawl and has no body spicules (except for the minute ones above the spiracular line); the second and third instars, which actively crawl, have conspicuously spiculate venters. For the fourth instar, spicules over all surfaces of its body probably relate to the fact that it feeds on its side as it circles the food mass. However, the nearly complete loss of body spicules of the fifth instar is difficult to understand.

Toward the end of the feeding phase and before spinning their cocoons, larvae start biting and ingesting the cell lining, presumably at first to eat the few pollen grains still

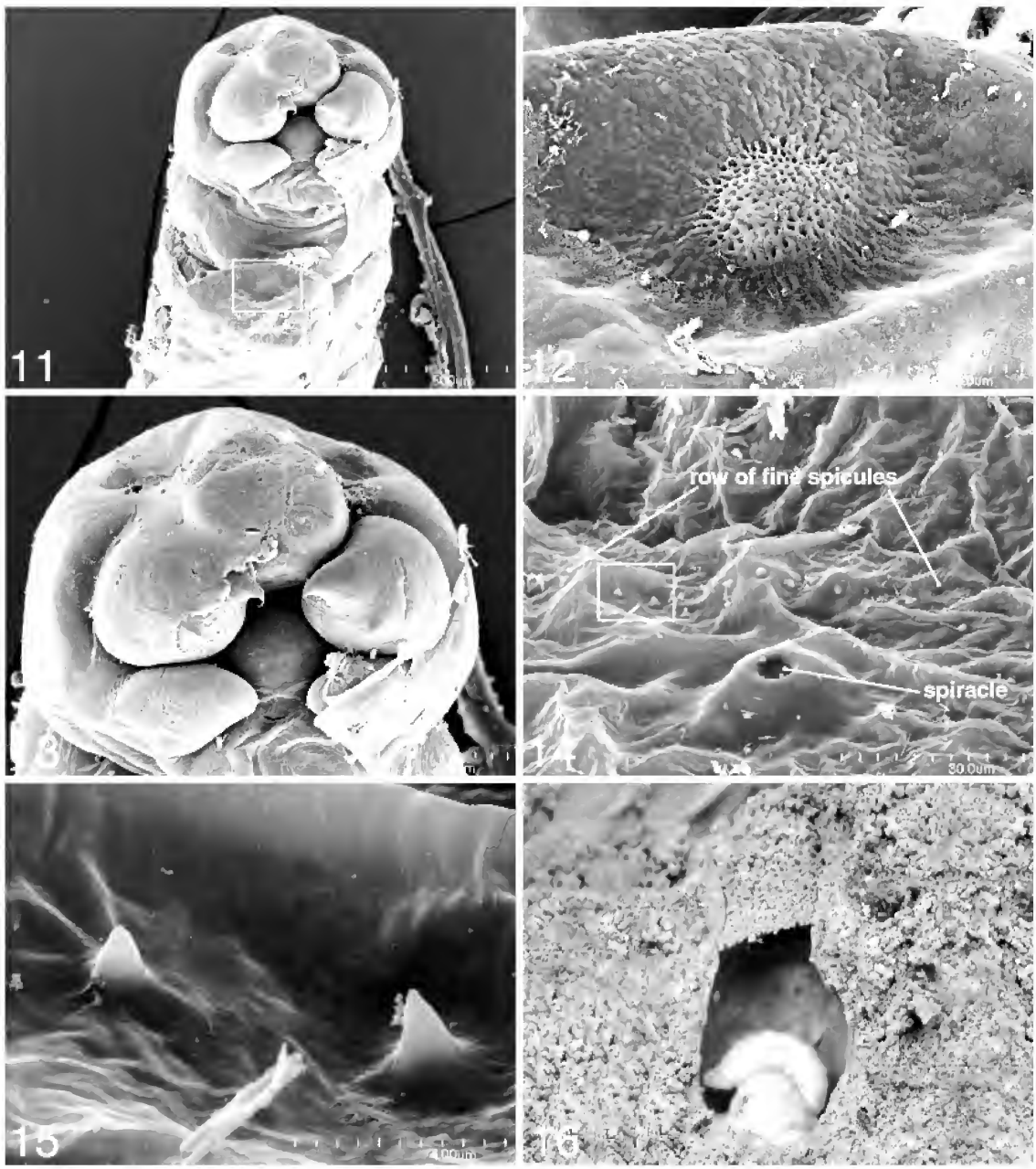

Figs. 11–15. SEM micrographs of first instar of *Monoeca haemorrhoidalis*. **11.** Anterior part of body, ventral view, with chorion partly broken away. **12.** Close-up of area identified by rectangle in fig. 11 enlarged, showing fragment of broken chorion with pores on inner surface of micropylar area that had been covering mandibular apices, hypopharynx, and one maxilla (for explanation, see text). **13.** Close-up of a head of first instar. **14.** Spiracle and row of fine, sharply pointed spicules running above spiracular line. **15.** Close-up of spicules identified by rectangle in fig. 14 (for explanation, see text). **16.** *Monoeca haemorrhoidalis*, probably third instar on top of provisions.

adhered to the wall, but later clearly consuming the lining. Inspection of cell walls and direct observations of live specimens collected in January 2005 indicate that the amount of lining removed by the larvae varies among cells. In some cases, only a few portions of the lining showed bite marks, while in others, the entire lining covering the bottom three-fourths of the cell was removed.

After provisions were entirely consumed, larvae of *Monoeca haemorrhoidalis* started to spin their cocoons, all of which occupied the lower (rear) end of the cells (fig. 10). Completed cocoons had the following dimensions: length measured from middle of the truncated upper end to the bottom (rear), 14.0–18.0 mm ($\bar{x}$ = 15.7 mm, N = 8); maximum diameter, 9.0–9.5 mm ($\bar{x}$ = 9.1 mm, N = 8); diameter of top, 7.0–7.5 mm ($\bar{x}$ = 7.1 mm, N = 6). Thus, considerable empty space (figs. 10, 23) remained between the top of the cocoon and the cell closure, a distance that measured 7.0–10.0 mm (N = 4). In most cells, mold hyphae grew in this space after cocoon construction (fig. 23). These brown hyphae grew from fine, whitish hyphae covering the bottom part of the cocoon, apparently developing on the bee feces. They grow over the cell wall, extending through the cell plug all the way to the lateral tunnel, where they produce dark spherical bodies (spore-producing bodies?). Similar mold hyphae were found in association with cocoons of *Tapinotaspoides serraticornis* by Rozen (1984b). The nearly ubiquitous presence of the hyphae in *Monoeca* cocoons and the position of the putative fruiting bodies, facilitating the contact of the emerging bees with the spores, suggest a strong, possibly mutualistic association.

Cocoons were elongate, occupying and conforming to the shape of the lower end of their cells. In side view, one side curved outward and the opposite side was nearly straight since it conformed only to the lower part of the cell (figs. 10. 17). The top of the cocoon was planar, with the perimeter usually slightly raised as a soft rim. The plane of the top angled downward so that the surface slanted toward the straighter side of the cocoon.

The entire cocoon, except for the top, consisted of an outer layer of fine, brown, silk fibers and an inner layer of thin, fenestrated sheets of fibrous silk intermixed with feces. The inside of the inner layers was coated with feces. On older cocoons, the inner surface was often blackened, perhaps resulting from bacterial action on the feces. When moist (i.e., when first excavated), the cocoon fabric had a soft, feltlike texture, which hardened on drying. The fabric of the cocoon was moderately thin in contrast to the thicker fabric of the *Protosiris* cocoon (see description of *Protosiris* cocoon, below).

The top of the cocoon (fig. 18) consisted of several fenestrated layers of silk well separated from one another but connected by a loose network of strands. Feces were not incorporated in this part of the cocoon, and the fabric was sufficiently open so that light was transmitted through the top end when it was held between a light source and the observer. Apparently, variation exists in the nature of the innermost layer of silk on the top. In one specimen this layer was a fine, transparent sheet of silk. However, in other specimens the two-dimensional, sheetlike material was absent, and a multidirectional network of individual strands existed. The latter appeared to be the more usual construction. Feces, while not occurring within the fabric at the top end, are dabbed on the margins to the inner surface of this end, though not usually on the center.

On eclosion, *Monoeca haemorrhoidalis* adults destroy the tops of the cocoons altogether so that only the sidewalls and bottoms of the cocoons remain (fig. 21). This contrasts with egress of adults of *Protosiris gigas*, a more slender bee, in which the outer rim of the top of the cocoon remains mostly intact while the center of the top is destroyed (fig. 22).

Monoeca haemorrhoidalis has a single generation per year. A sampling of the cocoons still containing live *Monoeca* offspring from 2002 was made at the nesting site on December 11, 2003. These cocoons contained 19 males (12 live adults, 7 live pupae), 11 live females (1 live adult, 10 live pupae), and 10 live postdefecating larvae, the sexes of which could not be determined. Obviously, the males were further advanced in their development than were the females, the pu-

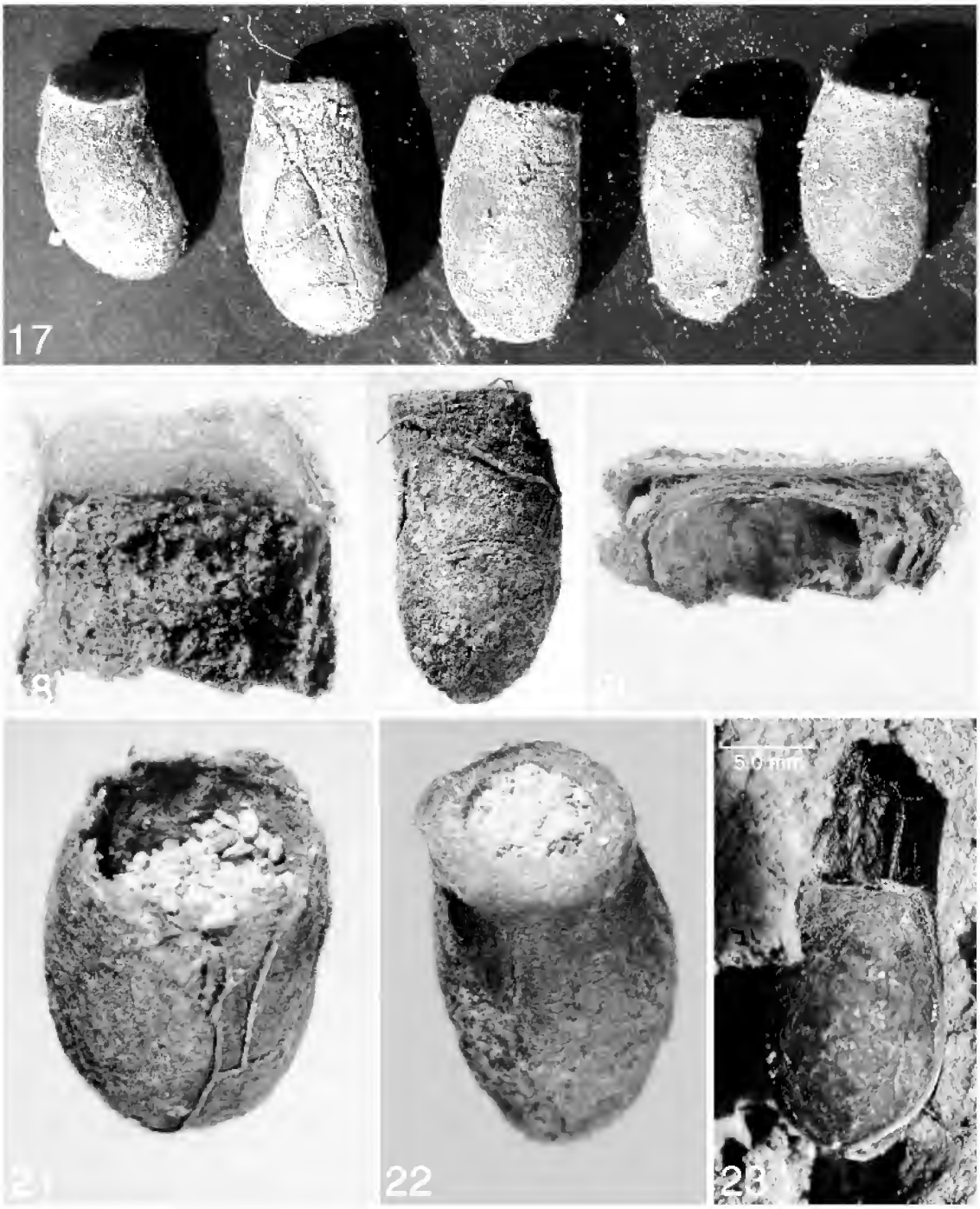

Fig. 17. Cocoons of *Monoeca haemorrhoidalis*, side view, showing variation in size and shape, front ends up. **Fig. 18.** Cross section of top of cocoon of *Monoeca haemorrhoidalis*, demonstrating loose arrangement of silk. **Fig. 19.** Cocoon of *Protosiris gigas*, side view. **Fig. 20.** Cross section of top of cocoon of *Protosiris gigas* showing dense layers of silk. **Fig. 21.** Cocoon from which adult *Monoeca haemorrhoidalis* has emerged (for explanation, see text). **Fig. 22.** Cocoon from which adult *Protosiris gigas* has emerged (for explanation, see text). **Fig. 23.** Cell and cocoon of *Monoeca haemorrhoidalis* showing space above cocoon with blackened mold hyphae.

pae of which tended to be not fully pigmented. The adults and pupae would have emerged later in the season, but we cannot be certain if the postdefecating larvae would have. If not, then, this would seem to be a case of parsivoltinism (Torchio and Tepedino, 1982).

Aguiar et al. (2004) presented a synopsis of the nesting biology of tapinotaspidine bees, including the biology of *M. haemorrhoidalis* presented here. Interestingly, the physical properties of the cell lining of *M. lanei* were as described above for *M. haemorrhoidalis*. As with that species, a piece of the lining from the previous investigation (Rozen, 1984), preserved in the collections of the American Museum of Natural History for the last 30 years, was melted on a glass slide placed on a warm hotplate. Despite the similarities in the cell linings, females of *M. lanei* do not have an indication of an epidermal gland on T6, as noted above.

BIOLOGY OF *PROTOSIRIS GIGAS* MELO

Protosiris gigas is a cleptoparasite of *Monoeca haemorrhoidalis*. Males and females were in abundance at the nesting site, immatures (eggs, larvae, and pupae) were recovered from host cells, and cleptoparasitic females were occasionally encountered in the host nests.

The similar appearance of males and females of *Protosiris gigas* in flight at the nesting site and the great abundance of males made it impossible to observe the female host-nest searching behavior. Males of *Protosiris gigas* were found in the late afternoon sleeping while clinging to leaves and stems of bushes adjacent to the site. With wings plated over their bodies, they clung to the vegetation holding on only with their mandibles (fig. 24). Females, few in number during our observations, were not observed sleeping, but they too probably sleep holding onto the vegetation with their mandibles. The abundance of males of this species at the site left little doubt that males were searching for females and that copulation occurred there.

We noticed no interaction between adults of *Monoeca haemorrhoidalis* and *Protosiris gigas* at the nest site; they seemed oblivious of one another.

Invariably, when we encountered parasitized cells that retained the cell closure, we found that the *Protosiris* female had created a large hole in the center of the spiral closure. Thus, this cleptoparasite attacks cells after they have been sealed by the host female. After the female *Protosiris gigas* oviposited, she plugged the hole with seemingly loose soil (figs. 5, 6) in each case. Three of these holes, roughly circular, measured 3.3 × 4.0, 3.5 × 3.75, and 2.5 × 3.5 mm. Host immatures (eggs or early instars) were found dead in cells containing unhatched *Protosiris* eggs on seven occasions. It therefore seems clear that the female cleptoparasite is primarily responsible for killing the host immature. The behavior and anatomy of the first-instar *Protosiris* indicate that it too can kill the host immature, should it survive the attack by the adult cleptoparasite.

Although not fully understood, eclosion of *Protosiris gigas* is different from that of the host, described above. Instead of being pharate, the first-instar *Protosiris* is active and crawls away from the chorion. A preserved first-instar specimen (fig. 28), studied with an SEM, showed it emerging from an opening at the anterior end of the egg while the longitudinally shriveled chorion with posterior end intact was left behind. A jagged rent (indicated by arrows in fig. 28) seemed to occur along one side of the chorion and may be comparable to the lateral longitudinal splitting of the *Monoeca* chorion along the spiracular line. A similar tearing of the chorion on the opposite side could not be certainly detected but may have been there. We were unable to identify a linear series of small spines or the spiracles on the specimen studied with the SEM, and a cleared specimen in glycerin examined with a compound microscope showed no such linear series even though the spiracles were clearly visible. Thus, it seems unlikely that the linear series of spines exists on this species.

The question remains how does the female *Protosiris* kills the immature *Monoeca*. Two ways have been documented by which a female cleptoparasitic bee eliminates the host offspring: (1) The cleptoparasite female opens the cell and kills the host immature

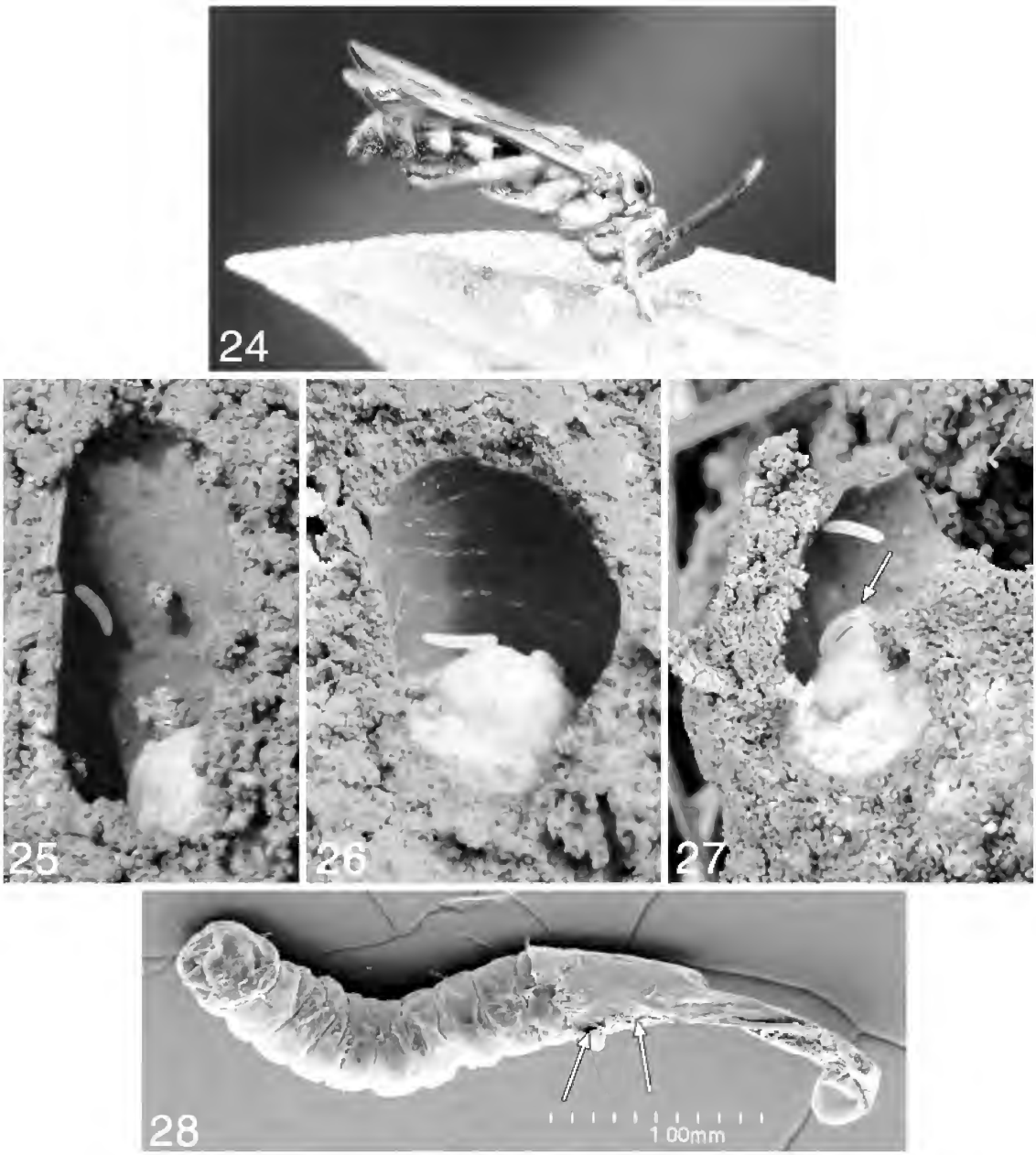

Fig. 24. Sleeping male *Protosiris gigas* with wings plated, holding onto edge of leaf with mandibles; forelegs not normally involved with grasping substrate. **Figs. 25–27.** Eggs of *Protosiris gigas*. **25.** On cell wall; note dead second instar of *Monoeca haemorrhoidalis* below. **26.** On summit of provisions; note egg of *Monoeca haemorrhoidalis* on provisions. **27.** Attached by posterior end to cell wall; note (arrow) droplet of liquid on dorsal anterior surface of host egg (for possible explanation, see text). **Fig. 28.** SEM micrograph of first instar of *Protosiris gigas* preserved as it was emerging from chorion; two arrows on side of chorion point to presumed tear in chorion.

with her mandibles (Bennett, 1966, for *Hoplostelis bilineolata* (Spinola); Bennett, 1972, for *Exaerete dentata* (Linnaeus)); and (2) the cleptoparasite female makes a small opening in the side of the host cells using her mandibles, reverses her position, and kills the host egg with her metasomal apex (Garófalo and Rozen, 2001, for *Exaerete smaragdina* (Guérin-Méneville)). All other known adult cleptoparasitic Apidae that introduce their eggs into sealed host cells do not kill the host offspring, but rather they have larvae that are hospicidal at one stage or another (Rozen, 2003: table 1 and references therein).

In the case of *Protosiris gigas*, indirect evidence supports the hypothesis that the female uses her metasomal apex, and perhaps the sting, to kill the *Monoeca* egg or early instar. A total of 5 eggs (and one shed chorion) of *Protosiris gigas* were found attached to cell walls approximately halfway between the cell closure and the top of the provisions (figs. 7, 25, 27), proof that the female must be able to extend her metasoma through the hole in the cell closure. In all of these instances, the host immatures (4 eggs, 1 second instar) were clearly dead, showing loss of turgor or even being misshapen, but none was removed from its normal position on the food mass, as might have been the case if it had been killed by the mandibles of the *Protosiris* female. Also, none was missing, as if it might have been eaten by the cleptoparasite. Because we found another 5 live *Protosiris* eggs at various locations on the provisions (e.g., on the summit, fig. 26; on the periphery), egg placement by *Protosiris gigas* may be variable, or the eggs may have originally been attached to the wall and the attachments failed, sending them onto the surface of the provisions.

On two other occasions a seemingly live host egg with an apparent fine puncture exuding a droplet of yellowish fluid on its anterior dorsal surface was noticed in a cell with a live *Protosiris* egg (fig. 27). This may have resulted from a puncture created by the parasite female's sting. We perhaps encountered these cells shortly after they had been attacked, so that the host eggs had not yet lost their turgor.

We reject the hypothesis that the female *Protosiris* used her mandibles to kill the host immature, both because there is no evidence that the *Monoeca* immatures were dislodged or missing from their normal positions and because it is doubtful that the opening of the cell closure made by the female would have been sufficiently large to allow her to reach into the cell. Furthermore, it seems unlikely that the *Protosiris* female would then reposition herself to attach her egg to the cell wall.

However, is it reasonable to think that the sting (and metasomal apex) of the *Protosiris* female can reach the host egg, that is, to the level of the top of the central mound of the provisions? In the laboratory, we measured the maximum metasomal diameter and the length of the female metasoma from the petiole to the apex of the sting on two dead females with the metasomas fully extended. In both cases, the maximum metasomal diameter was 3.0 mm, and the distance from petiole to sting apex was 15 mm. The size of the actual holes in the cell closures (given above) would certainly permit the metasomas to extend into the lumen of the cell. Three measurements of the distance between the cell closure and the top of the provisions were 12, 14, and 15 mm. We conclude partly on the basis of these distances that the female *Protosiris* probably inserts her entire metasoma through the hole in the cell closure so that the sting can damage the host egg or larva. At this time the cleptoparasite presumably places her egg on the cell wall (or drops it onto the provisions). This conclusion is also partly based on the fact that the evidence does not point to any other explanation.

The sting apparatus of *Protosiris gigas* is elongate relative to body size, presumably an adaptation for reaching the host egg and depositing its own, with the sting shaft, gonostyli, first and second rami, and furcula being longer than those of most of other bees. However, these structures are not as long as those of the related *Osiris* (Packer, 2003).

Certain matters, however, remain unclear. Might the posterior part of a female's mesosoma also be inserted through the cell closure, enhancing her ability to reach the host immature? How does the female manage to penetrate the thick soil-filled closure, or does she only reach the closure prior to the lateral

being filled? How does she position her legs when she extends her metasoma?

A host cell containing a dead *Monoeca* second instar and a live *Protosiris* egg (fig. 25) indicated that a parasite female can gain access to a cell that has been closed for some time after cell closure. Whether she is able to penetrate a soil-filled lateral is unknown. The presence of a live *Protosiris* first instar with a dead *Protosiris* egg in another cell indicated either that a cell can be attacked sequentially by two parasite females or (less likely) that one female parasite may places two eggs in a cell at a time.

In two cells in which the *Protosiris* egg was attached to the wall, the attachment was clearly by its posterior end (one egg so attached projected into the cell lumen at nearly a right angle to the cell wall; fig. 27). In all other cases cleptoparasite eggs seemed attached by their full lengths to the walls. SEM examination of an egg (fig. 76) did not reveal any special modification of the sculpturing of either the posterior end or other surfaces that might function to hold the egg to the wall. In the distantly related Melectini, which attach their eggs to the cell closures or upper cell walls by their posterior ends, the surface sculpturing of this end is quite different from the rest of the chorion (Rozen and Özbek, 2003: figs. 63, 65; 2005: fig. 11), being possible adaptations to enhance attachments to cell surfaces.

The chorion left behind by a newly emerged *Protosiris* larva was carefully examined for remnants of a cast first-instar exoskeleton. Since none was detected, we concluded that the active larva next to the chorion was the first instar (the five larval instars of this species are differentiated and described below). All first instars found were active and agile. One was observed crawling over the surface of the provisions and returning several times to chew at the remnant of the host egg. This larva was observed clinging to the substrate with the venter of the last three abdominal segments and raising the anterior part of its body until its body looped backward so that its head was posterior to its abdominal apex. The narrow, transverse anterior folds on the venter of abdominal segments 3–7 (see fig. 78) may assist the larva in this maneuver by providing extra ventral integument to elongate the larva's backward reach. With a microscope, we observed a larva crawling upside down on a glass surface. We saw that these folds also permitted the larva to crawl forward; as the abdominal apex pushed against the substrate, the larva's preceding segments stretched, one after another, so that the anterior end of the larva moved forward. The larva evinced no special structure (pygopod) at its abdominal apex to accomplish this, although the ventral surface of the larva including that of the abdominal apex was spiculate.

Although the female *Protosiris* presumably usually kills the host egg (or larva), the first-instar *Protosiris* seems perfectly capable of killing a host immature. We observed a first instar repeatedly attacking a dead host immature. Another attempted to bite the tip of a pin when teased, and it repeatedly opened and closed its mandibles as it searched the air for the pin. The anatomy of the head with its sharply pointed, strongly curved mandibles (figs. 77, 79–81) also indicates that the larva is capable of killing the host egg or larva. It is likely that the evolutionary driving force for these behavioral and anatomical adaptations is the need to be able to battle other cleptoparasites in the same cell rather than for host killing. In the case where a dead *Protosiris* egg and a live first-instar *Protosiris* were found together in a cell, we cannot be certain whether the egg was killed by the first instar or by the second *Protosiris* female to find the cell. Both scenarios are possible. We also observed a third-instar *Protosiris* responding to our probing forceps by turning its head in the direction of the attack and repeatedly opening and closing its sharply pointed mandibles (fig. 83) (see Other Larval Instars of *Protosiris*, below). Thus, this aggressive behavior appears to continue beyond the first stadium and indirectly implies that the successful ownership of the provisions may go undecided for the duration of several stadia. Interestingly, Garófalo and Rozen (2001) reported that the female of the distantly related cleptoparasite *Exaerete smaragdina* also normally destroys the host egg and that her offspring (but the second and not first instar) also are capable of battling with other cleptoparasites or with a host immature that might have survived.

Cocoons of *Protosiris gigas* (fig. 19) resemble closely those of the host externally. They are tan and composed of fine silk strands, and they have the same shape and adhered closely to the lower part of the cell. They exhibited the same planar, truncated top surface of the *Monoeca* cocoon. They have the following dimensions ($N = 5$): length, 14.5–18 mm ($\bar{x} = 16.3$ mm); maximum diameter, 8.0–9.0 mm ($\bar{x} = 8.6$ mm); diameter of top, 6.0–8.0 mm ($\bar{x} = 6.9$ mm).

The cocoon wall (i.e., except for the top) in cross section appeared thicker (at least on fresh, moist specimens) than that of *Monoeca haemorrhoidalis*. This was probably due to the fact that the cocoon consisted of three layers: an outer silken layer, an inner silken layer, and in between a layer composed of numerous fine sheets of silk sandwiching the entire meconial mass. Consequently, the inner surface of the cocoon exhibited no feces, contrasting with the cocoon of the host. Another noticeable difference between the host and parasite was in the tops of their cocoons. The cocoon top of *Protosiris* consisted of numerous densely layered fibrous sheets of silk (fig. 20), so that when held in front of a light source, no light penetrated through the top. Thus, the top is thicker, denser, and stronger than that of *Monoeca*. The open, meshlike outer surface of the *Monoeca* cocoon that loosely attaches to the inner surface is replaced in *Protosiris* with a sturdier fabric, the top surface of which is not easily compressed. On drying, the cocoons of both species shrink; the strong, dense disc of the top of the *Protosiris* cocoon shrinks less, giving the upper part of the cocoon a slight hourglass shape. On eclosion, the *Protosiris* adult does not demolish the top (front) end of the cocoons, as is characteristic of *Monoeca*; instead, the emerging adult chews its way out of the cocoon by burrowing through the middle of the top, leaving the periphery in place (fig. 22).

Although the ratio of *Monoeca haemorrhoidalis* to *Protosiris gigas* flying over the nesting site on December 4, 2003, appeared to be roughly 1:1, G.A.R.M. and A.A. inventoried the cells on January 24, 2003, when the site was quiescent. They recovered cells of 87 *Monoeca*, 8 *Protosiris*, and 28 containing *Tetraonyx* (*Paratetraonyx*) *distincticollis* Pic (Meloidae) (adults of which were tentatively identified by Dr. John Pinto).[6] When G.A.R.M. and A.A. sampled the nesting site on January 17, 2004, 96 cells contained *Monoeca* (36 eggs and active immatures + 60 postdefecating larvae in cocoons), 8 *Protosiris* postdefecating larvae in cocoons, and 25 *Tetraonyx distincticollis* and yielded a host/cleptoparasite ratio of approximately 11:1. The discrepancy between this ratio and the estimated ratio of 1:1 based on flying adults on December 4, 2003, was caused by the earlier emergence of the cleptoparasite compared with that of the host, by a briefer period of emergence of the parasite compared with a longer emergence period of the host, by host females being away foraging while the parasites were concentrated at the nesting site, or by some combination of these phenomena. There is a selective advantage for a host to prolong its emergence so that it outlasts the seasonal activity of the cleptoparasite. Data obtained in January 30, 2005, revealed an even lower host/cleptoparasite ratio: 63 cells contained *Monoeca* (17 predefecating larvae + 46 postdefecating larvae in cocoons, 6 of them dead), 2 *Protosiris* (1 dead larva and 1 dead male imago in their cocoons, both apparently from the previous season), and 2 *T. distincticollis*. The few cells containing young immatures had no indication of parasitism by *Protosiris* (only one cell had a young meloid larva).

[6] John Pinto, in an e-message sent after he had received adults of the beetle for identification, wrote: "They are of the genus *Tetraonyx*. Using the Selander and Martinez (1984) key to the Argentinian species, they fall at *T. distincticollis* Pic. It currently is the only species in the subgenus *Paratetraonyx* Kaszab, a poorly differentiated subgenus of questionable validity. S & M apparently never saw this species and simply used the literature to incorporate it into their key. It is not well known at all—recorded from Argentina (no localities specified) and, originally, from the state of Santa Catarina, Brazil.

Tetraonyx is an enormously complex genus; with about 101 named species, almost all of them from South America. Except for the faunal review of Selander and Martinez for Argentina, all we have is an 1879 publication of Haag-Rutenberg. I mention this because the taxonomy of the genus is in dire need of revision, and I don't know the group particularly well. Thus, the species identification has to be considered tentative."

Fig. 29. Nesting area (bank, middle background) of *Lanthanomelissa betinae* on campus of Universidade do Extremo Sul Catarinense, Criciúma. **Fig. 30.** A.A. looking at sloping nesting area of *Lanthanomelissa betinae* on the campus of Universidade Federal do Paraná, Curitiba.

BIOLOGY OF *LANTHANOMELISSA BETINAE* URBAN

The nesting biology of this species was original described by Sakagami and Laroca (1988) under the name of *Lanthanomelissa goeldiana* (Friese) from a nesting site in Castro, Paraná, Brazil. Urban (1995) assigned two females from that nesting site as paratypes of *L. betinae* when she described the species.

Our observations are from notes we gathered primarily on the campus of the Universidade do Extremo Sul Catarinense, Criciúma, in 2002 and 2003, although information observed at the Curitiba nesting site was similar. At both localities, burrow entrances were discovered on sloping surfaces (figs. 29, 30) close to grassy areas where the floral oil/pollen plant *Sisyrinchium micranthum* Cav. (Iridaceae) grew. Although both sites were ecologically degraded because of campus landscaping and lawn maintenance, adult bees also occurred at other localities with relatively unaltered landscapes. The presence of this bee on these campuses was possible because of the persistence of *Sisyrinchium* under such situations.

Early in the 2002 season in Curitiba, we observed males of *Lanthanomelissa betinae* patrolling flowers of *Sisyrinchium* and *Cuphea gracilis* Koehne (Lythraceae) and sleeping in aggregations when females were not yet present (thus indicating protandrous emergence). Fifty-eight sleeping male aggregations of *L. betinae* were sighted between October 13 and December 18, 2002, all of them along the bank where we found the nests (fig. 30). Most sleeping male aggregations were 10–80 cm above the ground, on the top leaves of four herbaceous plant species: *Chromolaena hirsuta* (Hooker and Arnott) R.M. King and H. Robinson (N = 27), *Eupatorium laevigatum* Lamarck (N = 3), *Chromolaena pedunculosa* (Hooker and Arnott) R.M. King and H. Robinson (N = 18), and *Solidago microglossa* de Candolle (N = 4) (Asteraceae). Few other males were found between the inflorescences of *Cuphea gracilis* (N = 3) and *Taraxacum officinale* G.H. Weber ex Wiggers (Asteraceae) (N = 2). The largest number of the males was observed on October 26, 2002, when 166 males were counted, distributed in 24 aggregations (μ = 6.91 $\pm$ 13.2). The largest sleeping aggregations were observed in *Chromolaena hirsuta* (N = 3; maximum numbers, 53, 39, 39) and *Solidago microglossa* (N = 1; maximum number, 18). Male activity started to drop by early November and ceased after mid-December. Females presumably slept in their nests.

Males were also previously found by I.A.S. in Criciúma sleeping on flowers of Asteraceae and in flowers of *Petunia integrifolia* (Hook.) Schinz and Thellung (Solanaceae). On Asteraceae, they were just resting

on the flowers with their head partly inserted into the flower. In Rio Grande do Sul, she once observed five males sleeping end-to-end around the ovary at the bottom of the corolla of *P. integrifolia*.

Nests, each occupied by a single female, were compact (maximum lateral spread of cells at most ca. 10 cm) and shallow (maximum depth ca. 15 cm) with cells close to one another. Dry tumuli (ca. 3.5 mm in diameter) were on the downhill side of entrances. Open entrance tunnels descended obliquely with some turning. Burrow walls were nonreflective and had no special lining. Cells were elongate ovals, 7.0–8.0 mm in maximum length and 4.5–5.0 mm in maximum diameter (based on actual measurements and on cocoon dimensions); thus, their lengths were somewhat more than 1.5 times their maximum diameters, contrasting with the elongate cells of *Monoeca haemorrhoidalis*. All were arranged singly (i.e., not in linear series). They were broadly rounded at the rear end, and their maximum diameter was one-third the distance from the rear end, forward from which they narrowed gradually to the front entrance, which was ca. 3.0 mm in diameter. Cells seemed to be radially symmetrical around their straight long axis, with one side not being straighter than the opposite one, contrary to the cells of *Monoeca* as described above. However, the true symmetry of the cells of *Lanthanomelissa* may have been obscured by their small size. Cell closures on the inside were a deep concave spiral of 3–4 coils.

The long axes of cells ranged from 35 to 80° from horizontal, with the front of the cell always higher than the rear. Cells possessed a conspicuous, waterproof, grayish lining beneath which the cell wall appeared dark, but whether the color resulted from mechanical compression of the substrate or from some applied substance (e.g., floral oils, glandular secretions) is unknown. When cell fragments dried, the lining tended to crack, but flakes could not be easily removed from the wall. When the lining was heated on a glass slide on a hotplate, it did not melt, as did the lining of the *Monoeca* cells. The source of the lining material is unknown. Laterals were of various lengths, with the shortest being ca. 1 cm long; all were filled with soil after cell closure.

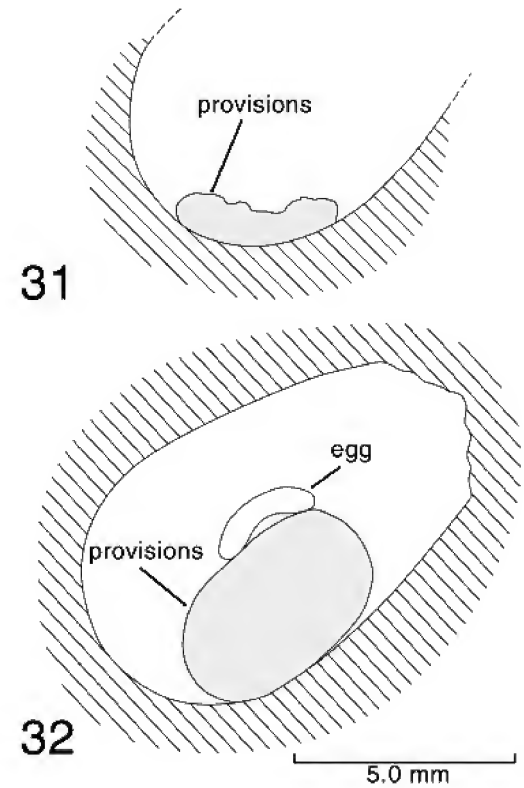

Figs. 31, 32. Cells of *Lanthanomelissa betinae*, diagrammatically represented. **31.** Early load of provisions. **32.** Egg on completed provisions in closed cell. Scale bar = 5.0 mm.

The first provisions brought into a cell were placed as an unshaped mass occupying the bottom of cell (fig. 31). The final provisions were shaped as an elongate, mealy-moist loaf, in one case 4.2 mm long and 2.8 mm high (fig. 32). When newly formed, the loaf was, at least in a few cases, attached by its ventral or posteroventral surface to the cell wall, so that the rear surface was separated from the rear of the cell, and sometimes the anteroventral surface was also separated from the cell wall (fig. 32).

The female deposited her egg on the top surface of the provisions near the front end (fig. 32). Young larvae crawled over the loaf while feeding, and intermediate-stage larvae circled the food mass, which had by this time slumped in the cell so that its posterior end became attached to the rear end of the cell.

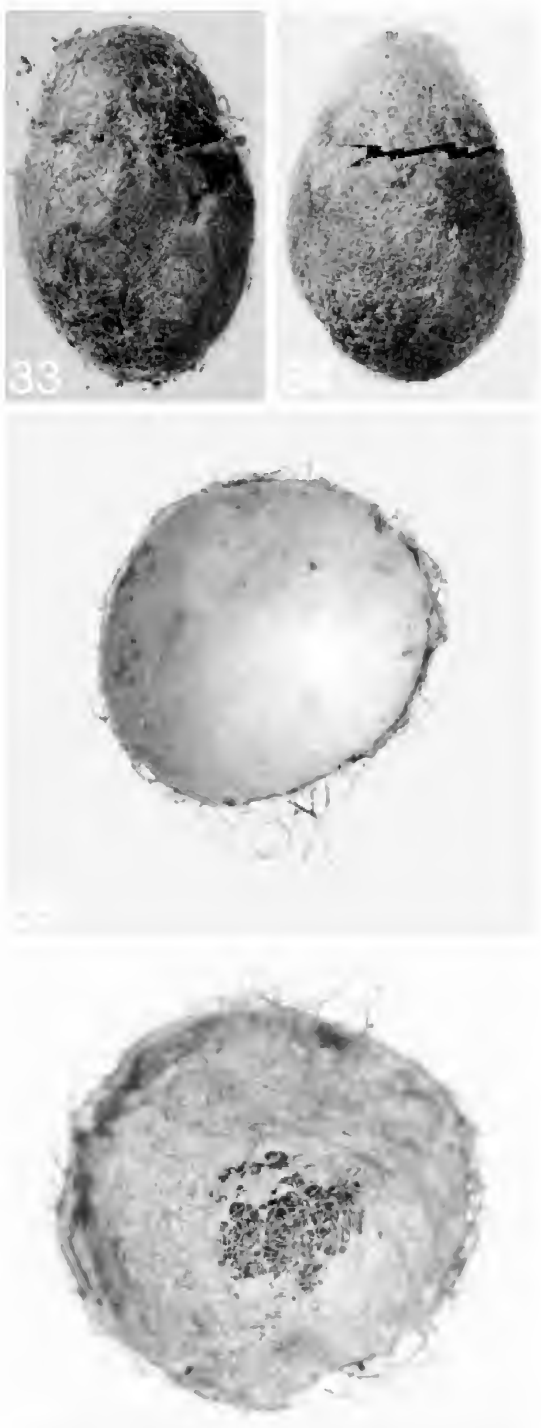

Fig. 33. Cocoon of *Lanthanomelissa betinae* from which larva had been removed, lateral view. **Fig. 34.** Cocoon of *Parepeolus minutus* from which larva had bee removed, lateral view. **Fig. 35.** Inner surface of front end of cocoon of *Lanthanomelissa betinae* showing complete covering by pale feces. **Fig. 36.** Inner surface of front end of cocoon of *Parepeolus minutus* showing central area that is not coated by feces.

Provisions at this time developed a central peak as the feeding larva circled the periphery with its dorsum against the cell wall. Information on the larva's final feeding position was not noted.

Externally brown, the cocoon of *Lanthanomelissa betinae* was 7.0–7.4 mm long ($\bar{x}$ = 7.3 mm) and 4.5–5.0 mm in maximum diameter ($\bar{x}$ = 4.8 mm) (N = 7). Each filled the entire cell and had a shape (fig. 33) identical to the inner topology of the cell (i.e., broadly round at the rear end), tapering forward from its maximum diameter to the narrowly rounded or faintly truncated front end. All but the front end of the cocoon was composed externally of fine, densely appressed silk strands. The anterior end consisted of coarser silk strands, openly and loosely arranged (thus, far less dense than elsewhere). The entire inner surface of the cocoon including the front end (fig. 35) was coated uniformly with a smooth layer of pale, almost white feces. Thus, in cross section, the cocoon consisted of two layers, a brown, silken outer layer (with the front end more open and less dense than elsewhere) and a somewhat thinner inner layer of feces.

The cocoons of *Lanthanomelissa betinae* and *Monoeca haemorrhoidalis* were similar in that their walls conformed to the similarly shaped cells, and both were composed of dense, fine, brown silk on the outside. However, they differed in a number of distinctive ways irrespective of dimensions: (1) Cocoon symmetry reflected the shape of the cell; thus, the cocoons of *L. betinae* appeared roughly radially symmetrical around their long axes whereas those of *M. haemorrhoidalis* were bilaterally symmetrical. (2) Whereas the front end of the cocoon of *M. haemorrhoidalis* was sharply truncated, with the periphery usually being accentuated by a slightly elevated rim, the front end of the cocoon of *L. betinae* was narrowly rounded, although on some specimens a small, flattened anterior surface was discernable. (3) Al-

though both taxa start spinning their cocoons before the onset of defecation, *L. betinae* spins its entire cocoon before applying feces to the inner surface. *Monoeca haemorrhoidalis* continues to spin layers of fiber while defecating, so that the feces are incorporated into the fabric of the cocoon as well as on the inner surface of the completed silken cocoon. (4) Feces of *L. betinae* completely cover the front interior surface of the cocoon as well as the rest of the cocoon, whereas the feces of *M. haemorrhoidalis* are incorporated throughout the cocoon except for the front surface. (5) The front end of the cocoon of *M. haemorrhoidalis* was far removed from the cell closure, whereas the front end of the cocoon of *L. betinae* approached the cell closure closely. This feature is the result of the more elongate cells of *M. haemorrhoidalis*.

Although several nests of *Lanthanomelissa betinae* with only a few cells were excavated, one nest seemed to contain 21 active cells, another had 11 cells, and a third had 9 cells. However, the first two nests mentioned included many other cells from which the adults had emerged, leaving behind vacated cocoons. This strongly suggests that these main burrows may have been used by more than one generation, a possibility supported by the fact that a single bee pupa[7] was encountered in one nest. Either the pupa was a member of the generation from the previous year or some members of the current generation may be bivoltine. So many cells in the nest favor the first alternative. Large nests contained offspring that had already constructed cocoons, freshly deposited eggs, and even open cells still being provisioned. The large range of developmental stages might be explained (assuming that only a single generation comprises the nest contents) either by a rapid development of immatures or, conversely, by a slow rate of emergence, nest construction, and provisioning. These matters cannot be determined by available data.

The observations on the nesting biology of *Lanthanomelissa betinae* (cited as *goeldiana* (Friese)) reported by Sakagami and Laroca (1988) concur with ours in that the species seems to prefer a sloping nesting surface, although the slope at their site appears to have been steeper than ours. In both cases, entrance turrets were absent, main tunnels tended to be short and remained open, and a single female inhabited each nest. Laterals tended to be short and were soil-filled after cell closure for both. Whereas cells we observed were arranged singly, they stated that cells were often in series of twos. Furthermore, they indicated that cells tended to be more vertical, whereas we found their orientation more variable, with their long axes ranging from 35 to 80° from horizontal. With both sets of observations, cell lengths were substantially less than twice their maximum diameters, and nests were quite compact and shallow because of short main tunnels and laterals. The provisions in both cases were arranged as loaves attached to the side of the cell, with eggs on the opposite surface from the attachment. They reported that intermediate larvae circled the provisions, so that they did not contact the cell wall, whereas we found such larvae circling the provisions while the food was still attached to the rear of the cell; this difference, however, may be a discrepancy in the ages of the two larvae observed. Sakagami and Laroca found no cleptoparasites associated with their nests.

The floral relationships of *Lanthanomelissa betinae* were reported by Cocucci and Vogel (2001) and Truylio et al. (2002). The latter found females of *L. betinae* to be the main visitors of *Sisyrinchium micranthum* in Rio Grande do Sul, Brazil. Roig-Alsina (1997) described the oil-collecting modifications of the foretarsus found in the genus *Lanthanomelissa*.

In an unpublished study in 1994, I.A.S. analyzed the provisions from 10 nests of *Lanthanomelissa betinae* in Rio Grande do Sul and found that all were provisioned with pollen only from *Sisyrinchium*. Thus, this bee species obtains both pollen and oil from the same plant.

[7] This pupa, a female, was badly damaged while being excavated and may have been either *Lanthanomelissa betinae* or *Parepeolus minutus*. However, the fact that the hindbasitarsus was not greatly enlarged suggests that it was the latter species. The pupa lacked mesoscutal tubercles, possessed low but distinct, paired, mesoscutellar tubercles, and an apical rows of rather large, sharply pointed tubercles on each of T2–T5, but not on T1. These are also features shared by *Monoeca haemorrhoidalis* and *Protosiris gigas*.

TABLE 1
Comparative Data on Number of Ovarioles and Number and Sizes of Mature Oocytes of Taxa in Current Study
Figures in the first three columns of figures are averages because more than one female of each species was measured. For further explanation, see section on Ovarian Statistics.

Taxon	Egg index	Total mature oocytes	Mature oocytes per ovariole	Ovariole formula	No. of specimens
Monoeca haemorrhoidalis	0.65	1	0.125	4:4	2
Protosiris gigas	0.82	2.33	0.29	4:4	3

BIOLOGY OF *PAREPEOLUS MINUTUS* ROIG-ALSINA

Adults of *Parepeolus minutus* were observed apparently searching for and entering nests of *Lanthanomelissa betinae* at the nesting areas at both Criciúma and Curitiba. Four postdefecating *Parepeolus* larvae, three of which came from one nest, were recovered from nests at Criciúma, confirming the host/parasite association. In external appearance their cocoons (fig. 34) were indistinguishable from those of the host, except that in two examples (the third was not noted) the front end of the cocoon contained no dark, slightly thicker strands of silk. However, from the inside, the cocoons of the two taxa could be immediately recognized because the fecal linings at the front ends of the cocoons of *P. minutus* were incomplete, leaving a hole through which the open silk fibers of the cocoon were easily visible (fig. 36) and light could be transmitted.

Information on the mode of parasitism of *Parepeolus minutus* is not available. Other parasites were not observed in the host nests.

OVARIAN STATISTICS

Table 1 provides comparative data on the number of ovarioles and number and sizes of mature oocytes of *Monoeca haemorrhoidalis* and *Protosiris gigas*. Although we attempted to dissect the ovaries of *Lanthanomelissa betinae* from four females, we were unable to retrieve information concerning ovarian anatomy or oocyte development, either because of poor preservation or because of unusual morphology. Females of *Parepeolus minutus* were not available for dissection.

The egg index of *Monoeca haemorrhoidalis* was 0.65, whether calculated on the basis of the length of its mature oocyte or of its egg (see Methods and Terminology for methods of calculating the egg index). This value falls in the category of *small*. The only other tapinotaspidine for which we have information is *Lanthanomelissa betinae*, reported below. This egg index, based on a single female and her egg, was 0.99, close to the upper limit of category *medium*. It is unknown if such a range in values within a single tribe of solitary bees is unusual.

The surprising statistics in table 1 are the range in values of the egg indices between *Protosiris gigas* and *Monoeca haemorrhoidalis*. Cleptoparasitic bees tend to have lower egg indices than do those of solitary bees (Rozen, 2003), but here we find that the egg length of the cleptoparasitic bees is nearly as long as that of its solitary host (compare figs. 37 and 38). The egg index of *P. gigas* is 0.82 based on the mature oocyte (table 1) and 0.86 based on a sampling of eggs from females (see Egg of *Protosiris gigas* Melo), with both values being well within the *medium* category.

We can partly account for this apparently anomalous situation in a number of ways. First, the egg of *Monoeca haemorrhoidalis* is curved and hence measures shorter than its curved length, in contrast to straighter egg of *Protosiris*. Second, the egg of *M. haemorrhoidalis* is more uniformly thick; it does not taper posteriorly, as does the egg of *P. gigas*. Third, the host, a robust bee, has a very wide mesosoma compared to its body length, whereas the cleptoparasite is slender, with a narrow mesosoma. Hence, the denominators in both calculations of the egg indices are skewed. Finally, the egg of *P. gigas* is obviously much thinner than that of its host. When the two eggs are viewed side by side

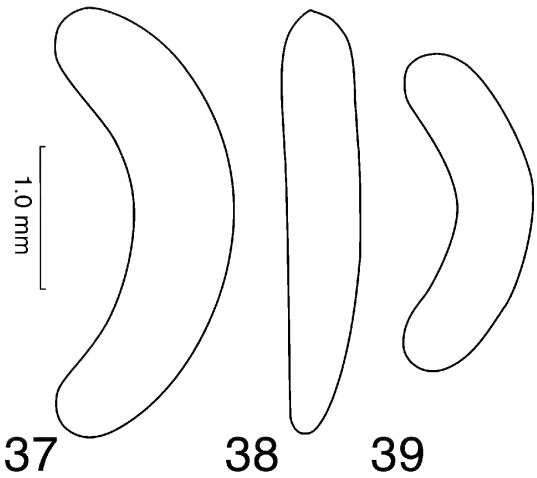

Figs. 37–39. Comparative diagrams of eggs, lateral views, anterior ends up, all drawn to same scale with camera lucida. **37.** *Monoeca haemorrhoidalis*. **38.** *Protosiris gigas*. **39.** *Lanthanomelissa betinae*.

(figs. 37 and 38), clearly the cleptoparasite has a considerably smaller egg volume. Part of the problem is with our having used egg length and intertegular distance, two linear statistics, to evaluate volume.

While this explanation may partly explain the large size of the egg of *Protosiris gigas*, other Osirini tend to have egg indices higher than those of many parasitic bees: *Epeoloides coecutiens* (Fabricius), 0.70 (*small*) (Rozen, 2001); *Osirinus lemniscatus* Roig, 0.79 (*medium*) (Alexander, 1996); and *Parepeolus aterrimus* (Friese), 0.88 (*medium*) (Alexander, 1996). Thus, it appears that osirines as a group do not have egg indices that fall into the *dwarf* category, as do many parasitic bees. Now that we know that females of *P. gigas* deposit their eggs into a closed host cell, we can probably interpret these relatively high indices as indicating that all members of the tribe invade a closed host cell for ovipositioning; as Rozen (2003) pointed out, cleptoparasitic taxa that invade closed host cells tend to have larger eggs than do those that hide their eggs in cells still being visited by host females.

The remaining statistics in table 1 are normal. Cleptoparasitic bees tend to have more mature oocytes than do solitary bees, presumably because of the need for cleptoparasites to lay eggs whenever appropriate host cells are discovered. Four ovarioles per ovary is plesiomorphic in the Apidae (Michener, 2000).

IMMATURE STAGES

In this section we describe the immature stages of *Monoeca haemorrhoidalis*, *Lanthanomelissa betinae*, *Protosiris gigas*, and *Parepeolus minutus*, respectively, to the extent that collected material permits. Most of the information presented under Methods and Terminology is applicable to this section. In the descriptions of the intermediate larval instars of both *M. haemorrhoidalis* and *P. gigas*, dates and collector names refer to exemplars that were cleared for careful study.

Egg of *Monoeca haemorrhoidalis* Smith)
Figures 7, 37, 40–42

Description: Length 2.9–3.2 mm; maximum diameter 07.3–0.75 mm ($N = 3$); egg index 0.65 (category *small*) (based on mean length of three eggs divided by mean intertegular width of five females selected at random). Shape approximately symmetrical along its strongly curved long axis; broadly rounded at both ends, anterior end slightly to distinctly wider than posterior end, widest about one-fourth length from anterior end; micropyle a tight cluster of small pores at anterior pole, these pores directed toward outcurved surface. Color nearly white. Chorion viewed through stereomicroscope somewhat shiny, much more so than that of *Protosiris gigas*. Chorion viewed by SEM without obvious patterning over most of surface but with faint polygonal sculpturing behind micropyle (fig. 41).

Material Examined: Three eggs, Brazil: Paraná, Mananciais da Serra, Piraquara, 20-XI-2002 (J.G. Rozen).

Remarks: The three eggs described above were quite similar to one another, and one of these was illustrated (fig. 37). Another egg (fig. 40) collected and preserved in 2003 was used for SEM examination and measured after being subjected to critical-point drying and coating with palladium/gold. It proved to be shorter (2.5 mm) and wider at maximum width (3.0 mm) than the others, and its posterior half tapered somewhat more than that

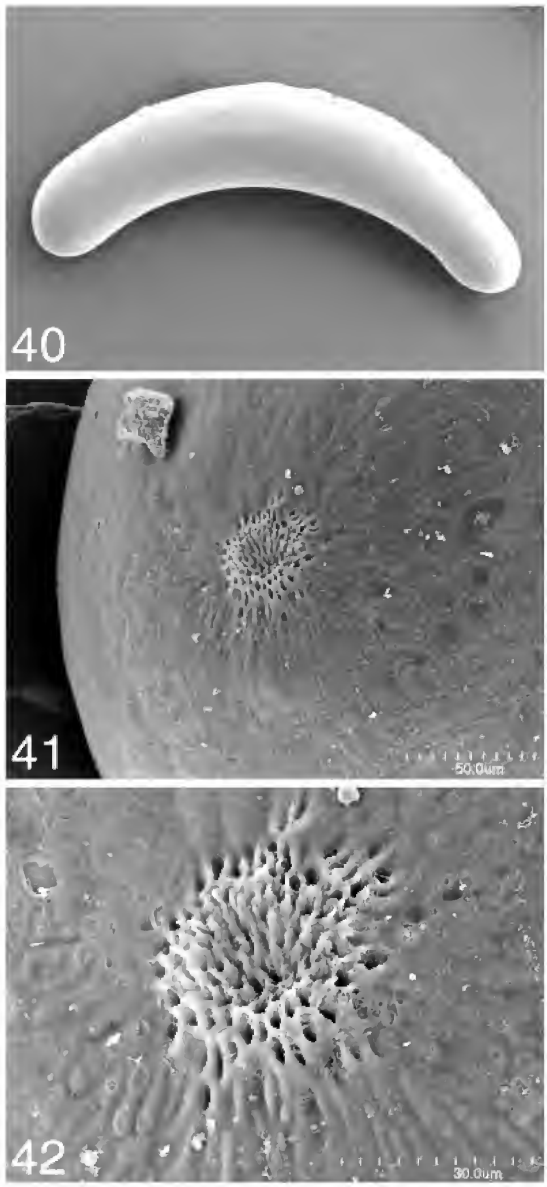

Figs. 40–42. SEM micrographs of egg of *Monoeca haemorrhoidalis*. **40.** Entire egg, lateral view. **41.** Front end, showing micropyle at anterior pole and surrounding chorion, out-curved surface toward top. **42.** Close-up of micropyle.

of the others (compare figs. 37 and 40). We are uncertain whether these differences are a result of different treatments, sex difference, or simply an error in random sampling resulting from a small sample, but we are convinced that they all represent the same species because of their identical micropylar areas observed with an SEM.

Although not examined with an SEM, an egg of *Tapinotaspoides serraticornis* in the collection of the American Museum of Natural History appears identical in shape and chorionic sculpturing to that of *Monoeca haemorrhoidalis*.

First Instar of *Monoeca haemorrhoidalis* (Smith)
Figures 11–15, 43–45

Diagnosis: The first instar of *Monoeca haemorrhoidalis*, mostly surrounded by the chorion, is unable to crawl, and has weakly sclerotized, unpigmented, broadly bidentate mandibles (figs. 13, 43, 44, 47). It therefore can be easily distinguished from the first instar of the cleptoparasite *Protosiris gigas*, which is free from its chorion, agilely crawls around the cell, and is quite capable of killing eggs or young larvae with its strongly curved, apically slender mandibles (figs. 77, 79–81).

Length: About 3.5 mm.

Head (figs. 43, 44): Integument of parietal weakly sclerotized, unpigmented; mandibular apices scarcely pigmented; head capsule and outer surface of mandibles with scattered, inconspicuous sensilla; hypopharynx, apex of maxilla indistinctly spiculate; inner apical surface of mandible more distinctly spiculate.

Head intermediate between hypognathous and prognathous (fig. 44). Tentorium moderately thin, complete; dorsal arms extremely thin; anterior and posterior tentorial pits moderate in size, normal in position; internal head ridges tending to be moderately weak except epistomal ridge weak laterad of anterior tentorial pits, absent between pits. Parietal bands absent. Antennal papilla much shorter than half basal diameter, not on projection, bearing about 3 sensilla. Frons and clypeus pronounced in lateral view (fig. 44); labrum moderately large, apically bearing low tubercles on outer corners, best seen in maximum profile; boundary between labrum and lower end of clypeus well defined.

Mandibles (figs. 43, 44, 47) weakly sclerotized, scarcely pigmented apically, basally large, stout, apically bearing flattened, sharp-

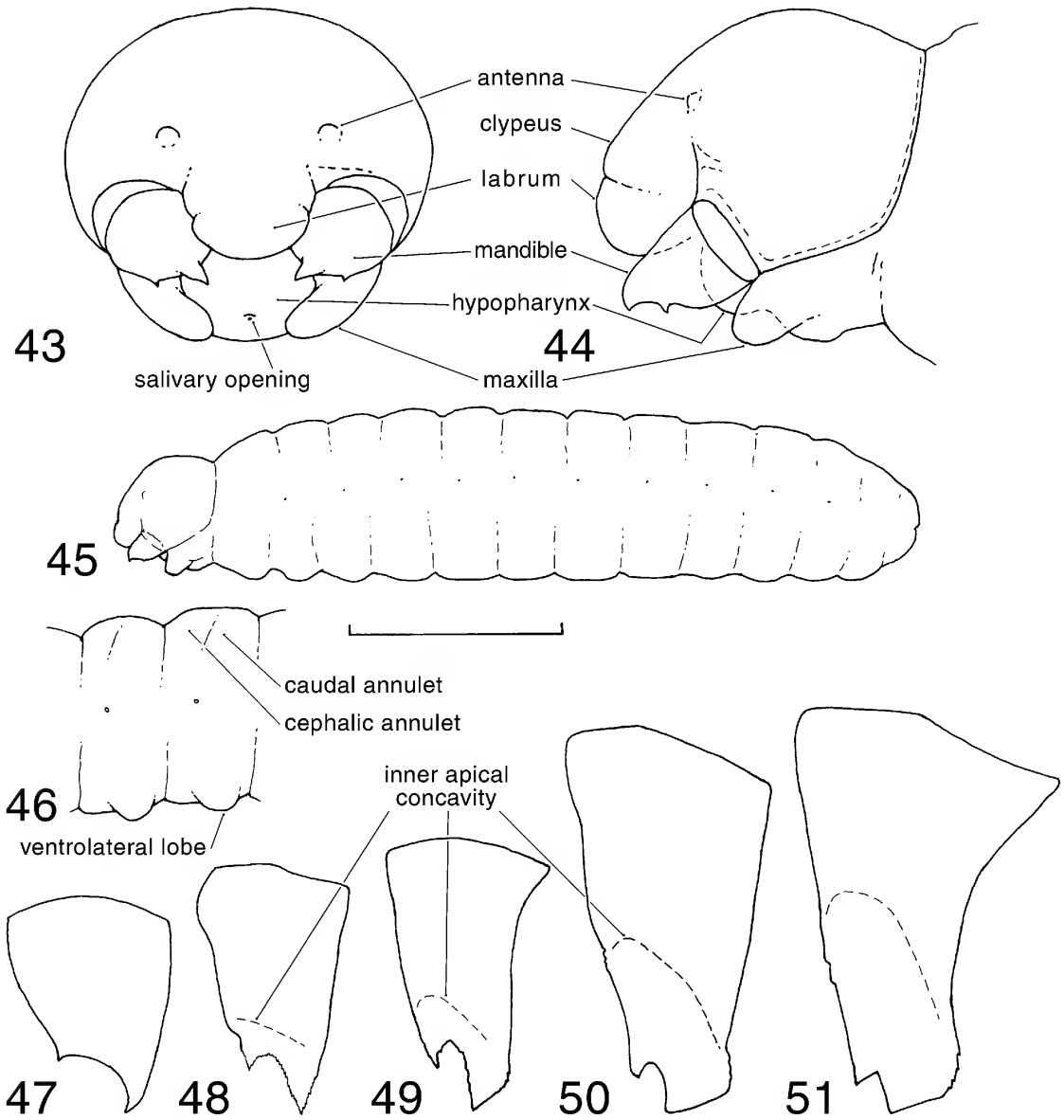

Figs. 43–51. *Monoeca haemorrhoidalis*. **43, 44.** Head of first instar with chorion removed, frontal and lateral views, respectively. **45.** Entire first instar with chorion removed, lateral view. **46.** Second instar, abdominal segments 3 (left) and 4, lateral view. **47–51.** Outer surface of right mandibles of first, second, third, fourth, and fifth instars, respectively, drawn to same scale, with apices in maximum profile. Scale bar (= 1.0 mm) refers to figs. 45, 46.

ly pointed, larger tooth and subapically bearing flattened, sharply pointed, smaller tooth; outer surface with a few fine sensilla. Each maxilla a strongly projecting, incurving lobe (figs. 43, 44); maxillary palpus not evident except presumably for inconspicuous sensilla; cardo, stipes, and articulating arm of stipes not evident. Labium greatly recessed relative to maxilla in lateral view (fig. 44); labial palpi not evident but presumably represented by inconspicuous sensilla. Salivary opening small, circular; salivary duct evident. Hypopharynx strongly projecting (fig. 44); hypopharyngeal groove faintly evident immedi-

ately above salivary opening. BODY: Integument without setae; spiculation pattern not discernable, except for faint (too fine to be depicted in fig. 45) linear pattern of granules (spicules) running longitudinally immediately above spiracular level on each side (figs. 14, 15). Form cylindrical (like that of egg) (fig. 45); intersegmental lines finely incised; body without dorsal tubercles; abdominal segments not divided dorsally into cephalic and caudal annulets and no abdominal segment ventrally with extra integumental folds; prothorax and abdominal segment 9 not protruding ventrally; abdominal segment 10 rounded posteriorly; anus apical. All spiracles present, small, coequal in diameter, more-or-less flush with body wall when viewed with stereomicroscope (but elevated when examined at high magnification with SEM, fig. 14).

MATERIAL STUDIED: 2 first instars, Paraná, Mananciais da Serra, Piraquara, 11-XII-2003 (J.G. Rozen); 2 first instars, same data except (J.G. Rozen, G.A.R. Melo, R.B. Gonçalves).

REMARKS: The lines of granules (spicules) (figs. 14, 15) extending longitudinally just above the spiracles would have been overlooked because of their faintness if we had not been aware of their possible presence from earlier studies (Alves-dos-Santos et al., 2002); they were detected only because the cleared specimen was examined with a compound microscope. Their shape and possible function are discussed in Biology of *Monoeca haemorrhoidalis*.

OTHER LARVAL INSTARS OF *MONOECA HAEMORRHOIDALIS* (SMITH)

The second instar (5-XI-2002 [J.G. Rozen, G.A.R. Melo]) is the first instar that feeds and crawls over the provisions. Because its mandibles are conspicuously pigmented apically, as are many of the internal head ridges, it can be immediately distinguished from the virtually unpigmented first instar. The antennal papilla is now nearly as long as its basal diameter, and it arises from a slight projection of the cranium. The internal ridges of the head capsule, as well as the capsule itself, are stronger than those of the first instar. The clypeus now bulges outward below the epistomal ridge in lateral view. The subapical tooth of the mandible is positioned closer to the apical tooth (fig. 48), and they are connected by a serrate ridge; the upper and lower apical mandibular edges are serrate, and the apical concavity is becoming pronounced. Maxillary and labial palpi are defined as low projections that are still much shorter than their basal diameters. The salivary opening is a transverse slit with faint papillae surrounding it, but without lips. The apex of the maxilla is strongly bent mesad of the palpus. The abdominal segments are dorsally weakly divided into cephalic and caudal annulets (fig. 46). Abdominal segments 1–9 each has a pair of ventrolateral lobes positioned posteriorly that presumably assist in crawling (fig. 46); they are densely spiculate, as is the rest of the venter including that of the thorax. By contrast, dorsal surfaces of the body appear almost nonspiculate, although widely scattered spicules may be present. The spiracular atrium is large and faintly denticulate, the true spiracular opening lacks a collar, and a peritreme is apparently absent.

The third and fourth instars (11-XII-2003 [J.G. Rozen, G.A.R. Melo, R.B. Gonçalves]) are quite similar to the second instar but, of course, become progressively larger. Figures 47–51 demonstrate the changes that take place in the mandibles from one instar to the next. With the third instar, salivary papillae appear immediately above the salivary opening and become even more pronounced on the fourth instar. The salivary opening of the fourth instar has slightly projecting salivary lips. Both instars continue to have a strongly spiculate venter, and by the fourth instar, dorsal surfaces are also conspicuously spiculate, contrasting with the nearly completely nonspiculate body integument of the fifth instar. It is only on the fifth instar (figs. 52–58) that the sclerotization of the cardo, stipes, and articulating arm of the stipes appear, as does the thickening of the cuticle of the dorsal body tubercles. The spiracular atrium becomes increasingly more clearly denticulate in the third and fourth instars, and a peritreme appears for the first time in the third instar. Although the subatrial area is differentiated from the trachea in these instars, distinct subatrial chambers do not appear until the fifth instar.

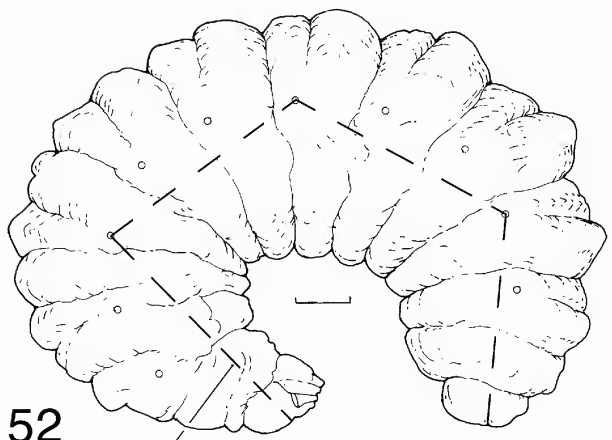

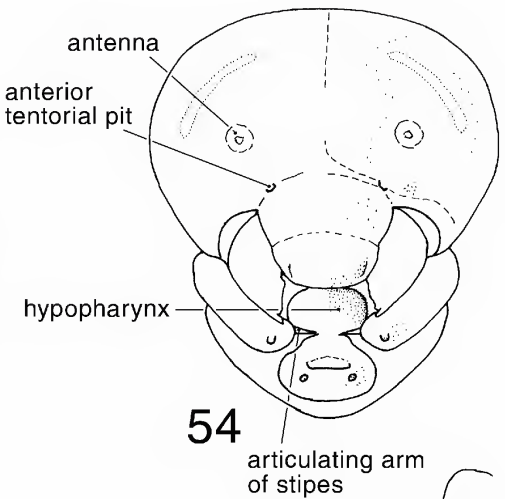

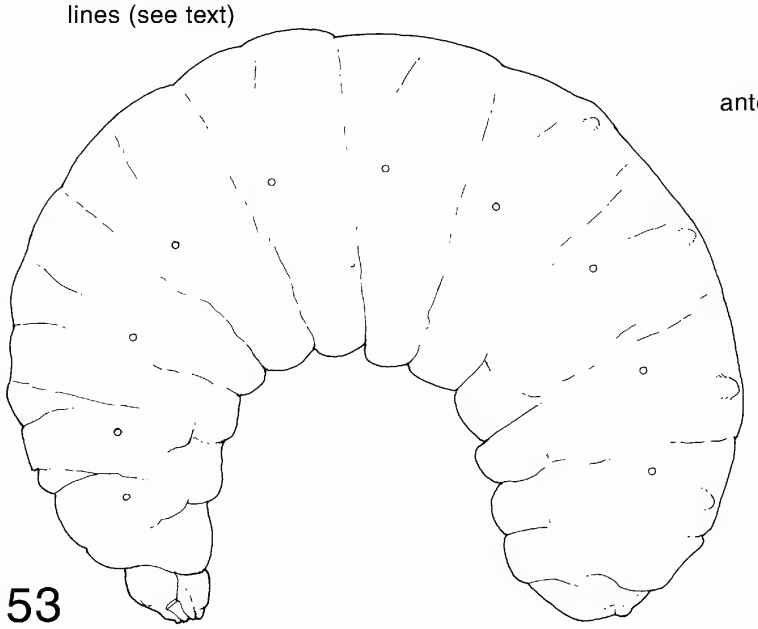

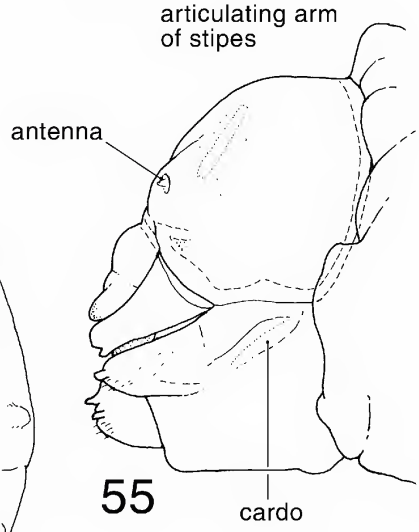

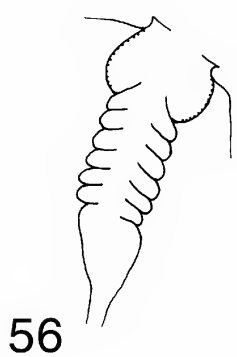

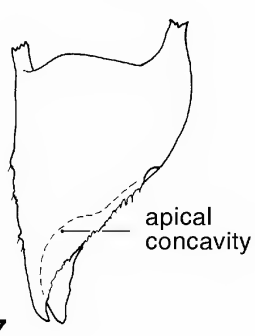

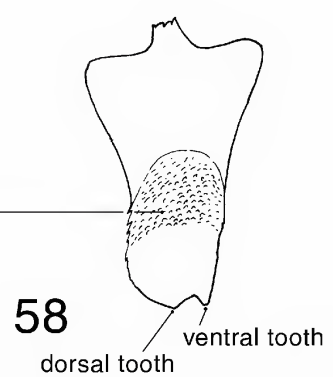

Figs. 52–58. *Monoeca haemorrhoidalis*. **52.** Postdefecating larva, lateral view. **53.** Predefecating larva, lateral view. **54, 55.** Head, postdefecating larva, frontal and lateral views. **56.** Spiracle of same. **57, 58.** Right mandible of same, dorsal and inner views. Scale bar (= 1.0 mm) refers to figs. 52, 53.

Postdefecating Larva of *Monoeca haemorrhoidalis* Smith)
Figures 52, 54–58

Diagnosis: Because of their coarsely wrinkled integument and low, paired dorsolateral body tubercles, postdefecating larvae of *Monoeca haemorrhoidalis* and *Lanthanomelissa betinae* appear similar, although they differ in body size. The larva of *Monoeca haemorrhoidalis* can easily be distinguished on the basis of its apically broad, scoop-shaped mandibles (figs. 57, 58) (also characteristic of *M. lanei*, unpubl.data), denticulate atrial wall (fig. 56), and projecting, spiculate hypopharynx (fig. 54). Larvae of *Lanthanomelissa betinae* have mandibles that taper apically and display a conspicuously denticulate cusp (figs. 72, 73) (also characteristic of *Paratetrapedia swainsonae* (Cockerell) studied by Rozen and Michener [1988]), a smooth atrial wall, and a flat (nonprojecting), nonspiculate hypopharynx. A cursory examination of the mature larvae of other tapinotaspidine taxa in the American Museum suggests that these features, and particularly those of the mandible, will be a good source of characters to distinguish the taxa.

Mature larvae of *Monoeca haemorrhoidalis* can be distinguished from those of its cleptoparasite, *Protosiris gigas*, on the basis of the following (*P. gigas* characters in parentheses): bidentate mandible (figs. 57, 58; acutely pointed mandible, figs. 90–93), denticulate atrial wall (fig. 56, smooth), labrum apically bilobed in maximum profile (fig. 59; simple curved apex, fig. 89), antennal papilla with about 3 sensilla (fig. 61; numerous sensilla, rarely only 3, fig. 95), and a moderately broad, moderately projecting salivary opening (fig. 54; extremely narrow, strongly projecting lips, figs. 89, 96). Live postdefecating larvae of *M. haemorrhoidalis* are quite yellowish, whereas those of *P. gigas* are nearly white.

Description: Length (if straight) about 15 mm.

Head (figs. 54, 55, 59): Integument of head capsule generally pigmented yellowish tan, concolorous with body integument, but following areas lacking pigment, therefore white: parietal band, median ecdysial line of cranium, epistomal ridge, postoccipital ridge; following areas of cleared head brownish: anterior and posterior tentorial pits, antennal papilla, cardo, stipes, articulating arm of stipes, salivary lips, mandible, and palpi; labral and maxillary apices and labrum brownish. Cranium (fig. 59) with scattered, small, setiform sensilla; sensilla of labral apex and labium longer than those of cranium, but not as long as palpi; following areas with spicules: inner apical surfaces of maxilla, lateral upper surface of hypopharynx, and epipharynx; upper surface and lower apical surface of salivary lips with elongate papillae, visible only with SEM (fig. 60).

Head size moderately small compared with body; head capsule moderately wider than long in frontal view (fig. 54). Tentorium complete, moderately robust; anterior tentorial pit distinctly closer to anterior mandibular articulation than to antenna; posterior tentorial pit well impressed, in normal position at junction of hypostomal and postoccipital ridges. Median longitudinal thickening of head capsule extending part way to level of antennae. Postoccipital, hypostomal ridges well developed; pleurostomal ridge broad, well developed; epistomal ridge complete; epistomal sulcus deeply incised, rather broad. Parietal band evident. Antennal prominence moderately weakly developed; antennal disc differentiated from papilla; papilla small, projecting slightly more than basal diameter, with approximately 3 sensilla. Front of head capsule in lateral view (fig. 55) sloping normally so that labrum extends beyond clypeus, and clypeus beyond frons; clypeus projecting strongly from frons. Labrum moderately wide, apically rounded in frontal view (fig. 54), but in maximum profile (i.e., dorsofrontal view) labrum bearing low mound on each side (fig. 59), apically extending beyond middle of labrum, these mounds bearing most of labral sensilla, thus tuberclelike; labral sclerite (as found in Megachilidae) absent; epipharyngeal surface with fine spicules on each side, these spicules nonsetiform and hence not forming brush.

Mandible (figs. 57, 58) short, robust at base; when viewed dorsally (fig. 57) or ventrally, mandible gradually tapering apically; when viewed adorally (fig. 58), mandible with large scoop-shaped apical concavity,

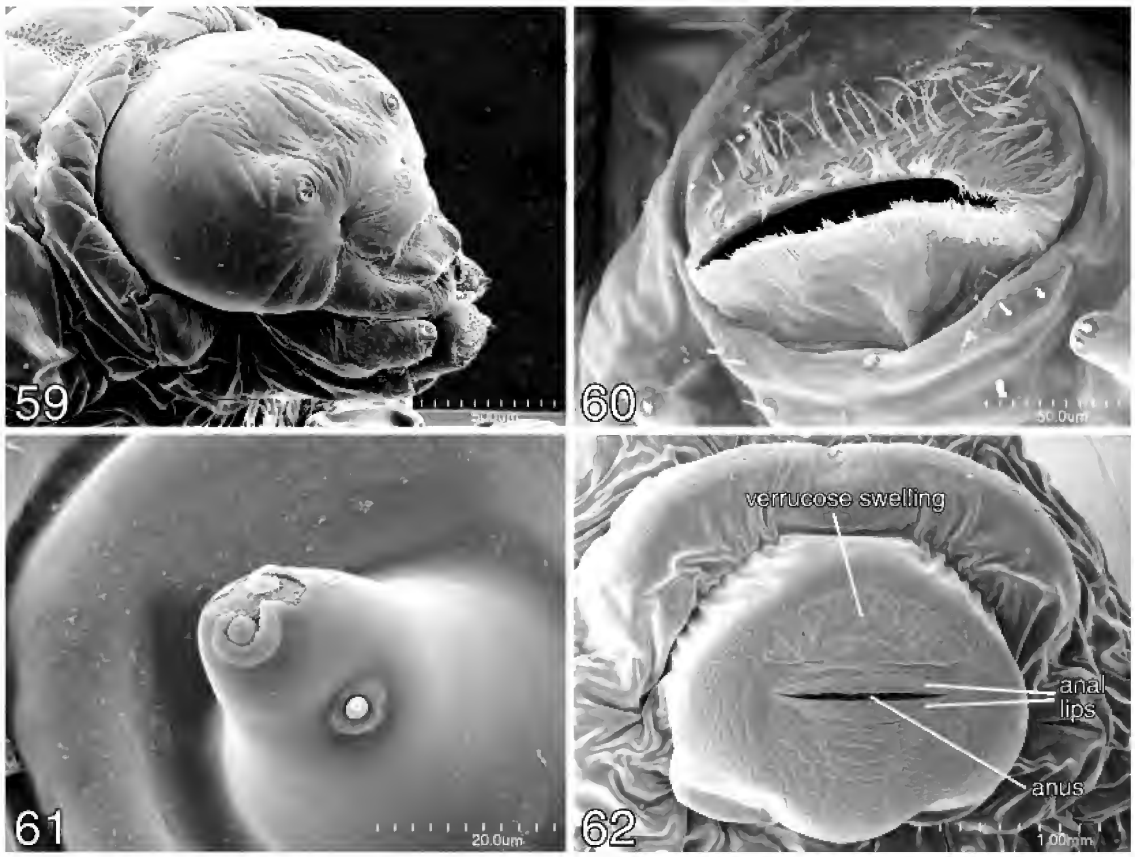

Figs. 59–62. SEM micrographs of postdefecating larva of *Monoeca haemorrhoidalis*. **59.** Head, dorsolateral view. **60.** Salivary lips, showing elongate papillae. **61.** Antennal papilla, with three sensilla. **62.** Abdominal apex, posterior view.

deep basal surface of which is weakly alveolate, apical surface of which is darkly pigmented, without sculpturing; dorsal apical edge of concavity finely, irregularly toothed; ventral apical edge without teeth, somewhat irregular; apex of mandible broad, bidentate, with broad dorsal tooth, which varies from being obtuse to broadly acute, and ventral narrowly acute tooth. Labiomaxillary region moderately strongly projecting in lateral view (fig. 55). Maxillary apex distinct, with palpus positioned slightly toward outer side; low mound bearing cluster of long, setiform sensilla immediately mesad of palpus possibly galea; palpus moderately large, about twice length of antennal papilla; cardo and stipes well developed; articulating arm of stipes evident. Labium divided into prementum and postmentum; premental sclerite evident on cleared head; labial palpus about as long as maxillary palpus. Salivary opening a transverse slit on projecting lips; lips in frontal view (fig. 54) moderately narrow, reflecting narrowness of prementum. Hypopharynx large, projecting, shallowly bilobed.

Body (fig. 52): Integument of postdefecating larva coarsely wrinkled (figs. 52, 62), without setae except for minute, scattered, setiform sensilla mostly on abdominal segment 10, below anus; body surface without spicules except as noted on abdominal segments 9 and 10, described below. Body form robust; intersegmental lines deeply incised; dorsal intrasegmental lines of meso- and metathorax and abdominal segments 1–9 deeply incised; pleural swelling (below spiracles) of most body segments moderately pronounced; very low paired dorsal tubercles on caudal annulets of meso- and metathorax and segments 1–8, these tubercles transverse

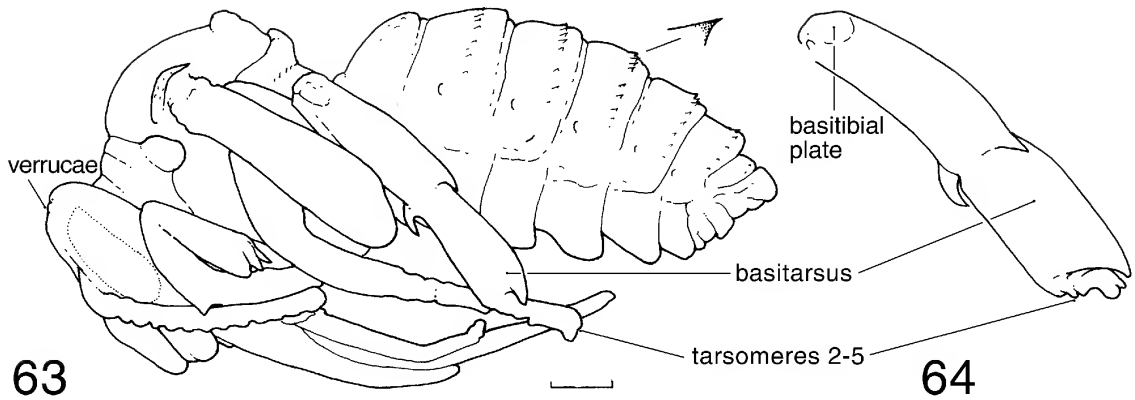

Figs. 63, 64. *Monoeca haemorrhoidalis*, pupa. **63.** Male, lateral view, with enlargement of tergal tubercle. **64.** Hindleg of female, lateral view. Scale bar (= 1.0 mm) refers to both figures.

but not meeting along midline; those of abdominal segmented 9 more nearly meeting at midline and finely spiculate, thus forming medially interrupted, narrow, transverse, spiculate band (fig. 62); abdominal segment 10 attached in approximate middle of segment 9 in lateral view (fig. 52); anus appearing to be positioned near middle of segment 10 in posterior view (fig. 62) but actually dorsal in position (see predefecating form, below); low transverse swelling curving above anus (fig. 62); surface of swelling distinctly verrucose; integument anterior to swelling finely spiculate laterally; anus (fig. 62) with transverse lips. Spiracles (figs. 52, 56) moderately small, pigmented, subequal in size; atrium globular, projecting above body wall, with rim; peritreme present; atrial inner surface with rows of sharp denticles concentric with primary tracheal opening; primary tracheal opening with collar; subatrium moderately short, with about 6 chambers.

Predefecating Form (fig. 53): As described for postdefecating form except for following: integument smooth, not wrinkled. Intersegmental lines scarcely incised dorsally, moderately incised ventrally; intrasegmental lines scarcely evident; paired dorsal tubercles scarcely evident, although on cleared, stained specimen, certainly present, with cuticle more than twice as thick as elsewhere; pleural swellings not developed. Anus clearly dorsal in position (fig. 53).

MATERIAL STUDIED: 12 postdefecating larvae, Brazil: Paraná: Mananciais da Serra, Piraquara, 20-XI-2002 (J.G. Rozen); 2 postdefecating larvae, same except 21-XI-2002; numerous predefecating and postdefecating larvae, same except 20-XII-2002 (G.A.R. Melo and A. Aguiar); numerous predefecating and postdefecating larvae, same except 4-11-XII-2003 (A. Aguiar, I. Alves-dos-Santos, R.B. Gonçalves, G.A.R. Melo, J.G. Rozen).

REMARKS: We could not detect evidence of mandibular wear in postdefecating larvae of this species, which might have resulted from eating the cell lining. Such evidence was discovered in the mandibles of *Protosiris gigas* (see Remarks in the treatment of its mature larva and also see Biology of *Monoeca haemorrhoidalis* (Smith), above).

PUPA OF *MONOECA HAEMORRHOIDALIS* (SMITH)
Figures 63, 64

DIAGNOSIS: Pupae of other *Monoeca* species have not been described. The only other pupal description of a tapinotaspidine was that of *Paratetrapedia swainsonae* (Cockerell) (Rozen and Michener, 1988). The undescribed pupa of *Tapinotaspoides serraticornis* is also represented in the collection of the American Museum of Natural History. Pupae of all three taxa are quite similar (except for size) and lack large mesoscutal tubercles while having obvious paired mesoscutellar tubercles; the very low mesoscutal tubercles reported for *P. swainsonae* may actually be homologs of the mesoscutal verrucose patches in front of the mesoscutellar tubercles of

M. haemorrhoidalis. The very low verrucae associated with the ocellar area of the pupa of *Monoeca haemorrhoidalis* are replaced in the other two species with sharply defined ocellar tubercles. The females of these two species have apical median projections of S4 and S5, which are lacking in *M. haemorrhoidalis*. Pupae of *P. swainsonae* tend to have more pronounced axillae than do either of the other two, and both *P. swainsonae* and *T. serraticornis* bear a very small but well-defined tubercle at the base of their forewings, and *M. haemorrhoidalis* does not. There are, no doubt, other differences to be identified among the taxa in the pupal stage, but these differences are probably subtle and difficult to define.

Although the pupae of *Monoeca haemorrhoidalis* and its cleptoparasite *Protosiris gigas* are found in cocoons of similar external appearance, the pupae can be immediately distinguished by body form (that of *M. haemorrhoidalis* is robust and that of *P. gigas* is slender). The basitarsus even of the male *M. haemorrhoidalis* is broad compared with the slender basitarsus of the pupa of *P. gigas*. The apex of the foretrochanter of *M. haemorrhoidalis* bears a pointed tubercle, whereas that of *P. gigas* is swollen and rounded.

HEAD: Integument without setae, spicules, tubercles, but with weakly defined verrucae above ocelli. Labrum apically rounded in frontal view; pupal ocelli scarcely defined, nontuberculate. Mandible with subapical ventral swelling accommodating developing adult setae. Paraglossa long, approximately equal in length to first segment of labial palpus.

MESOSOMA: Integument without setae; mesoscutum with pair of obscurely defined, paramedian, verrucose patches (not discernable in fig. 63) in front of mesoscutellar tubercles; pronotum with lateral angles finely verrucose dorsally; tegula dorsally verrucose. Lateral angles and posterior lobes of pronotum moderately produced. Mesepisternum without tubercles; mesoscutum without tubercles; mesoscutellum with paired, moderately low, paramedian tubercles accommodating developing adult setae; metanotum swollen especially medially but not tuberculate. Tegula not produced, without tubercle; wings without tubercles. All coxae with moderate-sized, sharply pointed, ventroapical tubercles that accommodate developing adult setae; foretrochanter with moderately small ventroapical tubercle; mid- and hindtrochanters with ventroapical angle but without clearly define tubercles; forefemur with rounded, ventrobasal tubercle; midfemur of both sexes without tubercles; hindfemur of female with very small apical tubercle in front of basitibial plate (fig. 64), in male this tubercle obscure; foretibia with small apical tubercle; midtibia without tubercle; hindtibia with slender apical tubercle on outer surface; hindtibial spurs curved; basitarsus with pronounced apical tubercle; basitarsus of male (fig. 63) narrower than that of female, which is broader than length of other tarsomeres combined (fig. 64).

METASOMA: Integument without spicules or setae. T1 without tubercles; T2–T6 (male), T2–T5 (female) with apical (or subapical) row of fine, sharply pointed tubercles, those of T2 less pronounced that those of other terga, which tend to have pigmented apices; sterna with apical margins unmodified, without rows of tubercles. Apex of metasoma without terminal spine, ending in rounded membranous lobe.

MATERIAL STUDIED: 3 female, 7 male pupae, Brazil: Paraná: Mananciais da Serra, Piraquara, 10-XII-2003 (J.G. Rozen); numerous female and male pupae, same except same except 4–11-XII-2003 (A. Aguiar, I. Alves-dos-Santos, R.B. Gonçalves, G.A.R. Melo, J.G. Rozen).

EGG OF *LANTHANOMELISSA BETINAE* URBAN
Figure 32

The single specimen upon which this description is based was lost before it could be examined with an SEM.

DESCRIPTION (fig. 32): Length 2.2 mm; maximum diameter 0.58 mm ($N = 1$); egg index 0.99 (category *medium*). Shape stout, approximately symmetrical along its strongly curved long axis; broadly rounded at both ends, anterior end presumably broader as in *Monoeca haemorrhoidalis*. Color nearly white. Chorion viewed through stereomicroscope somewhat shiny.

MATERIAL EXAMINED: One egg, Brazil: Pa-

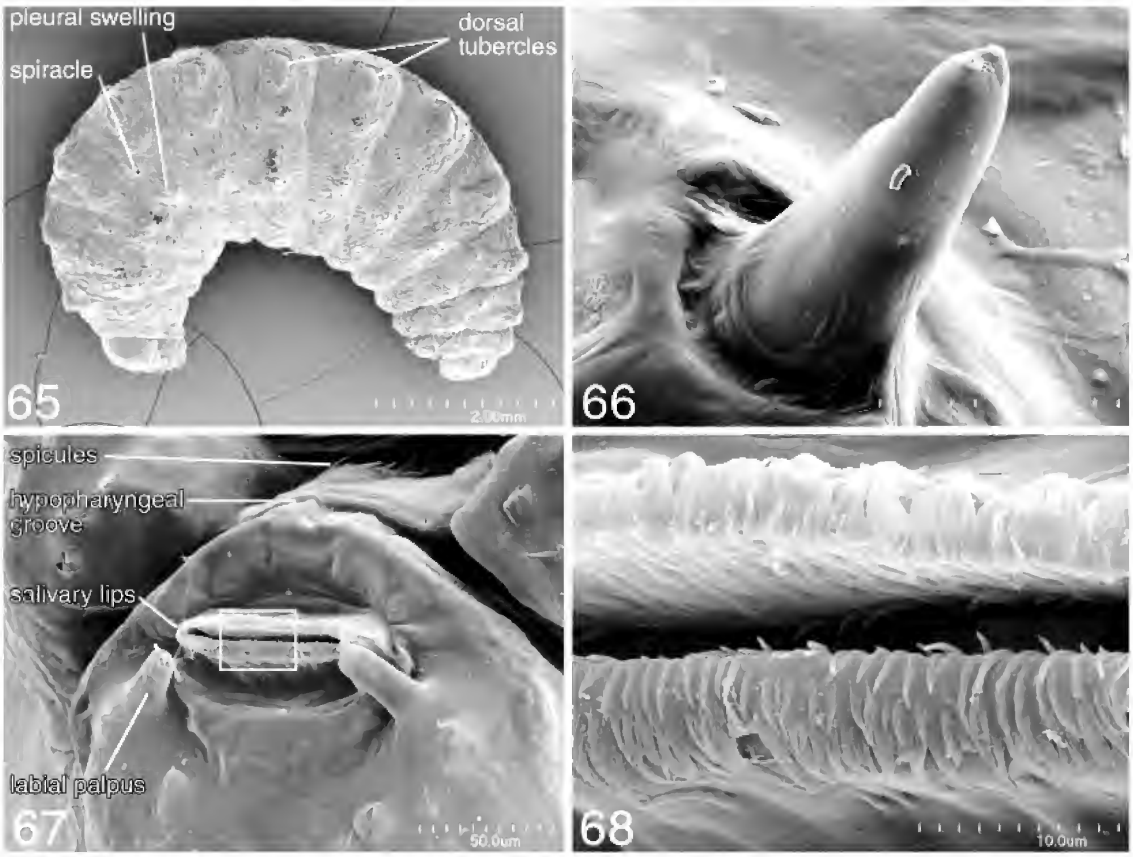

Figs. 65–68. SEM micrographs of postdefecating larva of *Lanthanomelissa betinae*. **65.** Entire body, lateral view. **66.** Close-up of antenna. **67.** Labral apex. **68.** Close-up of salivary lips showing elongate papillae, identified by rectangle in fig. 67.

raná, Curitiba, 25-XI-2002 (J.G. Rozen), nest no. 2.

REMARKS: The female collected from the nest provided the intertegular measurement for calculating the egg index.

POSTDEFECATING LARVA OF *LANTHANOMELISSA BETINAE* URBAN

Figures 65–73

DIAGNOSIS: See the Diagnosis of the postdefecating larva of *Monoeca haemorrhoidalis* to distinguish the mature larvae of these two species.

Because the postdefecating larva of *Lanthanomelissa betinae* is nearly white, its antennal papilla (figs. 66, 71) are long and slender, and its mandible (fig. 72, 73) is apically bidentate to subtruncate and bears a denticulate cusp, it can be separated from that of its cleptoparasite *Parepeolus minutus*, which has a more yellowish cream-color body, antennal papillae (fig. 97) that are more robust, and a mandible (figs. 103, 104) that is apically pointed and lacks a denticulate cusp.

Lucas-de-Oliveira (1966) described the predefecating larva of this species, under the name of *Lanthanomelissa* sp. Later Urban (1995) described and named the species *L. betinae*, based in part upon two adult paratypes from the nesting site from which the larva had been collected.

DESCRIPTION: Length (if straight) about 9 m.

Head (figs. 70, 71): Integument of head capsule at most faintly pigmented, hence appearing white, concolorous with body, except following brownish: mandibles, especially apically, and salivary lips. Cranium with very fine, scattered, mostly nonsetiform sen-

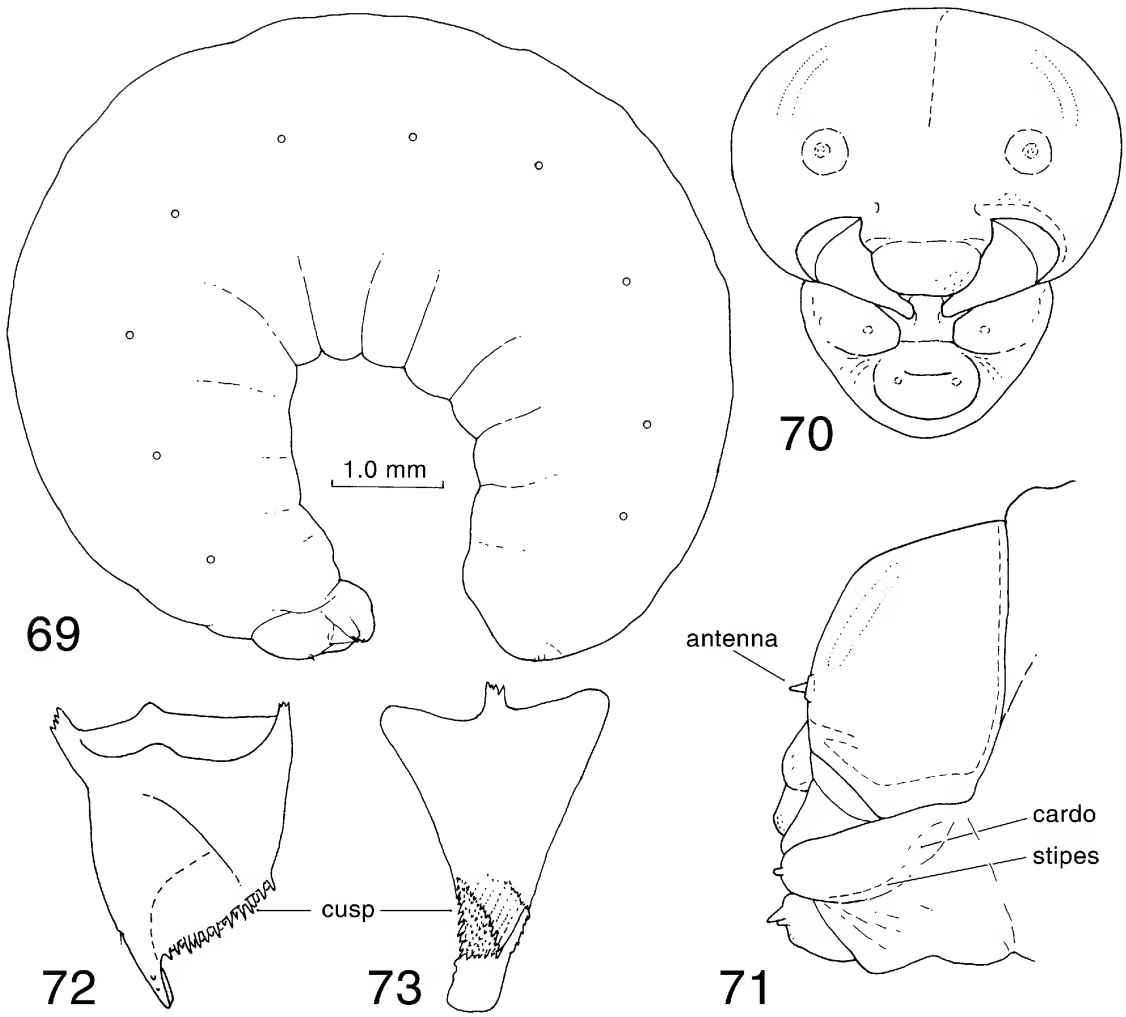

Figs. 69–73. *Lanthanomelissa betinae*. **69.** Predefecating larva, lateral view. **70, 71.** Head of postdefecating larva, frontal and lateral views. **72, 73.** Right mandible of same, dorsal and inner views. Scale bar (= 1.0 mm) refers to fig. 69.

silla; inner apical surfaces of maxilla and epipharynx apparently nonspiculate: hypopharynx (fig. 67) with a few elongate spicules laterally well behind hypopharyngeal groove. Salivary opening apically with elongate papillae apparently arising from within opening (visible with SEM: figs. 67, 68); external surfaces of lips without papillae.

Head moderate in size compared with body; head capsule moderately wider than long in frontal view (fig. 70). Tentorium complete, moderately robust; anterior tentorial pit distinctly closer to anterior mandibular articulation than to antenna; posterior tentorial pit well impressed, in normal position at junction of hypostomal and postoccipital ridges. Median longitudinal thickening of head capsule extending part way to level of antennae. Postoccipital, hypostomal, pleurostomal ridges well developed; epistomal ridge laterad of anterior tentorial pits short but well developed; epistomal ridge between pits scarcely evident, external sulcus shallow. Parietal band evident. Antennal prominence weak; antennal disc well differentiated from papilla, somewhat projecting; papilla long (two or more times basal diameter), longer than palpi, conical as seen in

lateral view, with approximately 3 apical sensilla. Front of head capsule in lateral view sloping normally so that labrum extends somewhat beyond clypeus, and clypeus somewhat beyond frons. Labrum moderately wide, apically subtruncate in frontal view (fig. 70) but in maximum profile (i.e., frontodorsal view) labrum apically weakly bilobed, these mounds bearing most of labral sensilla; labral sclerite (as found in Megachilidae) absent; epipharyngeal surface with brush of long setiform spicules on each side directed anteromesad.

Mandible broad at base when viewed dorsally (fig. 72) or ventrally and with short apex beyond base; when viewed adorally, mandible gradually tapering to narrow, nearly flat apex, which may be subtruncate (fig. 73), indistinctly toothed, or indistinctly bilobed with either dorsal or ventral lobe slightly longer than other; cuspal area strongly denticulate (figs. 72, 73); its teeth regularly spaced along dorsal and ventral edges of area and larger than teeth within area; dorsal apical edge beyond cusp without teeth or with one or two; ventral apical edge with linear series of irregular small denticles. Labiomaxillary region moderately strongly projecting in lateral view (fig. 71). Maxillary apex distinct, with palpus positioned slightly to outer side; galea possibly present, but only as sensilla mesad of palpus; palpus moderately large; cardo, stipes, and articulating arm of stipes evident but weakly developed and unpigmented. Labium divided into prementum and postmentum; premental sclerite not evident; labial palpus about as long as maxillary palpus. Salivary opening a transverse slit on moderately projecting lips; lips in frontal view (fig. 70) moderately narrow, reflecting narrowness of prementum. Hypopharynx not projecting, middle part nearly flat, extending backward toward mouth.

Body (fig. 65): Integument of postdefecating larva coarsely wrinkled, without setae except for minute, scattered, slightly setiform sensilla mostly below anus on abdominal segment 10; body surface mostly without spicules except paired abdominal tubercles apically each with weak patches of fine spicules; spicules weakly present laterally on abdominal segment 10. Body form robust; intersegmental lines deeply incised; dorsal intrasegmental lines of meso- and metathorax and abdominal segments 1–9 moderately incised; pleural swelling (below spiracle) on most body segments strongly pronounced, more so than in *Monoeca haemorrhoidalis*; low paired dorsal tubercles on prothorax, on caudal annulets of meso- and metathorax, and on caudal annulets of segments 1–8, these tubercles tending to be transverse but not meeting along midline; those of abdominal segment 9 more nearly meeting at midline; most dorsal tubercles tending to be more pronounced that those of *M. haemorrhoidalis*; abdominal segment 10 attached in approximate middle of segment 9 in lateral view (fig. 65); anus positioned somewhat above middle of segment 10; low transverse swelling curving above anus; surface of swelling less distinctly verrucose than in *Monoeca haemorrhoidalis*; anus with indistinct transverse lips. Spiracles moderately small, unpigmented, subequal in size; atrium globular, projecting above body wall, with rim; peritreme present; atrial inner surface smooth; primary tracheal opening with collar; subatrium moderately short, with about 6 chambers.

Predefecating Form (fig. 69): As described for postdefecating form except for following: integument smooth, not wrinkled. Intersegmental lines scarcely evident dorsally; intrasegmental lines not evident; pleural swelling not evident; paired dorsolateral body tubercles not evident on uncleared specimen, but visible on cleared, stained specimen as transverse, slightly roughened, dark patches. Anus almost certainly dorsal on segment 10, but ventral line between abdominal segments 9 and 10 not evident. Male with small paired cuticular scars on ventral midline of abdominal segment 9; female sex characters unknown.

MATERIAL STUDIED: 4 postdefecating and 1 predefecating larvae, Brazil: Santa Catarina: Criciúma, UNESC, 16-XI-2002 (J.G. Rozen), from nest no. 1; 1 postdefecating larva, same except from nest no. 4; 15 postdefecating larvae, same except 23, 26-XI-2003 (I. Alves-dos-Santos), nest nos. 1, 2.

REMARKS: Postdefecating larvae are coated with an extremely thin, colorless, transparent material that adheres to the integument.

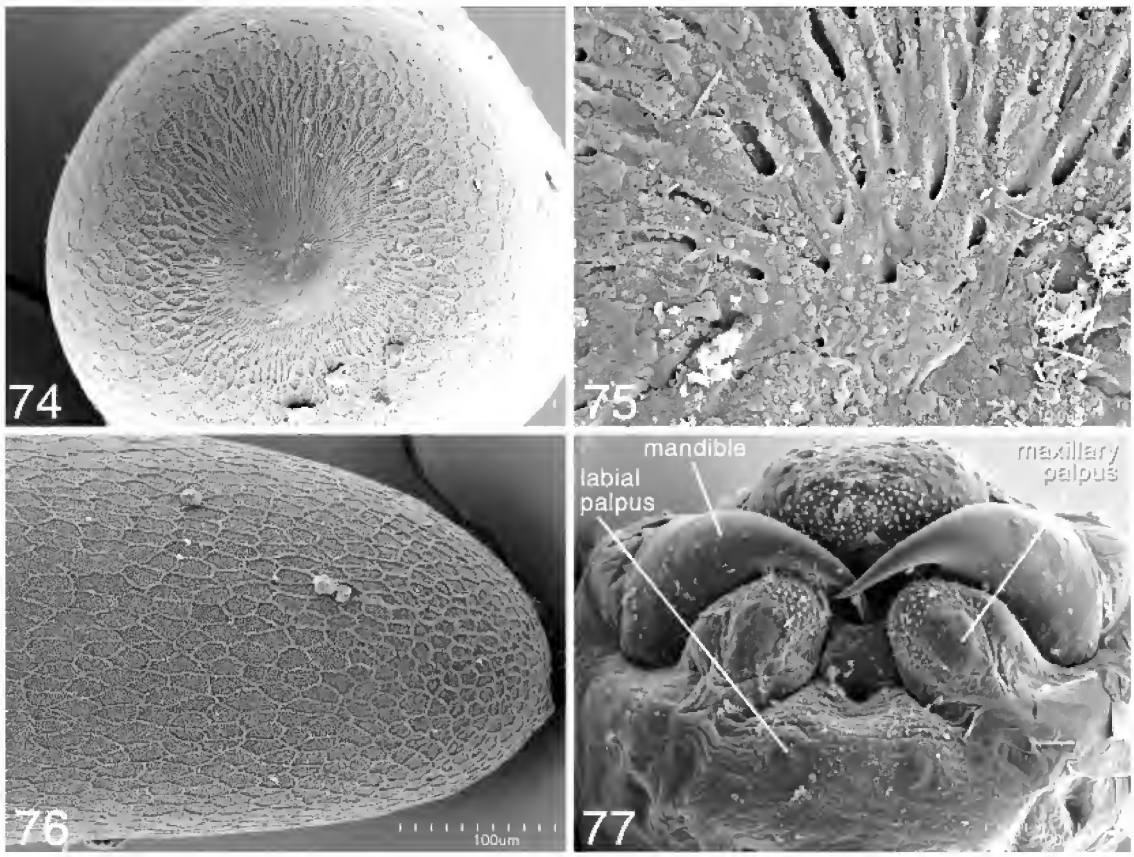

Figs. 74–77. SEM micrographs of egg and first instar of *Protosiris gigas*. **74.** Front end of egg, anterior view, outcurved surface toward top. **75.** Close-up of micropyle. **76.** Posterior end of egg, lateral view. **77.** Head of first instar, ventral view.

Egg of *Protosiris gigas* Melo
Figures 38, 74–76

Length 2.8–3.0 mm, maximum diameter 0.48–0.55 mm (N = 3); egg index 0.86 (based on average egg length divided by the average intertegular distance [3.39 mm] of five females collected at random) (category *medium*). Shape (fig. 38) slender, approximately symmetrical along its slightly curved long axis; rounded at both ends, with widest diameter slightly anterior to midbody; anterior end nearly parallel-sided; posterior end gradually tapering; anterior pole slightly produced; micropyle (fig. 75) a cluster of small pores on produced anterior pole; pores directed toward outcurved surface. Color nearly white except chorion of two eggs faintly tan at posterior end. Chorion viewed through stereomicroscope smooth, dull, without visible pattern except produced area at anterior pole somewhat shinier. As viewed with SEM, chorion at anterior pole showing fine elongate grooves radiating from micropylar pore directed only toward outcurved surface (fig. 75); somewhat farther away from micropyle but still at anterior end, chorion with radiating, strongly expressed polygons with raised borders that exhibit midline grooves (fig. 74); these grooves on outcurved surface extensions of grooves radiating from micropylar pores; polygonal grooves rapidly becoming less expressed posteriorly (fig. 74), fading to become faint polygonal patterning (lacking midline grooves) that extends over rest of chorion, except patterning becoming more pronounced, without midline grooves at extreme posterior end (fig. 76).

Material Examined: 3 eggs, Brazil: Pa-

raná, Mananciais da Serra, Piraquara, 20-XI-2002 (J.G. Rozen) from nests of *Monoeca haemorrhoidalis*

REMARKS: Among the taxa of the Osirini, the egg (as a mature oocyte) of *Epeoloides coecutiens* (Fabricius) was described and illustrated by Rozen (2001), and the presumably mature oocytes of *Osirinus lemniscatus* Roig-Alsina and *Parepeolus aterrimus* (Friese) were illustrated in the ovariole by Alexander (1996). Eggs of *Protosiris gigas* and *E. coecutiens* are classified as small, and those of *O. lemniscatus* and *Pa. aterrimus* are small and medium, respectively, according to Alexander (1996: table 1). Those of *E. coecutiens* are somewhat more curved (Rozen, 2001: fig. 3) than those of *Pr. gigas* (fig. 38) but otherwise are approximately similar in shape. The egg of *O. lemniscatus* appears to be slender (Alexander, 1996: fig.14), like that of *Pr. gigas*, but the egg shape of *Pa. aterrimus* is difficult to interpret (Alexander, 1996: fig. 15). The eggs of *Pr. gigas* and *E. coecutiens* differ considerably in chorionic surface sculpturing, with that of *E. coecutiens* being nodular (Alexander, 1996: figs. 10, 11) while that of *Pr. gigas* consists of a network of polygons with raised margins, all as seen with an SEM. However, the micropylar area of both (Alexander, 1996: fig. 12, and fig. 74 herein) consists of polygons narrowing toward the anterior pole, the polygons with raised margins each of which is divided by a fine groove. At the extreme anterior end of the eggs, the polygons are obliterated, and there remains only the raised borders and, on the outcurved surface, the fine, channellike grooves, which continue to the micropylar array. This feature, shared by both species, may be a synapomorphy. In *E. coecutiens*, the micropylar pores were not identified by Rozen (2001), but were probably obscured by follicular debris.[8] The pores of *Pr. gigas* become quite visible only under extremely high magnification (fig. 75).

[8] An early SEM study of the honey bee egg failed to detect the micropylar pores (Bronskill and Salkeld, 1978), but Erickson (1981: pl. 1.44) clearly demonstrated their presence.

FIRST INSTAR OF *PROTOSIRIS GIGAS* MELO
Figures 77–81

DIAGNOSIS: Because osirine first instars have not been collected and described before, a comparison of the first instar of *Protosiris gigas* with close relatives cannot be made. See the Discussion and table 2 for features that distinguish the first instar of this species from those of other cleptoparasitic apids.

Please see the diagnosis of the first instar of *Monoeca haemorrhoidalis* for ways to separate first instars of host and parasite.

LENGTH: About 3.0 mm.

HEAD (figs. 77, 79–81): Integument of parietal moderately sclerotized, somewhat pigmented; mandibular apices strongly pigmented; head capsule and mandibles at base with scattered, inconspicuous, minutely setiform sensilla, except parietals with indistinct line of slightly larger sensilla occupying position of spinulae as found in the Melectini (see remarks below); following areas spiculate: epipharyngeal surface, maxillary apices, and labium posterior to salivary opening (hypopharynx nonspiculate).

Head more or less prognathous (fig. 80); parietals faintly enlarged, moderately elongate in lateral view (fig. 80), somewhat constricted behind dorsally (fig. 80) but not laterally so that foramen not noticeably narrowed; sclerotization of parietal ending at hypostomal ridge, not invading labiomaxillary area; sclerotization of parietals ending posteriorly at postoccipital ridge. Tentorium complete but thin, with dorsal arms; anterior and posterior tentorial pits moderate in size; internal head ridges tending to be moderately developed except epistomal ridge weak laterad of anterior tentorial pits, absent between pits; integument near ridge not pebbled, wrinkled, or in other ways sculptured. Parietal bands absent. Antenna a low projection with the papilla fused with parietal and bearing 6–7 nonsetiform sensilla. Labrum moderate in size, apically subtruncate when seen in maximum profile (fig. 81) (but appearing rounded in frontal view, fig. 79); labrum weakly, if at all, sclerotized, with numerous nonsetiform sensilla, many on low elevations; labral tubercles absent; boundary between labrum and lower end of clypeus weakly defined.

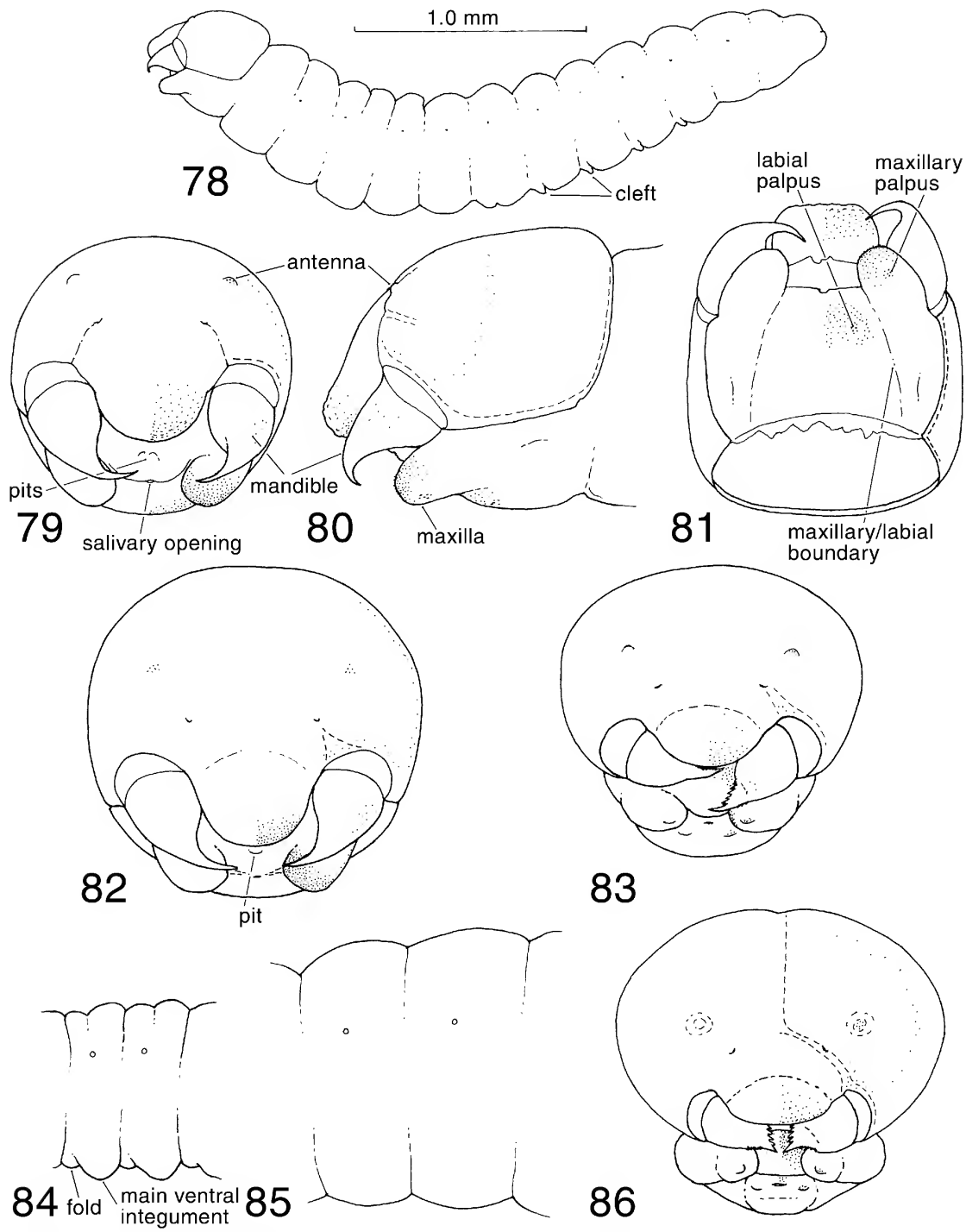

Figs. 78–86. Early instars of *Protosiris gigas*. **78.** First instar, entire larva, lateral view. **79–81.** Head, first instar, frontal, lateral, and ventral views, respectively. **82.** Head, second instar, frontal view. **83.** Head, third instar, frontal view. **84.** Abdominal segments 3 and 4, early third instar, lateral view. **85.** Abdominal segments 3 and 4, late third instar, lateral view; for explanation see text. **86.** Head, fourth instar, frontal view. Scale bar (= 1.0 mm) refers to fig. 78. Figures drawn in various scales, except 79–82 to same scale and 84, 85 to same scale.

Mandibles (figs. 77, 79–81) heavily sclerotized, moderately pigmented, basally stout, apically attenuate, strongly curved, ending in sharply pointed, simple apex, without tubercles on outer aspect but with scattered fine sensilla; inner surface smooth, without teeth or projections. Each maxilla a strongly projecting, apically heavily spiculate, rounded lobe; maxillary palpus not evident except for subapical cluster of about six, nonsetiform sensilla on ventrolateral surface (figs. 77, 81) on cleared specimen (these sensilla resembling those of labial palpus); under SEM examination maxillary palpus a low, nonspiculate, padlike structure (fig. 77); palpus, cardo, stipes (except for articulating arm) shallow depression near base of maxilla; thin sclerite leading from maxilla to salivary opening presumably articulating arm of stipital sclerite because of its position relative of maxilla and apex of labium; maxillae and labium basally forming continuous surface and seemingly fused, but actually separated by fine suture (fig. 81) extending to their bases; labium greatly recessed so that maxillary apices extend much farther forward than apex of labium; labial palpus not evident as projection on cleared specimen but identified by cluster of nonsetiform sensilla behind and laterad of salivary opening; under SEM examination, labial palpus faintly produced, nonspiculate (fig. 77). Salivary opening small, circular; salivary duct evident. Hypopharynx identified as area above articulating arms of stipital sclerites, nonspiculate, bearing two irregular pits, possibly indentations formed by mandibular apices when mandibles are closed.

BODY: Integument without setae; venter of each body segment with extensive patch of spicules, dorsal surface without spicules; linear series of fine granules immediately above spiracular line on each side (as found in *Monoeca haemorrhoidalis*) absent. Form elongate, linear (fig. 78); intersegmental lines deeply incised; body without dorsal tubercles; abdominal segments not divided dorsally into cephalic and caudal annulets; abdominal segments 4–7 each with distinct transverse cleft shortly behind intersegmental line, so that area in front becomes median, backward-sloping transverse fold, anterior surface of which is spiculate while the posterior surface is smooth; abdominal segment 3 with similar but less distinct anterior ventral fold; prothorax and abdominal segment 9 not protruding ventrally; abdominal segment 10 rounded posteriorly; anus apical. All spiracles present, small, coequal in diameter, flush with body wall (i.e., not on tubercles).

MATERIAL STUDIED: 2 first instars (one still partly enclosed in the chorion), Brazil: Paraná: Mananciais da Serra, Piraquara, 20-XI-2002 (J.G. Rozen) from nests of *Monoeca haemorrhoidalis*.

REMARKS: The single specimen whose head capsule and body were cleared in an aqueous solution of sodium hydroxide had a number of pollen grains lodged in its esophagus, an indication that it had started to feed although its midintestine contained no pollen.

The median, backward-sloping folds on the anterior venters of abdominal segments 3–7 are a feature unknown in other bee larvae. Their function is discussed in Biology of *Protosiris gigas*, above.

OTHER LARVAL INSTARS OF *PROTOSIRIS GIGAS* MELO

The four following larval instars increase in size incrementally, both in body length and head width. All material discussed in this section was collected at Brazil: Paraná, Mananciais da Serra, Piraquara; dates of collection and collectors are identified parenthetically.

The second instar (20–21-XI-2002 [J.G. Rozen]) is similar to the first, although it is somewhat larger (compare figs. 79 and 82), and the head is less elongate in lateral view. The antennae, composed of about the same number of sensilla, are perhaps less pronounced than those of the first instar. The mandibles continue to be sharply pointed, suggesting that this instar is also capable of killing conspecific and host immatures. Maxillary and labial palpi are still represented only by their sensilla (not examined with an SEM). The epistomal and pleurostomal ridges are less pronounced, and the spiculation of head and body is similar to the first instar. The two small pits in the hypopharynx of the first instar have given way to a single, larger, median, dimplelike pit, where the mandibular

apices might reside if the mandibles are closed. The transverse folds of integument on the anterior ventral surfaces of abdominal segments 3–7 are no longer evident. The spiracular atrium can be identified because it is now somewhat larger than the subatrium, but other features are unclear because of the small size of the spiracle.

With the third instars (5, 10-XII-2003 [G.A.R. Melo]; 6-XII-2003 [J.G. Rozen, G.A.R. Melo]), we see a gradual shift away from the rapacious features of the first and second instars, toward the anatomy of the fifth instar, adapted for feeding and cocoon spinning. This is most evident in the mandibles, which now start to broaden subapically where the surface takes on a faintly concave shape. This will transform into the scoop-shaped apical concavity in subsequent instars. For the first time a row of sharp teeth are visible along the dorsal and ventral apical mandibular margins. The mandible (fig. 83) is still acutely pointed and moderately strongly curved at the extreme apex. Observations recorded in the Biology of *Protosiris gigas*, above, suggest that this instar is behaviorally capable of attacking (or defending itself) in the event it encounters another larva in the cell. The antennal papilla is large but shorter than its basal diameter. The maxillary and labial palpi are slightly produced, blisterlike swellings. The salivary opening is slightly transverse but without lips. Spiculation is now faintly evident on the hypopharynx and the inner apex of the maxillae, and the ventral surface of the body is strongly retrorse spiculate. Fine spicules also occur dorsally on more posterior abdominal segments.

As indicated by the reshaped mandible, the third instar is primarily adapted for feeding. Because we were able to observe exemplars preserved in various stages of their feeding, we were able to record anatomical changes in their body shape. In its early stage (fig. 84) the body is quite linear, and abdominal segments at least 1–4 (but probably 1–8) are divided dorsally into cephalic and caudal annulets. Ventrally each of abdominal segments 2–8 posseses a narrow transverse fold of spiculate integument in front of the main ventral integument, similar to the folds found on segments 3–7 of the first instar. By the end of the third stadium (fig. 85), both the dorsal and ventral folds have disappeared because of the swollen midsection of the body. Thus, the greatly folded integument of the body midsection during the early part of the stadium allows the instar to ingest a large quantity of the provisions. The fully fed third instar appears quite physogastric, contrasting with its linear shape at the beginning of the stage. The spiracular atria are globular but much flattened; the primary tracheal opening is without a distinct collar and the subatrium cannot be recognized.

The fourth instar (fig. 86) (11, 20-XII-2002 [G.A.R. Melo]; 6-XII-2003 [J.G. Rozen, G.A.R. Melo]) in most ways is anatomically intermediate between the third and fifth instars. The mandible may no longer be effective (and presumably does not need to be) for attacking other cleptoparasites and probably serves well for ingesting provision because the scoop-shaped apex is more pronounced than in the third instar and is further broadened by the rows of apical teeth. The mandible changes little, except for size, between this instar and the final one. The hypopharynx has assumed a dorsally protruding form (which may actually have been the case in the preceding instar), its surface now distinctly spiculate, as in the last larval instars. Maxillary and labial palpi are projecting considerably more than in the previous instar but not as far as their basal diameters, which is also true for the antennal papillae. Parietal bands and the frontal depression above and mesad of each antenna are faintly present. Division of the labium into prementum and postmentum is questionably distinct in this instar. The salivary opening is narrowly transverse and has slightly projecting lips with papillae appearing on its dorsal surface and just above it. It is unknown if the abdominal segments exhibit intrasegmental lines early in this instar as they do in the third. The body integument is strongly spiculate ventrally, more weakly so dorsally. The spiracular atrium of the fourth instar is clearly globular but shallow compared with that of the last instar, possesses a peritreme, and the subatrium is sclerotized but lacks distinct chambers.

POSTDEFECATING LARVA OF *PROTOSIRIS GIGAS* MELO

Figures 87–93, 95, 96

DIAGNOSIS: Because of its much larger body, the mature larva of *Protosiris gigas* can immediately be distinguished from that of *Parepeolus minutus*, the only other osirine whose larva is known. Furthermore, the very narrow, strongly projecting, dorsally spiculate salivary lips of *Pr. gigas* (fig. 96) contrast with the broader, weakly projecting lips of *Pa. minutus* (fig. 98). The deep apical mandibular concavity of *Pr. gigas* (fig. 90–93) also separates this species from *Pa. minutus*, which has a very shallow, almost nonexistent apical mandibular concavity (figs. 103, 104).

See Diagnosis of the postdefecating larva of *Monoeca haemorrhoidalis* for characters to separate the postdefecating larva of *Protosiris gigas* from that of its host.

DESCRIPTION: Length (if straight) about 15 mm.

Head (figs. 88, 89): Integument of head capsule faintly pigmented; following areas of cleared head more darkly pigmented; posterior arms of tentorium (but not bridge), anterior arm of tentorium between pit and junction of dorsal arm; hypostomal, pleurostomal ridges, cardo, stipes, articulating arm of stipes, premental sclerite including apex of labium, salivary lips, mandible especially toward apex, and epipharyngeal surface. Cranium with fine sensilla widely scattered; labrum with sensilla clustered medioapically; following with papillae: (1) dorsal surface of upper salivary lip where they are long, nearly setiform, and forward curving (fig. 96); (2) median area immediately above lip; the following with spicules (1) upper surface of hypopharynx, (2) epipharyngeal surface of labrum, and (3) a few spicules on inner apical surface of maxilla.

Head size moderately small compared with body; head capsule much wider than long in frontal view. Tentorium complete, moderately stout; anterior tentorial pit about midway between antennal papilla and anterior mandibular articulation; posterior tentorial pit well impressed, in normal position at junction of hypostomal and postoccipital ridges. Median longitudinal thickening of head capsule faintly present. Postoccipital ridge very well developed; hypostomal, pleurostomal ridges, and lateral arms of epistomal ridge well developed; epistomal ridge between anterior tentorial pits evident. Parietal band faint. Antennal prominence moderately developed, accentuated dorsally by depression in frons above and slightly mesad of antenna; antennal disc differentiated from papilla (fig. 95); papilla projecting about as far as basal diameter, with sensilla varying in number from 3 to 10 (fig. 95). Front of head capsule in lateral view sloping normally, so that labrum extends beyond clypeus, and clypeus beyond frons. Labrum moderately wide, rather short, apically rounded in frontal view (fig. 89); tubercles absent; labral sclerite (as found in Megachilidae) absent; epipharyngeal surface without inner, trapezoidal, darkly pigmented sclerite.

Mandible (figs. 90, 91) moderately short, robust at base when viewed both dorsally and adorally; apex narrowing moderately abruptly to single, acute but rounded point when seen aborally (fig. 91); apex bearing large scoop-shaped apical concavity; concavity areolate basally; dorsal and ventral apical edges faintly but distinctly crenulate in postdefecating larva, but in predefecating larva, these crenulations distinct teeth (fig. 93); dorsal apical edge curved in aboral view; ventral apical edge nearly straight in aboral view; outer surface with apical cluster of small irregular tubercles that lack setae but may contain nonsetiform sensilla. Labiomaxillary region strongly projecting in lateral view (fig. 89). Maxillary apex distinct, subtruncate with palpus arising from outer corner when viewed dorsally; galea absent; palpus very large, longer and with greater diameter than antennal papilla; cardo and stipes well developed; articulating arm of stipes evident. Labium divided into prementum and postmentum; premental sclerite evident above salivary lips, fading on either side below lips; labial palpus distinctly smaller than maxillary palpus. Salivary opening an extremely narrow transverse slit on strongly projecting lips, which project about as far as apical width. Hypopharynx a narrow, strongly projecting lobe that extends forward as far as, if not farther than, maxillary apex (excluding palpus) (fig. 88).

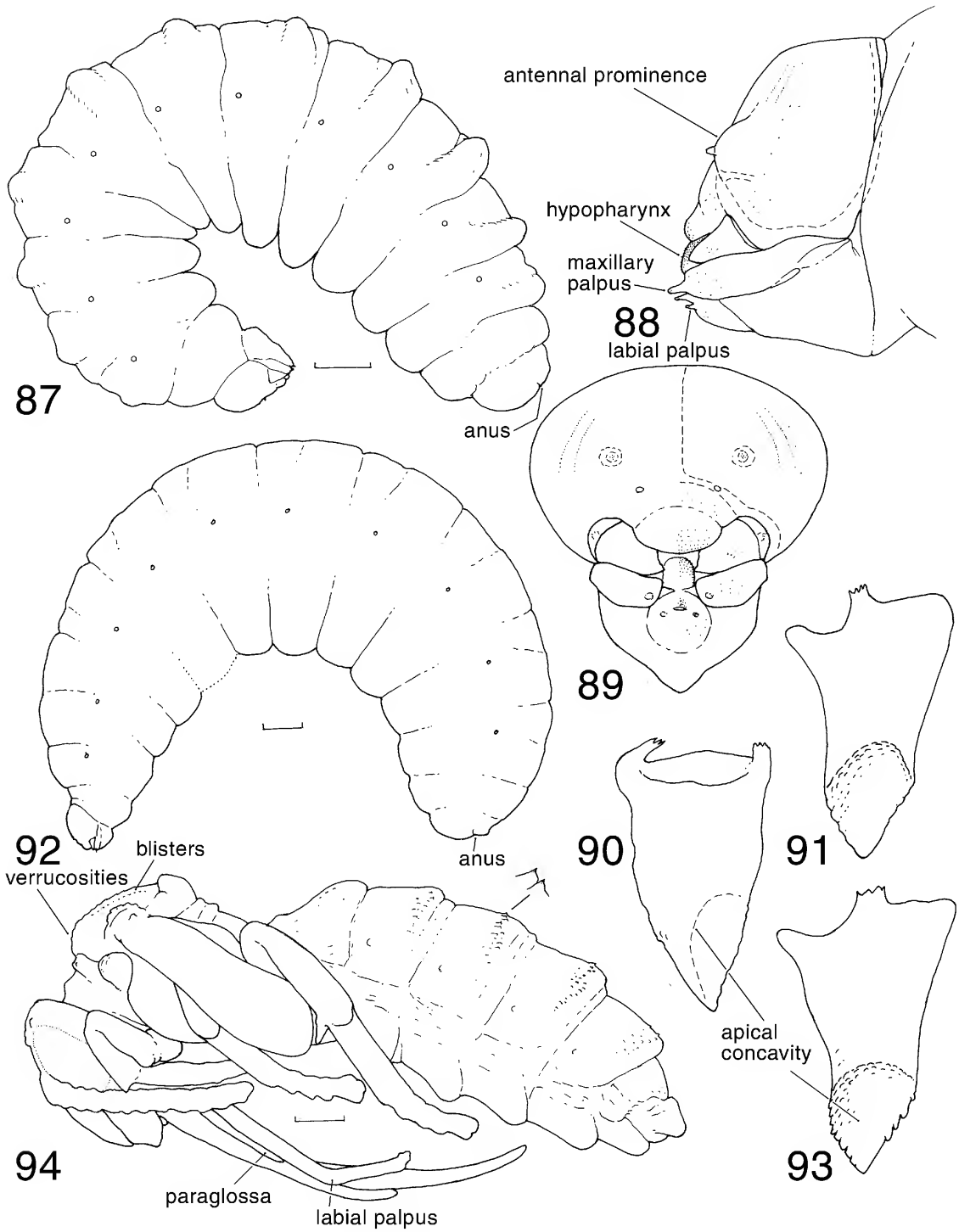

Figs. 87–94. *Protosiris gigas*. **87.** Postdefecating larva, entire body, lateral view. **88, 89.** Head, lateral and frontal views, respectively. **90, 91.** Right mandible, dorsal and inner views, respectively. **92.** Predefecating larva, lateral view. **93.** Right mandible of predefecating larva, inner view. **94.** Pupa, lateral view, with tergal tubercles enlarged. Scale bars (= 1.0 mm) refer to figs. 87, 92, 94, respectively.

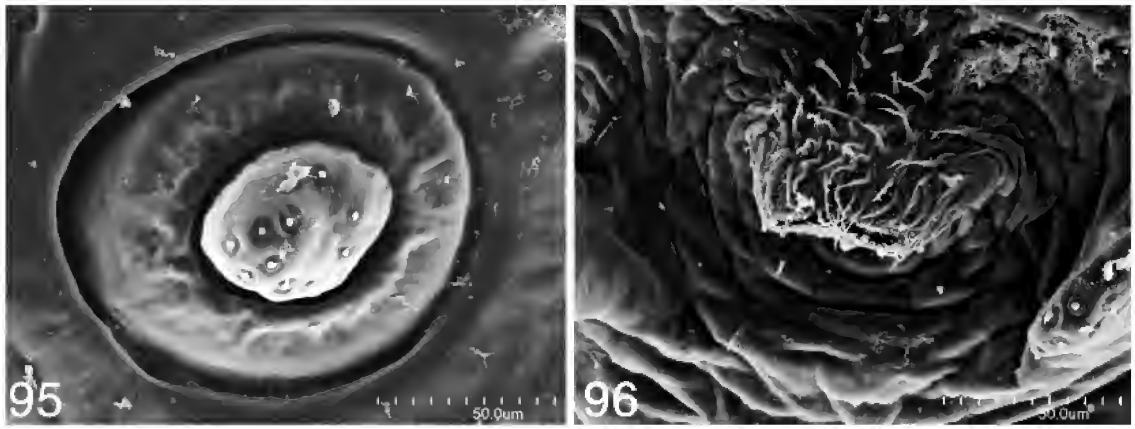

Figs. 95, 96. SEM micrographs of postdefecating larva of *Protosiris gigas*. **95.** Close-up of antenna, showing numerous sensilla. **96.** Apex of labium showing salivary lips with elongate papillae.

Body (fig. 87): Integument of postdefecating form finely wrinkled, without setae except for small cluster of minute sensilla mostly on abdominal segment 10, below anus; body surface nonspiculate except most body segments with patch of very fine spicules along ventral midline and for extremely fine scattered spicules dorsally on posterior abdominal segments (best seen on predefecating larva). Body form moderately slender in lateral view (fig. 87); intersegmental lines moderately deeply incised on abdominal segments, less so on thorax; dorsal intrasegmental lines obscured by pronounced transverse dorsolateral tubercles; pleural swelling (below spiracle) scarcely noticeable in lateral view (fig. 87); low, somewhat transverse, paired dorsolateral tubercles on thoracic segments; these tubercles becoming more strongly defined and more transverse on abdominal segments 1–7, less pronounced on segments 8 and 9; abdominal segment 10 attached in approximate middle of segment 9 in lateral view (fig. 97); anus dorsal on segment 10; transverse swelling curving above anus obscure on some specimens, somewhat express on others, its surface thickened; anus without distinct lips. Spiracles moderately small, faintly pigmented, subequal in size; atrium globular, projecting slightly above body wall, with rim; peritreme present; atrial inner surface smooth; primary tracheal opening with collar; subatrium moderate in length, with about 9 chambers, gradually decreasing in size inwardly.

Predefecating Form (fig. 92): As described for postdefecating form except for following: integument smooth, not wrinkled. Intersegmental lines shallowly incised dorsally, more evident ventrally; intrasegmental lines faintly evident on most abdominal segments dorsally, best defined on cleared specimen about halfway between midline and spiracles; pleural swelling not evident; paired dorsolateral body tubercles not evident on cleared or uncleared specimen; abdominal segment 10 with transverse swelling curving above anus present, its integument thickened. Anus positioned dorsally on segment 10, with paired lips. Sex characters unknown.

MATERIAL STUDIED: 5 postdefecating, 2 predefecating larvae, Brazil: Paraná, Mananciais da Serra, Piraquara, 20-XII-2002 (G.A.R. Melo, A. Aguiar), from nests of *Monoeca haemorrhoidalis*

REMARKS: Postdefecating larvae taken from cocoons were coated with a thin, dry, clear, colorless secretion, the source of which is unknown. When specimens were manipulated with forceps, the material flaked from the integument in patches with the exact topography of the wrinkled integument.

Although clearly the fifth larval instar, the specimen termed predefecating may possibly not have finished feeding yet. We cannot certainly explain why the mandibular teeth on this specimen are so pronounced whereas those of two cleared postdefecating specimens are reduced to crenulations. Because wear came to mind, we examined the surface

of a cell that contained a *Protosiris* cocoon and found there was no trace of the waxy cell lining, as has also been observed in many cells of *M. haemorrhoidalis*.

Pupa of *Protosiris gigas* Melo
Figure 94

Diagnosis: The only other osirine pupa that has been described was a species of *Osiris*, provisionally identified as *O. pallidus* Smith (Rozen, 2000a). Pupae of these two species share elongate bodies, paired mesoscutellar tubercles, similar (but not identical) verrucose patterns, and low, tuberclelike swellings (not visible in fig. 94) on the forewing. However, they are immediately separable on the basis of the tergal tubercles; those of *Protosiris gigas* each bears a single, usually pigmented, sharp point, whereas those of *O.* cf. *pallidus* are rounded and each usually has a patch of spicules.

The pupa of *P. gigas* cannot be successfully run in the generic key to cleptoparasitic pupae presented by Rozen (2000a). However, it can be distinguished from the known pupae of other parasitic lineages of bees as follows: Because it is enclosed in a cocoon, it contrasts with all parasitic Halictinae and Nomadinae, none of which spins cocoons. Because its labral apex is a simple curve, it is distinct from the Ericrocidini and Rhathymini, which have bituberculate labral apices. Unlike pupae of the Melectini, Isepeolini, and Protepeolini, it lacks paired mesoscutal tubercles. It does have paired mesoscutellar tubercles and apical transverse bands of small tubercles on most terga, unlike *Coelioxoides* (Tetrapediini). Finally, it contrasts with the parasitic Megachilidae because it lacks setae, whereas the pupae of the megachilids have conspicuous setae on their vertices and/or dorsal mesosomas. (Above data derived from Alves-dos-Santos et al. [2002]; Roig-Alsina and Rozen [1994]; Rozen et al. [1978]; and Rozen [2000a].)

See the diagnosis of the pupa of *Monoeca haemorrhoidalis* for features by which the pupae of the host and *Protosiris gigas* can be separated.

Head: Integument without setae and spicules, but with small cluster of verrucae immediately above ocelli, with single, minute tubercle centered on vertex, and with horizontal, parallel, low linear blisters immediately mesad of inner orbits on front of face. Scape possibly verrucose apically. Labrum apically rounded in frontal view. Mandible with subapical ventral swelling accommodating developing adult setae. Paraglossa moderately long, but clearly shorter than first segment of labial palpus (fig. 94).

Mesosoma: Integument without setae. Dorsal surface of angles of pronotum projecting and verrucose; lateral lobes of pronotum produced. Mesepisternum without tubercles; mesoscutum without tubercles but with low, paramedian, anterior verrucosities (fig. 94) behind which are more-or-less parallel series of low linear blisters, which appear to be minute rounded tubercles in lateral view; similar linear blisters appearing to radiate laterad of parapsidal lines; mesoscutellum with paired, moderately low, paramedian tubercles; metanotum neither swollen nor tuberculate. Tegula with outer edge verrucose; wings without distinct tubercles but with low tuberclelike mound midway to apex. All coxae swollen apically; in addition fore- and hindcoxae each with small, rounded, ventroapical, tuberclelike projection; midcoxa without such projection; all trochanters ventroapically swollen but not tuberculate; foretrochanter with moderately small, ventroapical tubercle; mid- and hindtrochanters with ventroapical angle but without clearly define tubercles; forefemur with rounded, ventrobasal swelling, too general to be called tubercle; all tibiae each with outer apical swelling; hindtibial spurs straight.

Metasoma: Integument without spicules or setae. T1 without tubercles; T2–T5 (female) each with apical (or subapical) transverse cluster fine tubercles, those of T2 less pronounced that those of other terga, which tend to have pigmented apices; sterna without rows of tubercles but S1-S3 with posterior median tubercle accommodating developing adult setae; T5 with paramedian pair of posterior tubercles accommodating developing adult setae. Apex of metasoma without terminal spine, ending in rounded membranous lobe.

Material Studied: 1 female pupa, Brazil: Paraná, Mananciais da Serra, Piraquara, 20-XI-2002 (J.G. Rozen).

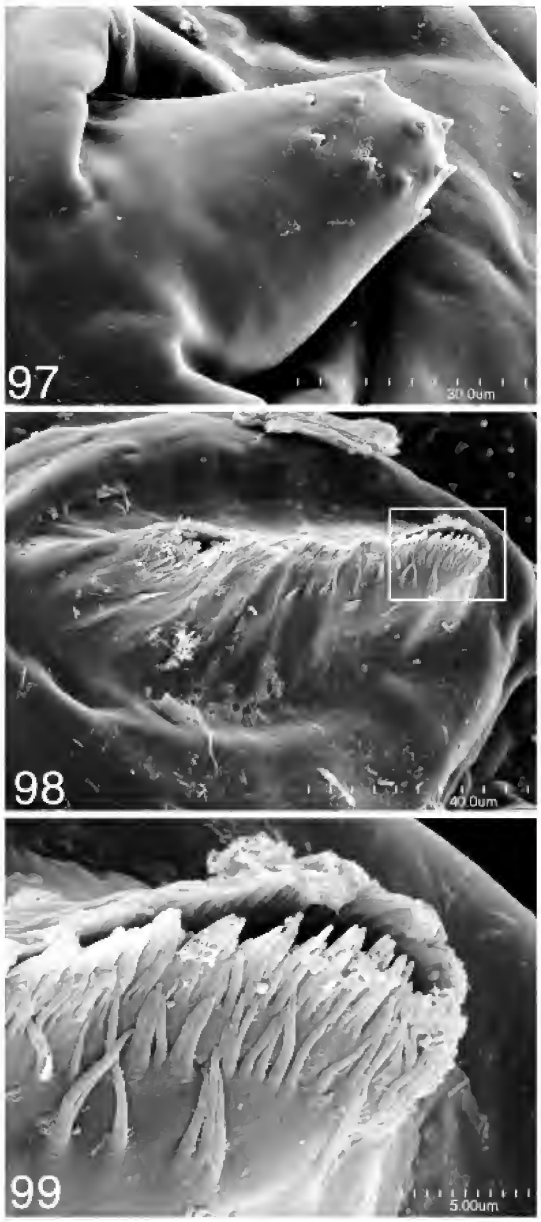

Figs. 97–99. SEM micrographs of postdefecating larva of *Parepeolus minutus*. **97.** Close-up of antennal papilla showing numerous sensilla, approximate lateral view. **98.** Salivary lips. **99.** Close-up of area identified by rectangle in fig. 98, showing elongate papillae.

Postdefecating Larva of *Parepeolus minutus* Roig-Alsina
Figures 97–104

Predefecating larvae of this species are unknown.

Diagnosis: The Diagnosis of the postdefecating larva of *Protosiris gigas* gives characters by which the mature larvae of these two species can be separated.

For features distinguishing the postdefecating larva of *Parepeolus minutus* from its host, please see Diagnosis of the postdefecating larva of *Lanthanomelissa betinae*.

Description: Length (if straight) about 8 mm.

Head (figs. 101, 102): Integument of head capsule faintly pigmented; following areas of cleared head brown: posterior arms of tentorium (but not bridge), anterior arm of tentorium between pit and junction of dorsal arm; hypostomal, pleurostomal ridges, epistomal ridge laterad of anterior tentorial pits, cardo, stipes, articulating arm of stipes, premental sclerite above salivary opening, fading laterally and below opening, mandible, and inner surface of epipharynx. Cranium with irregular band of fine setiform sensilla extending from mandibular coria, laterad of antennae and parietal bands to vertex; other similar sensilla widely scattered but most abundant on clypeus and labrum; labral apex with numerous sensilla; all setiform sensilla of mouthparts fine, inconspicuous; following areas with spicules: dorsal and apical surfaces of maxilla, upper surface of hypopharynx, leading edge of epipharynx; salivary lips apically with elongate papillae as seen with SEM (figs. 98, 99).

Head size moderately small compared with body; head capsule much wider than long in frontal view (fig. 102). Tentorium complete, moderately thin; anterior tentorial pit about midway between antenna and anterior mandibular articulation; posterior tentorial pit well impressed, in normal position at junction of hypostomal and postoccipital ridges. Median longitudinal thickening of head capsule absent. Postoccipital, hypostomal, pleurostomal ridges, and lateral arms of epistomal ridge moderately well developed; epistomal ridge between anterior tentorial pits absent. Parietal band weak. Antennal prominence moderately weakly developed; antennal disc differentiated from papilla; papilla projecting slightly more than basal diameter, with approximately 10 sensilla (fig. 97). Front of head capsule in lateral view (fig. 101) sloping normally, so that labrum

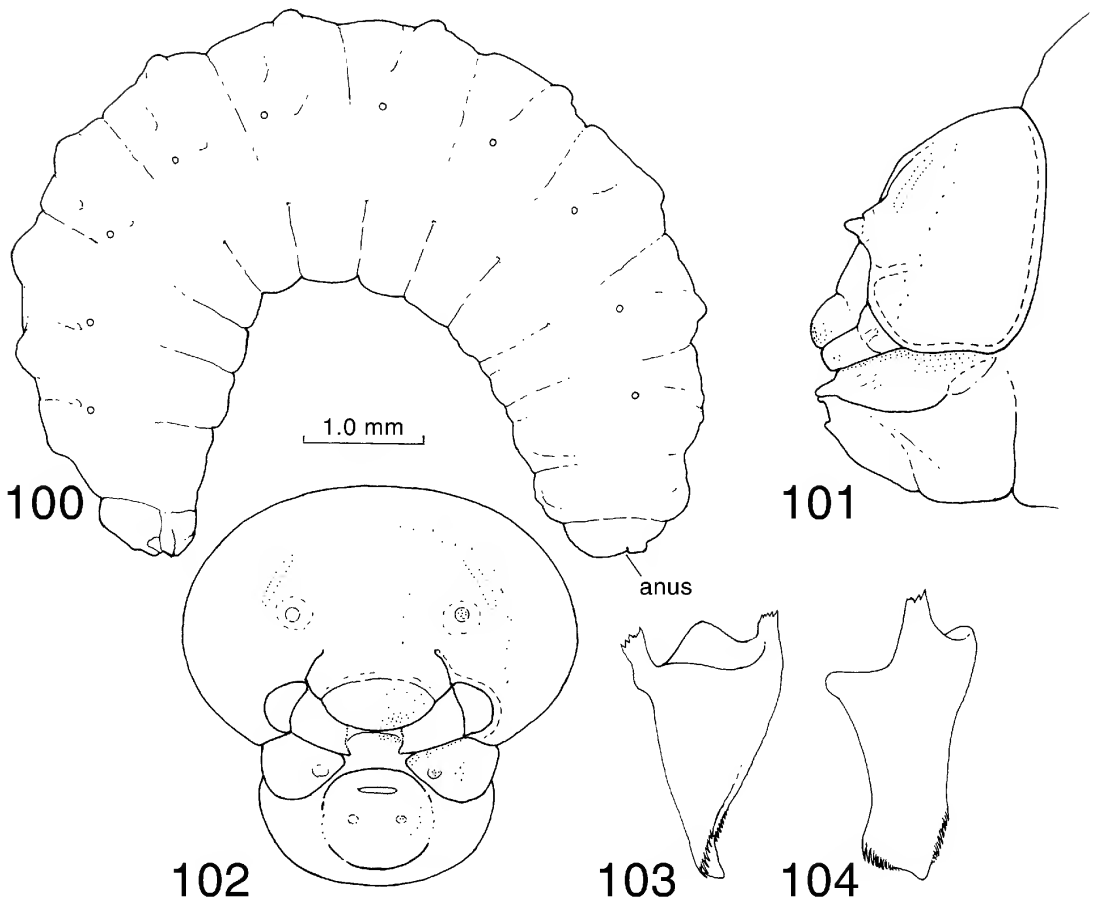

Figs. 100–104. Postdefecating larva of *Parepeolus minutus*. **100.** Entire body, lateral view. **101, 102.** Head, lateral, and dorsal views, respectively. **103, 104.** Right mandible, dorsal, and inner views, respectively. Scale bar (= 1.0 mm) refers to fig. 100.

extends beyond clypeus, and clypeus beyond frons. Labrum moderately wide, rather short, apically rounded in frontal view (fig. 102) but indistinctly bilobed in maximum profile; tubercles absent; labral sclerite (as found in Megachilidae) absent; epipharyngeal surface with outer surface nonpigmented, membranous but inner swollen area darkly pigmented (alternatively swollen area may be part of the esophagus).

Mandible (figs. 103, 104) short, robust at base; when viewed dorsally (fig. 103) or ventrally mandible gradually tapering apically; outer surface with 4 small setae on low tubercles on apical third; adoral surface shallowly, evenly concave; dorsal apical edge broadly expanded, bearing approximately 8 evenly space teeth; ventral apical edge not expanded so that two edges subparallel, thus apex of mandible shallowly scooplike; ventral apical edge with approximately 10 evenly spaced teeth, somewhat smaller than those of dorsal edge; apex of mandible acutely pointed (fig. 104). Labiomaxillary region moderately strongly projecting in lateral view (fig. 101). Maxillary apex distinct, with palpus positioned slightly subapically laterad of apex; galea absent; palpus large, perhaps slightly longer than antennal papilla; cardo and stipes well developed; articulating arm of stipes evident. Labium divided into prementum and postmentum; premental sclerite evident above salivary lips, fading on either side below lips; labial palpus distinctly smaller than maxillary palpus. Salivary opening a transverse slit on projecting lips;

lips in frontal view (fig. 102) moderately narrow, reflecting narrowness of prementum. Hypopharynx a dorsally projecting lobe, truncated on top, behind articulating arms of stipites and premental sclerite.

Body (fig. 101): Integument without setae except for small cluster of minute setiform sensilla mostly on abdominal segment 10, below anus; body surface spiculate dorsally and ventrally, but nonspiculate laterally in vicinity of spiracles and below them; integument without spines or sclerotized tubercles. Body form moderately robust; intersegmental lines moderately weakly incised; dorsal intrasegmental lines absent on thorax, weakly present on abdominal segments 1–9; pleural swelling (below spiracle) scarcely noticeable; very low paired dorsal tubercles on thoracic segments and on caudal annulets of abdominal segments 1–9; abdominal segment 10 attached in approximate middle of segment 9 in lateral view (fig. 100); anus somewhat dorsal on segment 10; distinct transverse swelling curving above anus; surface of swelling finely roughened but not verrucose; anus without distinct lips. Spiracles moderately small, darkly pigmented, subequal in size; atrium globular, projecting slightly above body wall, with rim; peritreme present; atrial inner surface smooth; primary tracheal opening with collar; subatrium short, usually with two larger outer chambers and one or two smaller inner chambers.

MATERIAL STUDIED: 1 postdefecating larva, Brazil, Santa Catarina, Criciúma, UNESC, 16-XI-2002 (J.G. Rozen), from nest no. 1 of *Lanthanomelissa betinae*; 1 postdefecating larva, same except 23-XI-2003 (I. Alves-dos-Santos), from nest no. 1 (different nest from previous year); 1 postdefecating larva, same except 26-XI-2003, from nest no. 2.

REMARKS: As with the other postdefecating larvae described herein, that of *Parepeolus minutus*, when removed from the cocoon, was found to be covered by a dry, clear, nearly colorless film that closely adhered to it body and tended to break into flakes after the larva was preserved in Kahle's solution.

DISCUSSION

The reader is referred to "Synopsis of the nesting biology of the Tapinotaspidini bees" (Aguiar et al., 2004) for a comparison of the nesting biology of the members of this tribe based on the information from this study and from previously published accounts. As the authors pointed out, members of the tribe nest in horizontal ground, earthen banks, and rotten wood. In addition, *Chalepogenus rozeni* Roig-Alsina has been observed 26 km south of Vicuña, Elqui Prov., Chile, nesting in deep cracks in the soil, as much as 30 cm below the surface. These nests have short main tunnels extending obliquely downward and cells appearing within 5 cm of the vertical crack surfaces (Rozen, unpubl. data). Such a nesting site can probably be considered akin to nesting in an earthen bank.

It would be interesting to compare the nesting biology and immatures of the Tapinotaspidini with those of the Exomalopsini because, until recently, the included taxa were placed in the same tribe, the Exomalopsini. However, such a comparison would be premature because so little has been published concerning the immatures and biologies of the various genera. Nonetheless, one biological feature seems to distinguish the Tapinotaspidini, that is, their behavior of collecting floral oils and their ability to transport and manipulate them.

The nonparasitic Ctenoplectrini do collect floral oils (Michener, 2000) and the postdefecating larva of one species has been described (Rozen, 1978). While this larva is remarkably similar to those of the Tapinotaspidini, the similarities (body form, details of the head and mouthparts) appear to be plesiomorphic. To the extent known, the Ctenoplectrini are cavity nesters, unlike the Tapinotaspidini. However, a more detailed analysis of larval features is warranted to determine if synapomorphies can be identified that show a relationship between these two tribes in light of some of the analyses of Roig-Alsina and Michener (1993) that show them to be sister groups.

In attempts to determine the nonparasitic ancestor that gave rise to cleptoparasites, host lineages are often identified as being likely ancestors. Is there evidence that the Osirini are derived from a tapinotaspidine-like ancestor? The fact that osirine larvae can metabolize floral oils mixed with pollen may be a synapomorphy of the two tribes. Mature

larvae of the two tribes show broad resemblances, but most of the features appear plesiomorphic and therefore are of little help in evaluating relationships.

The first instar of *Protosiris gigas* is obviously adapted to seek out and destroy host immatures and competing cleptoparasitic immatures. Its anatomy and biology therefore can be used to address the question whether *Protosiris* (and other Osirini) are closely related to other cleptoparasitic groups. Rozen (1991: table 1) identified 21 features of first instars that varied among the Nomadinae, Protepeolini, Melectini, Rhathymini, Isepeolini, and Ericrocidini. These same features are presented in table 2 here, to which two more columns have been added for *Coelioxoides* (Tetrapediini) and *Protosiris* (Osirini). Primitive features are scored 0, and derived features are scored 1, 2, and so on. Two features of the Isepeolini, then unknown, are now known: (1) females of *Isepeolus* introduce their eggs into host cells that are still open (scored 1), and (2) when deposited, the eggs are flat against the cell lining (Rozen, 2003). The latter is also scored 1, to be the same as "inserted in the cell wall" because of indirect evidence that the related *Melectoides* deposits its eggs this way in the cells of *Canephorula* (Michellete et al., 2000; Rozen, 2003). Data for *Coelioxoides* come from Alves-dos-Santos et al. (2002). It is now possible to analyze the behavioral and anatomical features of the first instar of *Protosiris* (the only member of the Osirini studied so far) with those of seven of the nine other cleptoparasitic lineages of the Apidae (Rozen, 2000b). Two cleptoparasitic lineages, *Exaerete* and *Aglae* (both Euglossini), are excluded, *Aglae* because its mode of parasitism is unknown, *Exaerete* because its second instar (not the first) is hospicidal (Garófalo and Rozen, 2001).

Table 3 shows the features of egg deposition and first-instar anatomy that *Protosiris* shares with each of the other seven lineages of cleptoparasitic apids. Based on the number of shared features, *Protosiris* and the Ericrocidini are the most similar, but they share no feature uniquely, a fact that suggests that these character states are not particularly strong. The complete sclerotization of the labiomaxillary region of the ericrocidines contrasts sharply with the totally membranous labiomaxillary region of *Protosiris*, as does the dorsoventrally flattened, large, projecting ericrocidine antenna with the small antennal papilla of *Protosiris*. The ericrocidine sclerotized labrum fused with the clypeus is also unlike the nearly membranous labrum of *Protosiris*. These strong dissimilarities do not support the idea that these two taxa are related. The only possibly unique character shared by *Protosiris* with any of the lineages is character 6, the presence of spinulae found also in Melectini. While spinulae have been a unique feature of melectines, present in all of them, the microscopic morphology of a spinula (Rozen, 1991: fig. 22) is not that of a simple setiform sensillum as appears to be true in *Protosiris*. Thus, while the spinulae of the Melectini and the band of setiform sensilla of *Protosiris* occupy the same position on the head capsule, they may not be homologous. The numerous differences between the first instars of these two groups also argue against a close relationship (table 2). One is left with the impression that *Protosiris* and thus the Osirini represent an independent origin of cleptoparasitism in the Apidae. The presence of the unique, ventral, integumental folds on the anterior edges of segments 3–7 seems to support the concept that many hospicidal bee larvae must be able to move with agility in order to find and kill host eggs (or larvae) and those of competing cleptoparasites, and that *Protosiris* (or its ancestor) found a new way to crawl. It is not out of the question that the Osirini arose from a tapinotaspidine-like ancestor despite the lack of evidence supporting such a conclusion at present.

ACKNOWLEDGMENTS

Robert G. Goelet, Chairman Emeritus, Board of Trustees, American Museum of Natural History, kindly supported the two fieldtrips to Brazil undertaken by J.G.R. to carry out this investigation.

We thank the State of Paraná water company SANEPAR for granting permission to G.A.R.M. to conduct the studies on *Monoeca* at the Mananciais da Serra.

John Pinto, University of California, Riverside, tentatively identified meloid adults

TABLE 2

Comparison of the Modes of Parasitism and of Anatomical Features of First Instars of Cleptoparasitic Apidae

Character	1. Nomadinae	2. Protepeolini	3. Melectini
0. Introduction of Cleptoparasite Egg into Host Cell	**1** Into open cell while host female foraging	**1** Into open cell while host female foraging	**2** Through closure after cell is closed
1. Egg Deposition	**1** Embedded in cell wall	**1** Embedded in cell wall	**2** Free in cell, usually adhering to closure
2. Head Shape	**1** Prognathous, rarely (*Townsendiella, Neolarra*) somewhat hypognathous	**0** More-or-less hypognathous	**1** More-or-less prognathous
3. Parietals	**0** Not swollen to somewhat swollen just in front of posterior head margin	**1** Extending upwards and backwards	**0** Normal, unmodified
4. Ventral Sclerotized Postoccipital Bridge	**1** Present, not fused with labiomaxillary region	**0** Absent	**2** Present, fused with labiomaxillary region
5. Head Sclerotization	**0** Ending at posterior margin	**0** Ending at posterior margin	**0** Ending at posterior margin
6. Cranial Band of Spinulae	**0** Absent	**0** Absent	**1** Distinct
7. Troughlike External Hypostomal Groove	**1** Present, at least in most cases	**0** Absent	**1** Present
8. Angle of Posterior Margin of Head to Hypostomal Groove	**0** Right angles or rarely obtuse	**1** Broadly curved	**0** Variable
9. Antennal Size	**1** Almost always small, obscure	**0** Low but distinct swelling	**2** Large, elongate
10. Antennal Shape	**0** Not flattened	**0** Not flattened	**0** Not flattened
11. Antennal Fusion	**1** Fused with head capsule	**1** Fused with head capsule	**0** Set off by ring from head capsule
12. Labrum	**1** Nonsclerotized, not fused with clypeus	**0** Sclerotized, articulating with clypeus	**2** Sclerotized, fused with clypeus
13. Labral Tubercle(s)	**1** Paired, long to very long, separately articulating	**2** Three pairs, fixed to labrum	**1** Paired, nonarticulating
14. Mandible	**1** Moderately long to very long	**0** Not elongate	**1** Moderately long
15. Labiomaxillary Sclerotization	**1** Present mesad of hypostomal grooves but absent in middle	**0** Absent	**1** Somewhat on sides and behind palpi
16. Labium and Maxillae	**1** Extensively fused	**0** Separate	**0** Separate
17. Maxillary Palpus	**1** Well developed, sometimes greatly elongate	**2** Short, large, padlike	**0** Small but distinct
18. Abdominal Segment 10	**1** Bearing forked or trilobed, eversible pygopod	**1** Bilobed	**0** Rounded
19. Body Setae	**0** Absent	**1** Present	**0** Absent
20. Spiracles of Abdominal Segment 8	**0** Normal in position and size	**0** Normal in position and size	**0** Normal in position and size

TABLE 2 (*Extended*)

[Data in table 2 from Rozen (1991: table 1, except as noted in Discussion), from *Coelioxoides* (Alves-dos-Santos et al., 2002), and from *Protosiris* (current study)].

4. Rhathymini	5. Isepeolini	6. Ericrocidini	7. *Coelioxoides*	8. *Protosiris*
2 Through closure after cell is closed	1 Into open cell while host female foraging	2 Through closure after cell is closed	2 Through closure after cell is closed	2 Through closure after cell is closed
2 Free in cell, adhering to closure	1 Flat against cell lining	2 Free in cell, adhering to closure	2 Free in cell, in food mass	2 Free in cell
0 Hypognathous	1 Prognathous	1 Prognathous	0 Hypognathous	1 More-or-less prognathous
2 Swollen, globose	0 Not swollen	0 Not swollen	2 Swollen	2 Slightly swollen
1 Present, not fused with labiomaxillary region	2 Present, fused with sclerotized labiomaxillary region	2 Present, fused with sclerotized labiomaxillary region	3 Partly present, not fused with labiomaxillary region	0 Absent
0 Ending at posterior margin	1 Extending onto prothorax	0 Ending at posterior margin	0 Ending at posterior margin	0 Ending at posterior margin
0 Absent	0 Absent	0 Absent	0 Absent	? Band of sensilla
0 Absent	0 Absent	0 Absent, except in *Ericrocis*	0 Absent	0 Absent
2 Nearly straight	? Impossible to interpret	0 Right angle	0 Right angle	0 More-or-less right angle
1 Scarcely evident	0 Small, well defined	2 Large, projecting	3 Absent	0 Small
0 Not flattened	1 Dorsoventrally flattened	1 ~ Dorsoventrally flattened	NA	0 Not flattened
1 Fused with head capsule	1 Fused with head capsule	1 Fused with head capsule	NA	1 Fused with head capsule
0 Perhaps faintly sclerotized, not fused with clypeus	2 Sclerotized, fused with clypeus	2 Sclerotized, fused with clypeus	2 Huge, fused with clypeus	0 Nonsclerotized, not fused with clypeus
1 Paired, nonarticulating	3 Single median	? Vague at best	0 Absent	0 Absent
1 Moderately long	1 Very long, slender	1 Long, robust	0 Not elongate	0 Not elongate
1 Only on sides of maxillae	2 Complete	2 Complete	0 Absent	0 Absent
0 Separate	1 Extensively fused	1 Extensively fused	1 Extensively fused	1 Topologically fused posteriorly
3 Evident only because of sensilla	3 Scarcely evident	3 Scarcely evident	4 Absent	3 Evident only because of sensilla
1 Bilobed	2 Truncate, small, greatly fused to IX	2 Truncate, trilobed, fused to IX	3 Pointed	0 Rounded
0 Absent	1 Present	0 Absent	0 Absent	0 Absent
0 Normal in position and size	1 Larger than preceding ones and at posterior margin of segment	1 Usually larger than preceding ones and at posterior margin of segment	0 Normal in position	0 Normal in position

TABLE 3
Derived Character States of Egg Deposition Features and First Instars
(Shared by *Protosiris gigas* with other Cleptoparasitic Apidae; for explanation, see Discussion)

Taxa	Shared derived character states	No. of states
Protosiris/Nomadinae	2, 11, 16	3
Protosiris/Protepeolini	11	1
Protosiris/Melectini	0, 1, 2, 6[a]	4
Protosiris/Rhathymini	0, 1, 3, 11, 17	5
Protosiris/Isepeolini	2, 11, 16, 17	4
Protosiris/Ericrocidini	0, 1, 2, 11, 16, 17	6
Protosiris/*Coelioxoides*	0, 1, 3, 16	4

[a] The homology of this feature is questionable; see Discussion.

taken from the nesting site of *Monoeca haemorrhoidalis* as *Tetraonyx* (*Paratetraonyx*) *distincticollis* Pic.

We thank the following Scientific Assistants of the American Museum of Natural History for their contributions to this project: Valerie Giles prepared all larval specimens for SEM examination and took the micrographs; Steve Thurtson arranged and labeled the illustrations for publication. Division Secretary Joanna Bilz assisted in numerous ways, including the formatting of table 2.

We also express our appreciation to John S. Ascher and two anonymous reviewers for their thoughtful suggestions and comments that have improved the manuscript.

REFERENCES

Aguiar, A.J.C., G.A.R. Melo, J.G. Rozen, Jr., and I. Alves-dos-Santos. 2004. Synopsis of the nesting biology of Tapinotaspidini bees (Apidae: Apinae). Proceedings of the 8th IBRA International Conference on Tropical Bees and VI Encontro sobre Abelhas, pp. 80–85. Ribeirão Preto, Brazil; CD-ROM.

Alexander, B.A. 1996. Comparative morphology of the female reproductive system of nomadine bees (Hymenoptera: Apidae: Nomadinae). Memoirs of the Entomological Society of Washington 17: 14–35.

Alves-dos-Santos, I., G.A.R. Melo, and J.G. Rozen, Jr. 2002. Biology and immature stages of the bee tribe Tetrapediini (Hymenoptera: Apidae). American Museum Novitates 3377: 1–45.

Bennett, F.D. 1966. Notes on the biology of *Stelis* (*Odontostelis*) *bilineolata* (Spinola), a parasite of *Euglossa cordata* (Linnaeus) (Hymenoptera: Apoidea: Megachilidae). Journal of the New York Entomological Society 74: 42–79.

Bennett, F.D. 1972. Observations on *Exaerete* spp. and their hosts *Eulaema terminata* and *Euplusia surinamensis* (Hymen., Apidae, Euglossinae) in Trinidad. Journal of the New York Entomological Society 80: 118–124.

Bronskill, J.F., and E.H. Salkeld. 1978. The micropylar area of some hymenopterous eggs. Canadian Entomologist 95: 663–665.

Cocucci, A.A., and S. Vogel. 2001. Oil-producing flowers of *Sisyrinchium* species (Iridaceae) and their pollinators in southern South America. Flora 196: 26–46.

Erickson, E.H., Jr., S.D. Carlson, and M.B. Garment. 1981. A scanning electron microscope atlas of the honey bee. Ames: Iowa State University Press.

Garófalo, C.A., and J.G. Rozen, Jr. 2001. Parasitic behavior of *Exaerete smaragdina* with descriptions of its mature oocyte and larval instars (Hymenoptera: Apidae: Euglossini). American Museum Novitates 3349: 1–26.

Iwata, K., and S.F. Sakagami. 1966. Gigantism and dwarfism in bee eggs in relation to the mode of life, with notes on the number of ovarioles. Japanese Journal of Ecology 16: 4–16.

Lucas-de-Oliveira, B. 1966. Descrição de estádios imaturos de *Lanthanomelissa* sp., com inferência sôbre a posição filogenética dêste gênero entre os Exomalopsinae (Hym. Apoidea). Studia Entomologica 9: 429–440.

Michelette, E., J.M.F. Camargo, and J.G. Rozen, Jr. 2000. Biology of *Canephorula apiformis* and its cleptoparasite *Melectoides bellus* (Hymenoptera, Apoidea): nesting habits, floral preferences, and immature stages. American Museum Novitates 3308: 1–23.

Michener, C.D. 2000. The bees of the world. Baltimore, MD: Johns Hopkins University Press, 913 pp.

Packer, L. 2003. Comparative morphology of the skeletal parts of the sting apparatus of bees (Hymenoptera: Apoidea). Zoological Journal of the Linnean Society 138: 1–38.

Roig-Alsina, A. 1989. The tribe Osirini, its scope, classification, and revisions of the genera *Parepeolus*, and *Osirinus* (Hymenoptera, Apoidea, Anthophoridae). The University of Kansas Science Bulletin 54: 1–23.

Roig-Alsina, A. 1997. A generic study of the bees of the tribe Tapinotaspidini, with notes on the evolution of their oil-collecting structures (Hymenoptera, Apidae). Mitteilungen der Münchner Entomologischen Gesellschaft 87: 3–21.

Roig-Alsina, A., and C.D. Michener. 1993. Stud-

ies of the phylogeny and classification of long-tongued bees (Hymenoptera: Apoidea). The University of Kansas Science Bulletin 55: 123–173.

Roig-Alsina, A., and J.G. Rozen, Jr. 1994. Revision of the cleptoparasitic bee tribe Protepeolini, including biologies and immature stages (Hymenoptera: Apoidea: Apidae). American Museum Novitates 3099: 1–27.

Rozen, J.G., Jr. 1964. The biology of *Svastra obliqua obliqua* (Say), with a taxonomic description of its larvae (Apoidea, Anthophoridae). American Museum Novitates 2170: 1–13.

Rozen, J.G., Jr. 1969. The biology and description of a new species of African *Thyreus*, with life history notes on two species of *Anthophora* (Hymenoptera: Anthophoridae). Journal of the New York Entomological Society 78: 51–60.

Rozen, J.G., Jr. 1978. The relationships of the bee subfamily Ctenoplectrinae as revealed by its biology and mature larva (Apoidea: Melittidae). Journal of the Kansas Entomological Society 51: 637–652.

Rozen, J.G., Jr. 1984a. Nesting biology of diphaglossine bees (Hymenoptera, Colletidae). American Museum Novitates 2786: 1–33.

Rozen, J.G., Jr. 1984b. Comparative nesting biology of the bee tribe Exomalopsini (Apoidea, Anthophoridae). American Museum Novitates 2798: 1–37.

Rozen, J.G., Jr. 1991. Evolution of cleptoparasitism in anthophorid bees as revealed by their mode of parasitism and first instars (Hymenoptera: Apoidea). American Museum Novitates 3029: 1–36.

Rozen, J.G., Jr. 2000a. Pupal descriptions of some cleptoparasitic bees (Apidae), with a preliminary generic key to pupae of cleptoparasitic bees. American Museum Novitates 3289: 1–19.

Rozen, J.G., Jr. 2000b. Systematic and geographic distributions of Neotropical cleptoparasitic bees, with notes on their modes of parasitism. *In* M.M.G. Bitondi, K. Hartfelder, et al. (editors), Anais do IV Encontro sobre Abelhas, pp. 204–210. Ribeirão Preto, Brazil.

Rozen, J.G., Jr. 2001. Ovarioles and oocytes of two old world cleptoparasitic bees with biological notes on *Ammobatoides* (Apoidea: Apidae). American Museum Novitates 3326: 1–9.

Rozen, J.G., Jr. 2003. Eggs, ovariole numbers, and modes of parasitism of cleptoparasitic bees, with emphasis on Neotropical species (Hymenoptera: Apoidea). American Museum Novitates 3413: 1–36.

Rozen, J.G., Jr., and S.L. Buchmann. 1990. Nesting biology and immature stages of the bees *Centris caesalpiniae*, *C. pallida*, and the cleptoparasite *Ericrocis lata* (Hymenoptera: Apoidea: Anthophoridae). American Museum Novitates 2985: 1–30.

Rozen, J.G., Jr., K.R. Eickwort, and G.C. Eickwort. 1978. The bionomics and immature stages of the cleptoparasitic bee genus *Protepeolus* (Anthophoridae, Nomadinae). American Museum Novitates 2640: 1–24.

Rozen, J.G., Jr., and C.D. Michener. 1988. Nests and immature stages of the bee *Paratetrapedia swainsonae* (Hymenoptera: Anthophoridae). American Museum Novitates 2909: 1–13.

Rozen, J.G., Jr., and H. Özbek. 2003. Oocytes, eggs, and ovarioles of some long-tongued bees (Hymenoptera: Apoidea). Appendix: *Parammobatodes rozeni*, a new bee species from Israel, by M. Schwarz. American Museum Novitates 3393: 1–35.

Rozen, J.G., Jr., and H. Özbek. 2005. Notes on the egg and egg deposition of the cleptoparasite *Thyreus ramosus* (Hymenoptera: Apidae: Melectini). Journal of the Kansas Entomological Society 78(1): 34–40.

Sakagami, S.F., and S. Laroca. 1988. Nests of an exomalopsine bee *Lanthanomelissa goeldiana* (Hymenoptera: Anthophoridae). Journal of the Kansas Entomological Society 61: 347–349.

Santos, C.G., J.M. Oliveira, K.S. Ramos, and B. Blochtein. 2004. Plasticidade de glândulas tegumentares abdominais em *Monoeca xanthopyga* Harter-Marques, Cunha & Moure (Hymenoptera, Apidae, Tapinotaspidini). Revista Brasileira de Entomologia 48: 221–225.

Torchio, P.F. 1989a. In-nest biologies and development of immature stages of three *Osmia* species (Hymenoptera: Megachilidae). Annals of the Entomological Society of America 82: 599–615.

Torchio, P.F. 1989b. Biology, immature development, and adaptive behavior of *Stelis montana*, a cleptoparasite of *Osmia* (Hymenoptera: Megachilidae). Annals of the Entomological Society of America 82: 616–632.

Torchio, P.F., and V.J. Tepedino. 1982. Parsivoltinism in three species of *Osmia* bees. Psyche 89: 221–238.

Torchio, P.F., and G.E. Trostle. 1986. Biological notes on *Anthophora urbana urbana* and its parasite, *Xeromelecta californica* (Hymenoptera: Anthophoridae), including descriptions of late embryogenesis and hatching. Annals of the Entomological Society of America 79: 434–447.

Torchio, P.F., G.E. Trostle, and D.J. Burdick. 1988. The nesting biology of *Colletes kincaidii* Cockerell (Hymenoptera: Colletidae) and development of its immature forms. Annals of the Entomological Society of America 81: 605–625.

Truylio, B., B. Harter-Marques, and W. Engels.

2002. Biologia floral e polinização de *Sisyrinchium micranthum* (Iridaceae) na região do Planalto das Araucárias do Rio Grande do Sul, Brasil. Biociências 10: 11–24.

Urban, D. 1995. Espécies de *Lanthanomelissa* Holmberg e *Lanthanella* Michener & Moure (Hymenoptera, Anthophoridae, Exomalopsinae). Revista Brasileira de Zoologia 12: 767–777.

APPENDIX

Taxonomic Notes on *Monoeca* and Description of a New Species of *Protosiris* (Hymenoptera: Apidae)

by Gabriel A.R. Melo

INTRODUCTION

This short note deals with the identity of the species of *Monoeca* from southeastern Brazil and describes the new species of *Protosiris* associated with the nesting site of *Monoeca haemorrhoidalis*, described above. The acronyms used herein refer to the following collections: AMNH, American Museum of Natural History, New York; BMNH, The Natural History Museum, London; DZUP, Departamento de Zoologia, Universidade Federal do Paraná, Curitiba, Brazil; MPEG, Museu Paraense Emilio Goeldi, Belém, Brazil; MZSP, Museu de Zoologia, Universidade de São Paulo, São Paulo; NHMW, Naturhistoriches Museum Wien, Wien, Austria; ZMHB, Museum für Naturkunde der Humboldt Universität zu Berlin, Berlin.

Monoeca haemorrhoidalis (Smith)

Melissodes haemorrhoidalis Smith, 1854: 313. Type female, South America (BMNH).

Tetralonia reversa Smith, 1879: 111. Type female, Brazil: Rio de Janeiro, Tijuca (BMNH). Synonymy indicated by LaBerge and Moure (1962: 11).

Tetrapedia piliventris Friese, 1899: 293. Holotype male, Brazil: São Paulo, Santos (NHMW). **NEW SYNONYMY.**

The specimens from the population studied in Piraquara, Paraná, agree with the type material listed above, as well as with additional specimens from Rio de Janeiro (listed below). This species is most similar to *M. schrottkyi* (Friese, 1902) and *M. xanthopyga* Harter-Marques, Cunha, and Moure, 2001. These three species, together with *M. pluricincta* (Vachal, 1909), represent the largest members of *Monoeca* (from 10 to 14 mm in length); also, they possess relatively long pubescence on the mesoscutum and scutellum (longest plumose setae about 2.5–3.1× as long as diameter of flagellum). *Monoeca pluricincta* is readily distinguished by its conspicuous yellow integumental tergal bands and by its shallower medial sulcus on the upper frons. The other three species differ mostly by details of the pubescence and structure of the metasomal terga and sterna (figs. A1–A6) and can be separated using the key presented below. Females of *M. haemorrhoidalis* and *M. schrottkyi* can be readily separated from one another based on the pattern of pubescence on the metasomal terga. Many males of *M. haemorrhoidalis*, however, are quite similar to *M. schrottkyi* in possessing broad bands of yellow pubescence on the terga.

Among the six species of *Monoeca* examined (see Biology of *Monoeca haemorrhoidalis*, above), females of the four species mentioned here have a large, wax-extruding area at the base of T6 (figs. A7, A8).

The specimens of *M. haemorrhoidalis* from Piraquara, especially the males, vary considerably in color of the body pubescence and in the distribution of the pubescence on the metasomal terga. The females are less variable; most of them have the marginal zone of T2 and entire T3–T4 covered with bright yellow setae, while only a few females have the metasomal terga covered with dark pubescence. The males vary from having very light colored (pale yellow to light orange) to entirely black pubescence on the head, thorax, and legs, including all sorts of combinations. The setation on the metasomal terga also varies from very dense, with broad marginal bands on the terga, to very sparse, with only a few scattered setae along the tergal margin.

Material Examined: Female type of *Melissodes haemorrhoidalis*, "Type H. T.", "B. M. Type / Hym / 17.B. 858", "Melissodes / haemorrhoidalis / S. Amer. Sm." and "F. Sm. coll. / 79.22"; female type of *Tetralonia reversa*, "Type B. M.", "B. M. Type / Hym / 17.B.8111", "Tetralonia / reversa / Type Smith" and "TEJUCA / Jan 1. 1857 / J. Gray"; male holotype of *Tetrapedia piliventris*, "Santos / Brasilien / Dr. Brauns. / 18.10.97", "Tetrapedia / piliventris / det. Friese 1898 / n. sp." (♂) and "Holotype"; 1 female (DZUP), "Tijuca—R.J. / 16.I.56 / Moure leg." and "Monoeca / reversa / (Smith, 1879) / Det.

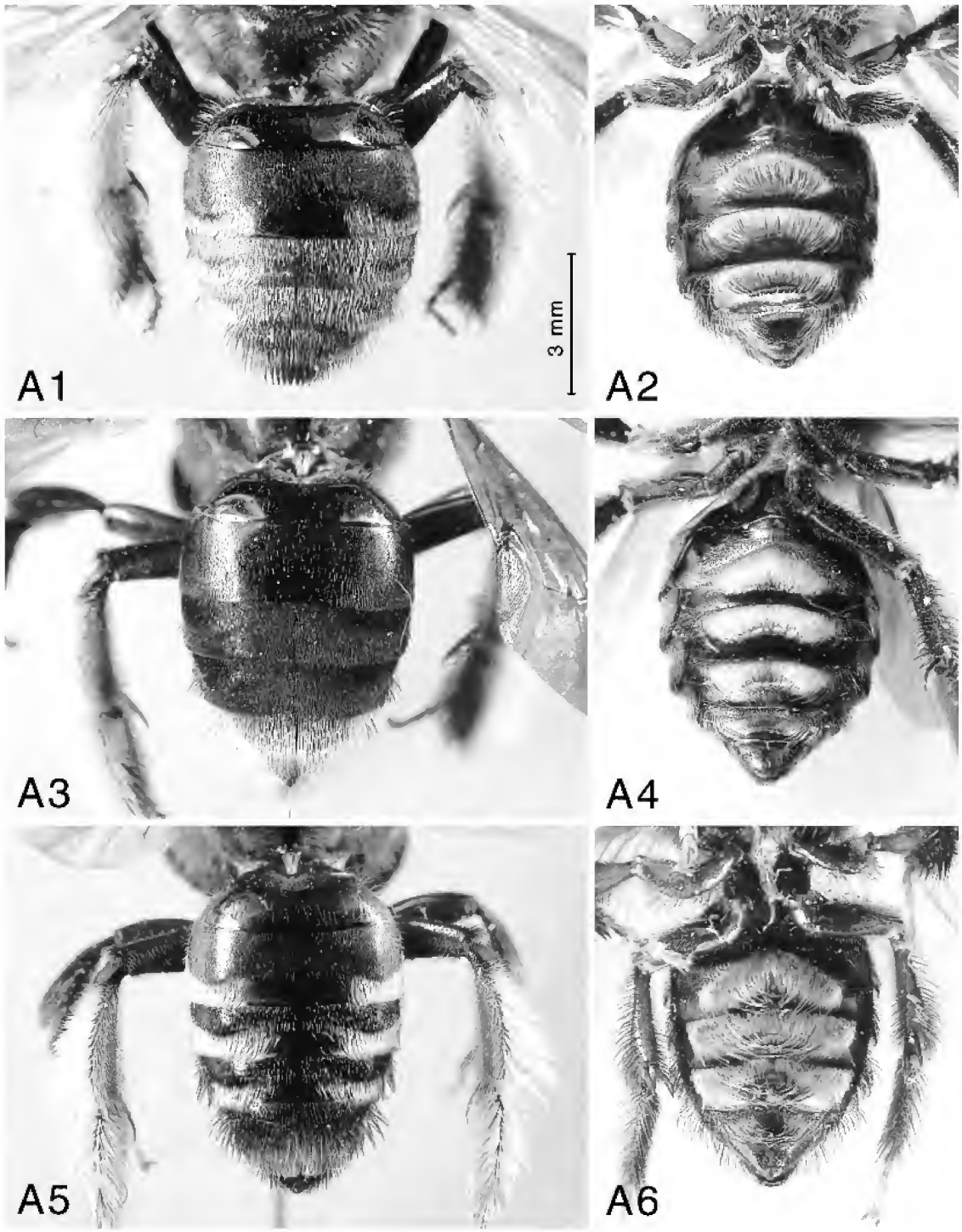

Figs. A1, A2. *Monoeca haemorrhoidalis*. **A1.** Female metasoma, dorsal view. **A2.** Male metasoma, ventral view. **Figs. A3, A4.** *Monoeca xanthopyga*. **A3.** Female metasoma, dorsal view. **A4.** Male metasoma, ventral view. **Figs. A5, A6.** *Monoeca schrottkyi*. **A5.** Female metasoma, dorsal view. **A6.** Male metasoma, ventral view. Scale = 3 mm, refers to all figures.

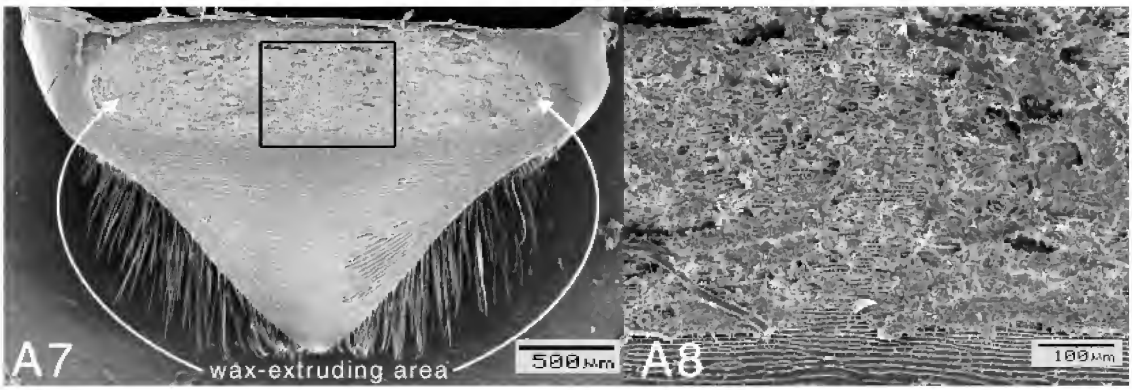

Figs. A7, A8. Sixth tergum of *Monoeca haemorrhoidalis*, female. **A7.** Dorsal view of sclerite, showing well-developed pygidial plate and broad wax extruding area at base associated with epidermal gland. **A8.** Close-up of wax release surface as indicated by rectangle in fig. A7.

Moure 1980"; 1 male (DZUP), "Floresta da Tijuca / D. Federal BRASIL / I-1954 / C.A.C. Seabra Coll." and "Monoeca / brasiliensis / Lep. Serv. / Det. J. S. Moure 1957"; 1 female (DZUP), "Praia Lagoinha do Leste / Florianópolis, SC, Brazil / 27.XII.2002 / A. Zillikens leg." and "In nest aggregation of / Monoeca sp."; plus numerous males and females collected at the nesting site, as well as additional older specimens collected in the same locality and deposited in the DZUP collection.

Monoeca schrottkyi (Friese)

Pachycentris schrottkyi Friese in Schrottky (1901: 215), nomen nudum.

Pachycentris schrottkyi Friese, 1902:187. Lectotype female (presently designated), Brazil: São Paulo, Jundiaí (ZMHB).

In order to properly identify the material from Piraquara, we also studied the type material of *M. schrottkyi* (see Comments under *M. haemorrhoidalis*). Friese described this species based on females collected by Schrottky in a nest aggregation found in Jundiaí, São Paulo. To help stabilize the taxonomy of the genus, we designate here as lectotype one of the syntype females (see label data below).

Material Examined: Lectotype female (ZMHB), "Brasil / Jundiahy / 16.11.1899 / Schrottky", "Pachycentris / schrottkyi / 1900 Friese det. / Fr." (♀) and "Typus"; 1 female (MZSP), "1.374" and "PARATYPE / Monoeca / schrottkyi (Friese, 1902) / J. S. Moure 1993" (the registry book of the MZSP contains the following data under the number 1.374: "Pachycentris schrottkyi Friese (cotipo), 16.xi.1899, Jundiahy, Schrottky"); 1 female (MPEG), "JUNDIAHY / E. S. PAULO", "Brasil / Jundiahy / 18.11.1899 / Schrottky" and "Pachycentris / schrottkyi Friese" (Ducke's handwritten label); 1 male (DZUP), "São Paulo / cidade / Melzer leg. / 1914." and "Tetralonia / (Thygater.)"; 1 male (DZUP), "Barueri / São Paulo—Brasil / 8-IV-61 / K. Lenko col." and "Monoeca / schrottkyi / (Friese, 1902) / Pe J S Moure 1993"; 1 female (MZSP), "Est. Biol. Boracéia / Salesópolis, SP / W. Wilms, col. / 14.12.1992" and "Monoeca / piliventris / (Friese, 1899) / det. W. Wilms, 1994"; 1 female (DZUP), "Caiobá / XII-1942" and "Fiorentina / schrottkyi / P. Moure det. 1947"; 1 female (DZUP), "CORUPÁ / S. Catarina BRASIL / XI-1953 A. Maller" and "Monoeca / schrottkyi / (Fr.) / Det. J. S. Moure 1957" (on the reverse "C. W. cotype / MZ-USP / Pe. J. S. Moure / XII-1954").

Key to the Large Species of *Monoeca* from Southeastern Brazil

1. Wing membrane darkly infumated. Lateral portion of tergum 2 and entire terga 3 and 4 densely covered with simple dark setae, discs not distinctly different from marginal zones, except for short lateral bands of plumose dark setae on T3–T4 (fig. A3). Simple setae on mesoscutum about as long as plumose setae. Female: medial portion of clypeus entirely punctured, except for a narrow basal stripe .... *xanthopyga* (Paraná, Rio Grande do Sul, Santa Catarina)

— Wing membrane with a yellow tint. Marginal zones of T2–T4 with distinct bands of plumose setae, usually pale yellow (sometimes black), setae on tergal discs distinctly shorter compared to those on marginal zones (figs. A1, A5). Female: a few simple

setae on the mesoscutum distinctly longer than plumose pubescence; medial portion of clypeus with a narrow longitudinal stripe without punctures 2

2. Marginal zones of T2–T4 only weakly depressed in relation to discs laterally (fig. A1). Pubescence on lateral portions of discs of T3–T4 not particularly sparser than on T2, except on T4 of a few males with weakly pubescent terga. Female: last three metasomal terga usually with integument bright reddish brown (rarely dark brown); clypeus with only a medial longitudinal depression or at most with a faint ridge; punctures on disc of tergum 2 almost reaching center of sclerite. Male: sternal pads less developed and occupying less than three-fourths of the sclerite width, tips of setae of posterior fringe not meeting in the middle portion of sclerite (fig. A2) ..... *haemorrhoidalis* (Paraná, Rio de Janeiro, Santa Catarina, São Paulo)

— Marginal zones of T2–T4 distinctly depressed in relation to discs laterally (fig. A5). Pubescence on lateral portion of discs of T3–T4 distinctly sparser than on T2. Female: metasomal terga with a dark brown to black integument; clypeus with a weak, but distinct, medial longitudinal ridge; central one-third of tergum 2 almost impunctate. Male: sternal pads strongly developed and occupying over three-fourths of the sclerite widths, setae of posterior fringe distinctly long, their tips meeting in the middle portion of sclerite (fig. A6) *schrottkyi* ..... (Paraná, Santa Catarina, São Paulo)

Protosiris gigas Melo, new species
Figures A9–A21

COMMENTS AND DIAGNOSIS: The genus *Protosiris* contains four described and a few additional undescribed species (Roig-Alsina, 1989; Shanks, 1986; Melo, unpubl.). The new species proposed here, *Protosiris gigas*, is most similar, both in size and structure, to *P. caligneus* (Shanks) (comparisons based on male and female paratypes from the type locality deposited at AMNH and MZSP). *Protosiris gigas* can be separated from *P. caligneus* by its abundant yellow marks (uniformly reddish to dark brown in *P. caligneus*), lower paraocular area covered by plumose pubescence (mostly simple in *P. caligneus*), slightly longer decumbent hairs on middle portion of upper frons, mesoscutum strongly protruding on its midanterior portion (more pronounced in the female), and with a corresponding deep sulcus along the midline (fig. A18), posterior portion of male scutellum more evenly convex, medial sulcus only weakly indicated (scutellum more bulging in *P. caligneus*, medial sulcus more deeply marked), basal depression of metaposnotum smooth and without rugulae (fig. A12) (finely microreticulate and with lateral rugulae in *P. caligneus*), tergal setal punctures relatively sparse (very dense in *P. caligneus*, punctures about 1–2 puncture diameters apart) and lateral portions of terga 2–4 with only erect setae (in *P. caligneus*, with abundant short, decumbent hairs, similar to those of tergum disc).

DESCRIPTION: *Holotype male.* Body length: 14 mm; maximum head width: 3.1 mm; forewing length: 11.5 mm. Color: head and thorax mostly pale yellow, with many reddish to dark brown areas, as shown in figures A9 and A10; scape, pedicel, and 1st flagellomere dark brown, remaining flagellomeres dark reddish brown. Wing membrane brownish yellow infuscated, veins brown, pterostigma reddish brown. Metasomal terga 1–5 pale yellow at base and broadly brown apically; T6–T7 entirely dark brown. Sternum 1 dark brown at base and apically, its middle portion pale yellow; S2–S4 largely pale yellow basally and with triangular-shaped, apical brown band (in middle, band occupying about half of sclerite's length); S5–S6 mostly dark brown. Pubescence: lower paraocular area covered with plumose pubescence. Longest erect setae on lateral portion of mesepisternum about as long as width of 2nd flagellomere (0.3–0.32:0.31). Lateral ventral portions of metasomal terga with only erect setae; S5 with a distinct apical band of plumose pubescence, setae directed to the middle portion of sclerite. Integumental surface: integument very smooth and polished. Setal punctures fine and inconspicuous, except for a few relatively strong punctures laterally on the clypeus and posteriorly on lateral portion of mesepisternum (weaker than those on clypeus). Metapostnotum mostly smooth, microreticulation almost imperceptible, basal depression well developed, its surface without longitudinal rugulae and only with a few transverse, inconspicuous rugulae laterally at the base (fig. A12). Setal punctures on posterior halves of discs of terga 1–4 about 3–4 puncture diameters apart transversely and 5–10 diameters apart longitudinally, slightly denser on basal halves of sclerites. Structure (measurements in mm): head about 1.3× wider than long (3.10:2.40); inner orbits nearly straight and parallel (upper to lower interorbital distance, 1.69:1.70); eye 1.8× as long as width at eye's midlength (1.85:1.02); mandible bidentate apically, about 2.9× longer than its outer basal width (1.58:0.55); clypeus about 2.4× wider than long (1.69:0.71), distinctly protuberant, mid-

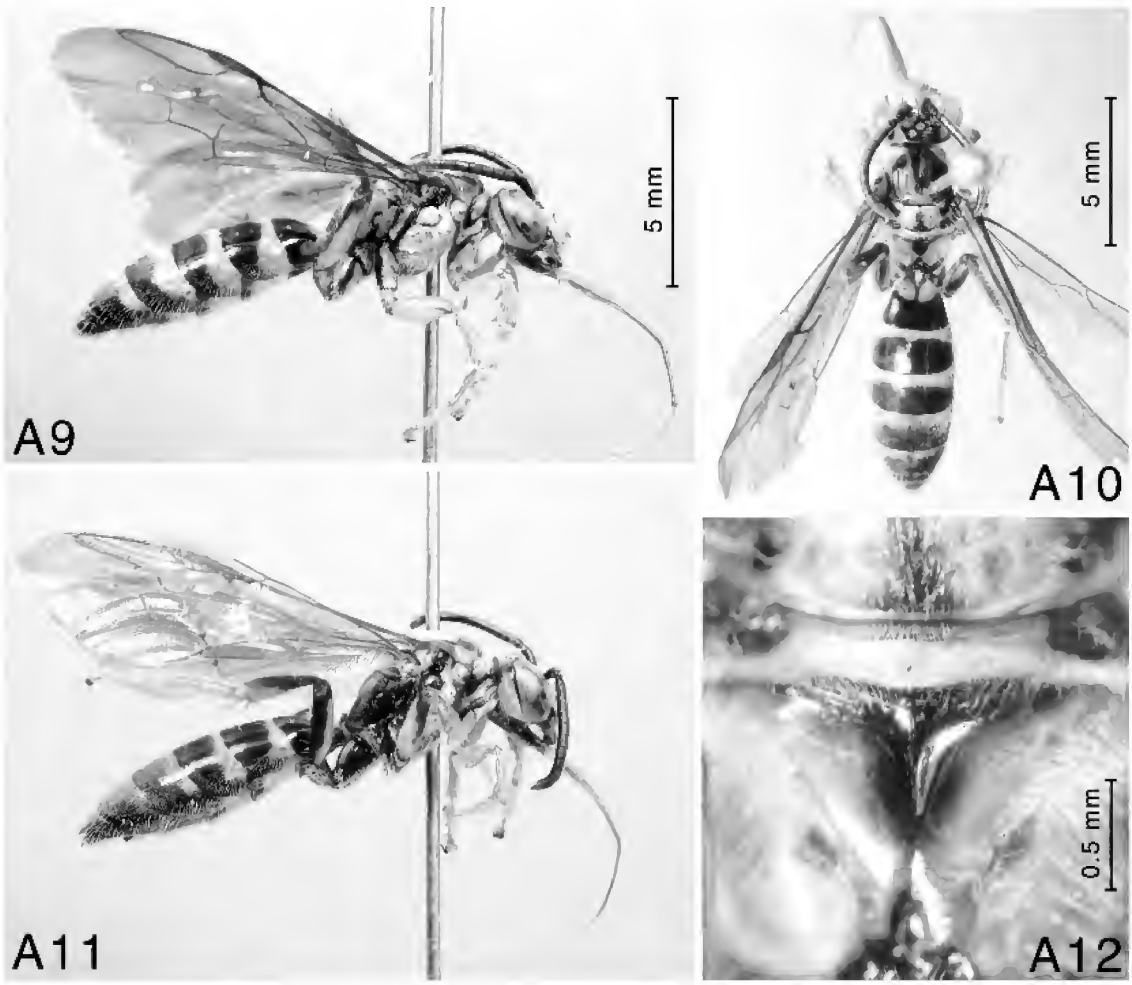

Figs. A9–A12. *Protosiris gigas*, new species. **A9.** Male holotype, lateral view. **A10.** Male holotype, dorsal view. **A11.** Male paratype, lateral view. **A12.** Close-up of metapostnotum of male holotype, posterodorsal view. Figs. A9 and A11 at same scale.

apical portion of disc with relatively flat, triangular-shaped area; supraclypeal area about as protuberant as clypeus, its middle portion relatively flat. First flagellomere conical, about 0.8× as long as its maximum width (0.24:0.31), and about 0.61× as long as 2nd flagellomere (0.24:0.39). Labial palpus 4-segmented, apical segment about as long as third. Hindtibia, in posterior view, about 4.3× longer than wide (2.56:0.59). Forewing M and Cu diverging distinctly distal to cu-a; proportion of lengths of submarginal cells on posterior margin 1.7:1:1.7 (1.18:0.71:1.18). Midanterior portion of mesoscutum distinctly protruding (as in fig. A18), median line forming deep sulcus; mesoscutum as long as wide (1.97:1.97). Pygidial plate narrowly truncate apically.

Female. Body length: 14–16 mm; maximum head width: 3.35–3.62 mm; forewing length: 11–12 mm. Agreeing with male in color, pubescence, sculpturing and structure, except as follows (measurements taken on two females, somewhat representative of size variation): head about 1.27–1.29× wider than long (3.35:2.60/3.62:2.84); upper to lower interorbital distance, 1.89:1.97/2.05:2.13; eye about 1.9–2× as long as width at eye's midlength (2.01:1.04/2.21:1.10); mandible simple apically, about 2.8–2.9× longer than its outer basal width (1.69:0.59/1.77:0.63); clypeus about 2.6–2.7× wider than long (1.93:0.71/2.09:0.79). Pygidial plate well developed, about as long as its basal width (1.14:0.98/1.22:1.10).

VARIATION: Some specimens have more extensive darker areas, especially on the thorax and propodeum (fig. A11).

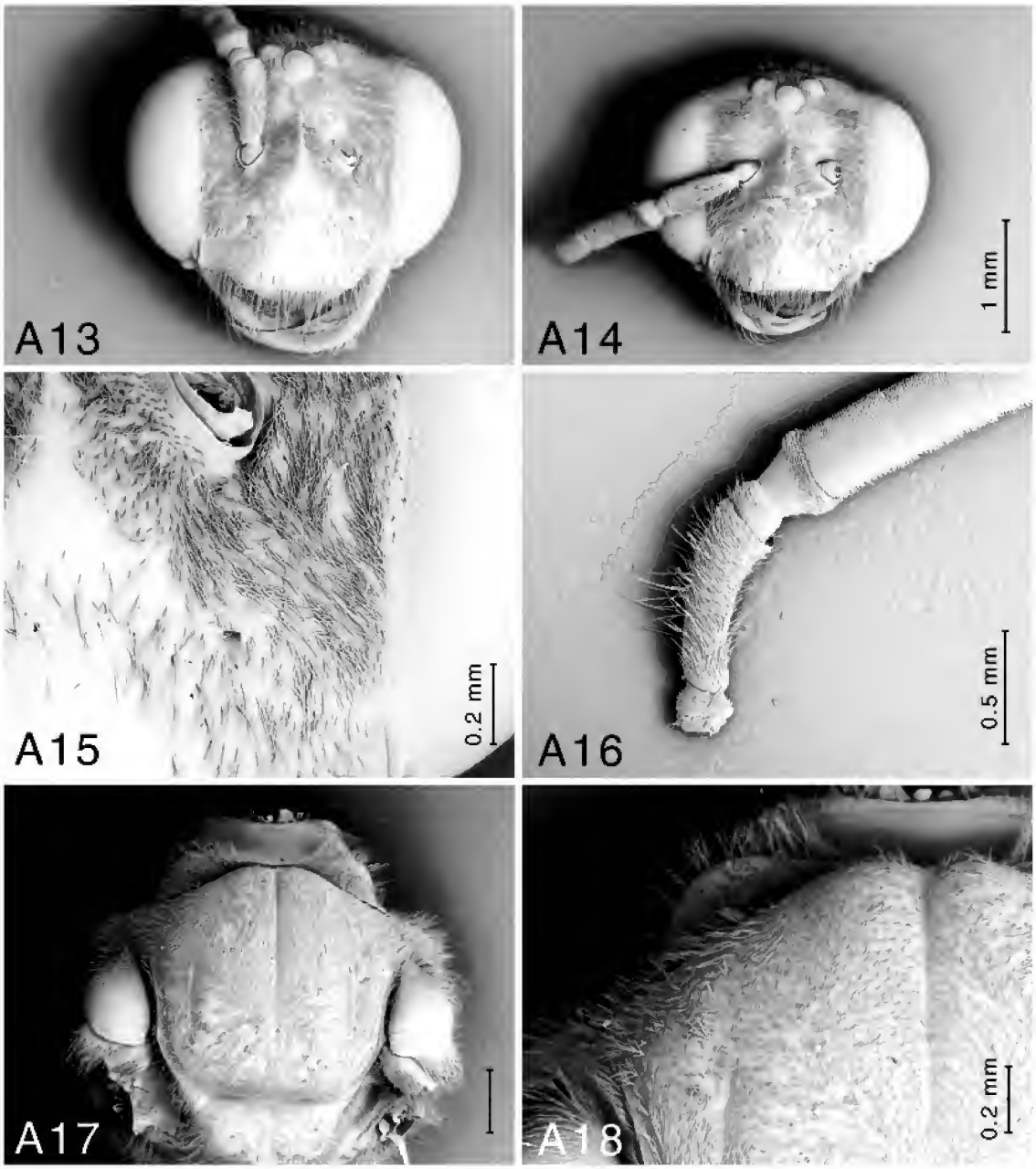

Figs. A13–A18. *Protosiris gigas*, new species. **A13.** Female head, frontal view. **A14.** Male head, frontal view. **A15.** Close-up of lower paraocular area of female, frontal view. **A16.** Basal portion of female antenna, frontal view. **A17.** Male mesosoma, dorsal view. **A18.** Close-up of anterior portion of male mesoscutum, dorsal view. Figs. A13 and A14 at the same scale.

TYPE MATERIAL: Holotype male, "Brasil, Paraná, Piraquara, / Mananciais da Serra, / 25°28′40″S 48°58′04″W, / 1140m, 20.xi.2002, / Melo, Aguiar & Rozen". Paratypes: several males and females, from the same locality as the holotype, but specific dates and collectors varying (20 November–13 December 2002, and 3–11 December 2003); 1 female, "UCAD / Florianópolis, SC, Brasil / 23.XI.2002 / A. Zillikens leg." and "Neoregelia laevis / (Mez) L. B. Smith. / Bromeliaceae

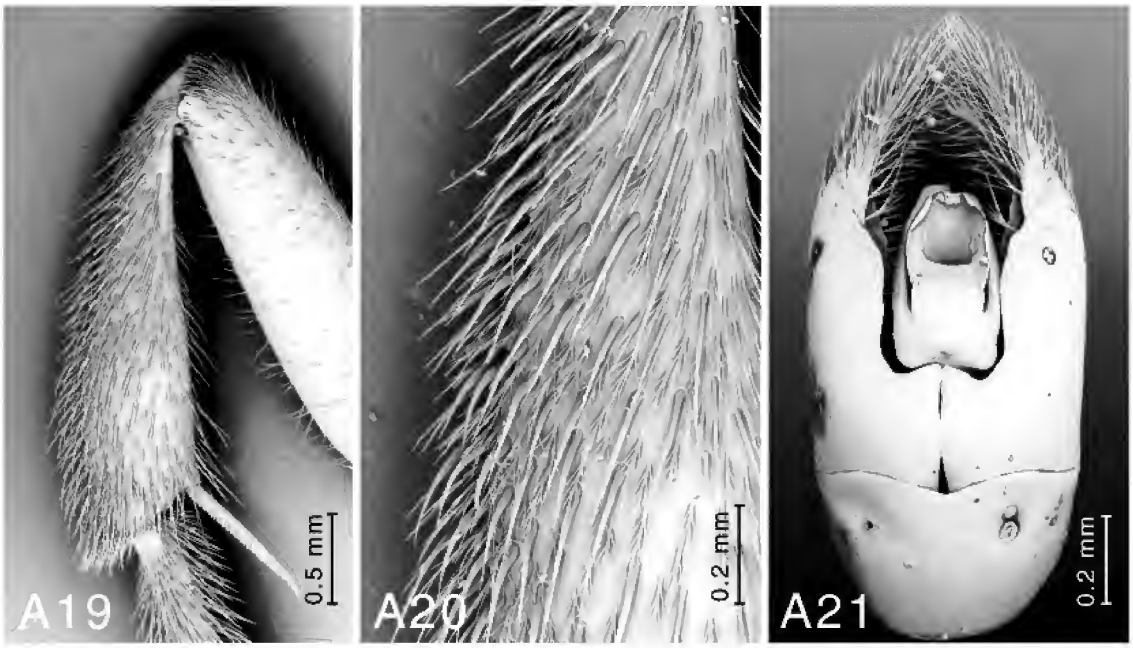

Figs. A19–A21. *Protosiris gigas*, new species. **A19.** Detail of the female hindleg, outer view. **A20.** Close-up of the midportion of the female hindtibia, outer view. **A21.** Male genitalia, dorsal view.

/ flor''; 1 female, ''Praia Lagoinha do Leste / Florianópolis, SC, Brazil / 27.XII.2002, A. Zillikens leg.'' and ''In nest aggregation of / Monoeca sp.''. Holotype in DZUP and paratypes in DZUP and AMNH.

ETYMOLOGY: This species is named for its relatively large body size, compared to other *Protosiris*, from the Latin *gigas*, giant.

ACKNOWLEDGMENTS TO APPENDIX

I thank A.J.C. Aguiar for providing information on the types of *Melissodes haemorrhoidalis* and *Tetralonia reversa* and for his help on preparing the key to the species of *Monoeca* presented here. A. Zillikens kindly provided the specimens of *Protosiris* collected in Florianópolis. The ''Centro de Microscopia Eletrônica'' (UFPR) is acknowledged for the SEM images of the adult *Protosiris*.

REFERENCES TO APPENDIX

Friese, H. 1899. Monographie der Bienengattungen *Exomalopsis*, *Ptilothrix*, *Melitoma* und *Tetrapedia*. Annalen des K.K. Naturhistorischen Hofmuseums 14: 247–304.

Friese, H. 1902. Zwei neue Bienengattungen (Hym.). Zeitschrift für Systematische Hymenopterologie und Dipterologie 2: 186–187.

LaBerge, W.E., and J.S. Moure. 1962. Type specimens of American eucerine bees deposited in the British Museum. Boletim da Universidade do Paraná, Zoologia 1(11): 1–12.

Roig-Alsina, A. 1989. The tribe Osirini, its scope, classification, and revisions of the genera *Parepeolus* and *Osirinus* (Hymenoptera, Apoidea, Anthophoridae). The University of Kansas Science Bulletin 54: 1–23.

Schrottky, C. 1901. Biologische Notizen solitärer Bienen von S. Paulo (Brasilien). Allgemeine Zeitschrift für Entomologie 6: 209–216.

Shanks, S. 1986. A revision of the Neotropical bee genus *Osiris* (Hymenoptera: Anthophoridae). The Wasmann Journal of Biology 44: 1–56.

Smith, F. 1854. Catalogue of hymenopterous insects of the collection of the British Museum. Part 2: 199–465. London: British Museum.

Smith, F. 1879. Descriptions of new species of Hymenoptera in the collection of the British Museum. London: British Museum, xxi + 240 pp.